8-18-2015 12:00 AM

Stimuli-Responsive Polymersomes and Surface Functionalized Dendrimersomes: Platforms for Biomedical Applications

J Trevor McIntosh
The University of Western Ontario

Supervisor
Dr. Elizabeth R Gillies
The University of Western Ontario

Graduate Program in Chemistry
A thesis submitted in partial fulfillment of the requirements for the degree in Master of Science

STIMULI-RESPONSIVE POLYMERSOMES AND SURFACE FUNCTIONALIZED DENDRIMERSOMES: PLATFORMS FOR BIOMEDICAL APPLICATIONS

(Thesis format: Integrated Article)

by

J. Trevor McIntosh

Graduate Program in Chemistry

A thesis submitted in partial fulfillment
of the requirements for the degree of
Master of Science

The School of Graduate and Postdoctoral Studies
The University of Western Ontario
London, Ontario, Canada

Abstract

Amphiphilic block copolymers (BCPs) and dendrimers are known to self-assemble in aqueous solution to form a number of aggregate morphologies. These different architectures are largely a function of the hydrophilic volume or weight fractions of the different components of the polymer system. One possible morphology is a vesicle, also referred to as a polymersome or dendrimersome when BCPs or dendrimers, respectively, are used. Vesicles are multi-functional, supramolecular, bilayer assemblies, whose potential for stimuli-responsiveness and surface functionalization make them promising materials for a variety of biomedical applications. This thesis demonstrates the use of UV-sensitive block copolymers forming photodegradable vesicles, as well as the use of dendrimersomes as a platform for surface functionalization. Polymersomes were formed from an amphiphilic triblock copolymer consisting of a UV-sensitive *o*-nitrobenzyl ester homopolymer functionalized with poly(ethylene glycol) chains at its termini. The assembled polymersomes degraded upon exposure to UV light and reassembled into smaller aggregate morphologies demonstrating their potential for encapsulation and targeted delivery of cargo. Surface functionalizable dendrimersomes were prepared using a combination of Janus dendrimers and their azide-terminated analogues. The dendrimersome surface was functionalized with a 2 kg/mol poly(ethylene oxide)-alkyne derivative showing that it may be functionalized with a variety of ligands using copper-catalyzed azide-alkyne click chemistry. Combined, these examples demonstrate the versatility of stimuli-responsive and surface functionalized vesicle systems for a wide range of applications.

Key words: Janus dendrimer, Dendrimersome, Surface functionalization, Polymersome, Photoresponsive, Self-assembly

Co-Authorship Statement

The work discussed in this thesis is the result of the author's work as well as the work of coworkers at Western University, collaborators from the Université de Bordeaux and the University of Toulouse and supervisor Dr. Elizabeth Gillies whose exact contributions are described here.

Chapter 2 describes a project proposed by Dr. Ali Nazemi and Dr. Elizabeth Gillies. The manuscript was drafted by the author while editing and final preparations were provided by Dr. Gillies. All small molecule and polymer synthesis, self-assembly, particle characterization and degradation was performed by the author while other self-assembly protocols were performed by co-authors Dr. Elizabeth Gillies, Dr. Sebastian Lecommandoux and Dr. Colin Bonduelle.

Chapter 3 describes an ongoing project proposed by Dr. Ali Nazemi and Dr. Elizabeth Gillies. All small molecule and dendrimer synthesis, as well as self-assembly and particle characterization was performed by the author, except for the synthesis of 2 kg/mol Poly(ethylene oxide)-alkyne which was performed by coworker Andrew Wong.

Acknowledgements

First and foremost I would like to thank my supervisor Dr. Elizabeth Gillies, who gave me the opportunity to learn and develop as a chemist as a part of her research group. I would like to thank her for her support, guidance and tireless efforts over the last three years helping to make me successful.

I would also like to thank the Gillies research group, past and present, for making the lab such a pleasant place to be and work. Everyone was always so willing to help whenever it was needed, whatever the task might be. In particular, Dr. Ali Nazemi always provided guidance and mentorship during my time. I would also like to thank Anita Borecki who was always so willing to provide analytical assistance.

Furthermore I'd like to thank my friends and family who have always been supportive and understanding of the time and work I've put in over the last two years. I'd very much like to extend my appreciation towards Sara O'Halloran who provided endless moral support and picked up my slack at home during those late nights in the lab and writing.

Most of all though, I'd like to dedicate this thesis to my recently passed grandmother, Margaret McIntosh. She was a hard working and loving woman who was loved and will be missed.

Table of Contents

List of Tables

List of Figures

List of Schemes

List of Abbreviations

BCP	Block copolymer
bis-MPA	2,2-bis(hydroxymethyl) propionic acid
Bp	Boiling point
CuAAC	Copper catalyzed azide-alkyne cycloaddition
Đ	Dispersity
DCC	*N*,*N*'-dicyclohexylcarbodiimide
DIPEA	*N*,*N*-diisopropylethylamine
DLS	Dynamic light scattering
DMAP	4-dimethylaminopyridine
DMF	*N*,*N*-dimethylformamide
DMSO	Dimethylsulfoxide
DSC	Differential scanning calorimetry
EDC	*N*-(3-dimethylaminopropyl)-*N*'-ethylcarbodiimide
EtOAc	Ethyl acetate
$f_{hydrophilic}$	Hydrophilic volume fraction
G1	First generation dendron
G2	Second generation dendron
G3	Third generation dendron
G4	Fourth generation dendron
GPC	Gel permeation chromatography
HCl	Hydrochloric acid

HCTU	*O*-(6-chlorobenzotriazol-1-yl)-*N*,*N*,*N*',*N*'-tetramethyluronium hexafluorophosphate
HRMS	High resolution mass spectrometry
IR	Infrared spectroscopy
IUPAC	International Union of Pure and Applied Chemistry
Ln	Ligand
LRMS	Low resolution mass spectrometry
M_i	Mass of polymers in polymer set i
M_n	Number average molecular weight
Mp	Melting point
M_w	Weight average molecular weight
MWCO	Molecular weight cutoff
N_i	Number of polymers in polymer set i
NMR	Nuclear magnetic resonance imaging
PEG	Poly(ethylene glycol)
PEO	Poly(ethylene oxide)
SEC	Size exclusion chromatography
TEM	Transmission electron microscopy
T_g	Glass transition temperature
THF	Tetrahydrofuran
TLC	Thin layer chromatography
T_m	Melting temperature
UV	Ultra violet

Chapter 1

1 Polymersomes and Dendrimersomes in Biomedical Applications

1.1 Introduction to Polymers

Polymer science dates back to ancient Mesoamerica.[1] The indigenous peoples were able to mix the juice from morning glory vines with the latex from rubber trees to make rubber. This rubber was tunable by varying the amount of either component, thereby providing them the ability to make products with different physical properties, such as hard soles for sandals or figurines, sticky adhesives, stretchy rubber bands and bouncy balls. Now, more than 3000 years later, the field has evolved and greatly advanced into what it is today. The term *polymer* comes from the Greek, *pols*, meaning "many" and *meros*, meaning "part", and was first used in 1833 by Swedish chemist, Jons Jakob Berzelius.[2] The International Union of Pure and Applied Chemistry (IUPAC), defines the word as follows

> "a molecule of high relative molecular mass, the structure of which essentially comprises the multiple repetition of units derived, actually or conceptually, from molecules of low relative molecular mass."

With this in mind, we can subcategorize these molecules into natural and synthetic polymers. Natural polymers, as their name suggests, are made via cellular processes in nature and include the building blocks of life such as DNA, polysaccharides and proteins, or other products like silk from the silkworm, wool from sheep, and cellulose in plants. Synthetic polymers like Teflon, polyester, nylon 6.6, polystyrene, or dendrimers are those made in a lab or a factory by scientists for academic or commercial purposes.

In comparison to small molecules, which have well defined molecular weights and physical properties, polymers have molecular weight distributions and broadly defined physical properties. These properties are governed by the chain entanglement characteristics intrinsic to the polymer as well as the dispersity ($Đ$) of the material. $Đ$

refers to the distribution of size or molecular weight of a given polymer sample, and is defined by the equation,

$$Đ = \frac{M_w}{M_n}$$

where M_w is the weighted molecular weight average,

$$M_w = \frac{\Sigma_i N_i M_i^2}{\Sigma_i N_i M_i}$$

and M_n is the molecular weight number average,

$$M_n = \frac{\Sigma_i N_i M_i}{\Sigma_i N_i}$$

where N_i is the number of molecules with specific molecular mass M_i.

A perfectly monodisperse or uniform sample is represented by $Đ$=1.0 where M_w=M_n. This situation is termed "monodisperse" and describes a polymer sample consisting entirely of chains of equal length, such as with dendrimers or naturally occurring polymers like proteins. Conversely, when $Đ$>1.0, the polymer sample contains chains of varying length, such as is the case with most types of synthetic polymers where the width of the dispersity is dependent upon the polymerization technique; termed "polydisperse".

Polymer molecular weight is commonly determined through size exclusion chromatography (SEC), also known as gel permeation chromatography (GPC). This method fractionates samples based on hydrodynamic volume by using a stationary phase with a range of pore sizes. The polymers with larger hydrodynamic volume will elute first and the smaller ones will elute last. The size of the polymer is inversely proportional to the elution time because the smaller the polymer, the more pores it may enter and therefore increase its path length and time on the column. The elution times or volumes of the analyte fractions are compared to those of a series of polymer standards of known molecular weight which gives an accurate approximation of the molecular weight of the analyte. The more closely the analyte chemically resembles the polymer standard the more accurate the measurement will be.

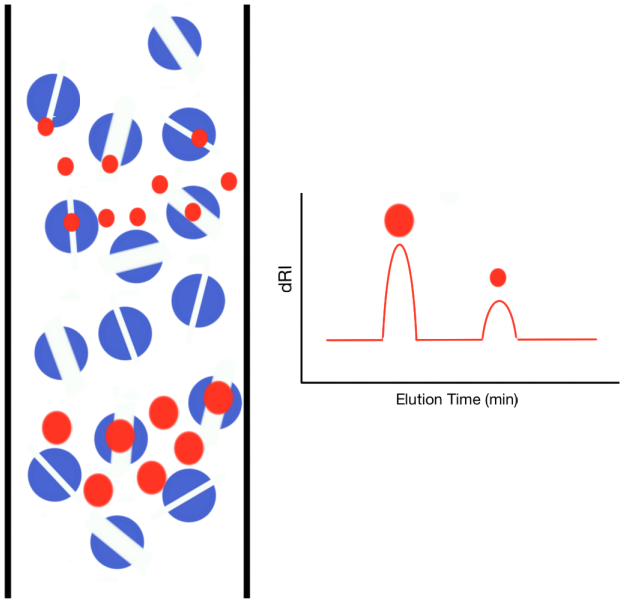

Figure 1.1. GPC cartoon schematic showing separation of large and small analytes measuring change in refractive index versus elution time.

Beyond molecular weight, polymers are typically characterized using their state transition temperatures to justify their physical properties. Small molecule species can exist in the solid, liquid or gaseous phases which are separated by phase-transition temperatures: melting point (mp) and boiling point (bp). Polymers, however, can exist in a glassy state, amorphous/semicrystalline state and melt or fluid-like state, which are separated by the glass-transition temperature (T_g) and melting temperature (T_m). Below the T_g the polymer chains are frozen in place and the polymer is hard and brittle. Above the T_g the chains exist in both a frozen and mobile state where the sample is soft and rubbery until above the T_m where the chains are completely mobile and fluid-like. The phase-transition temperatures are determined using differential scanning calorimetry (DSC) which is a thermoanalytical method by which the heat flux of a polymer sample is measured over heating and cooling cycles. The thermal flux of a reference and an analyte is measured as the two are heated and cooled at the same temperatures. When a phase transition occurs it

will require more or less heat to maintain the sample at the given temperature thus indicating at which temperatures (T_g and T_m) the phase transitions occur.

Scheme 1.1. Phase transition temperatures of polymer species.

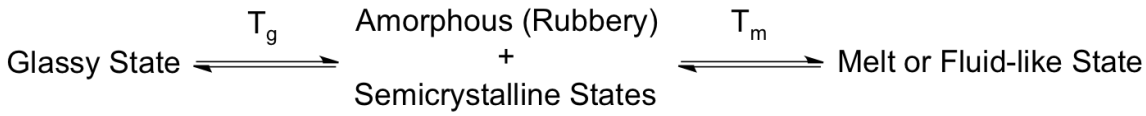

1.2 Block Copolymers

As the term polymer describes a molecule composed of repeating smaller units, a block copolymer (BCP) is two or more chemically distinct homopolymers linked together. Its physical properties are dependent upon such molecular characteristics as chemical structure, size, dispersity and block ratios. One polymer A can be linked to another polymer B, or polymer B can be grown from polymer A using B monomers. These are two methods for creating a diblock copolymer. There are however, other architectures that can be made, such as tri and tetraBCPs, or star and mixed-star BCPs.

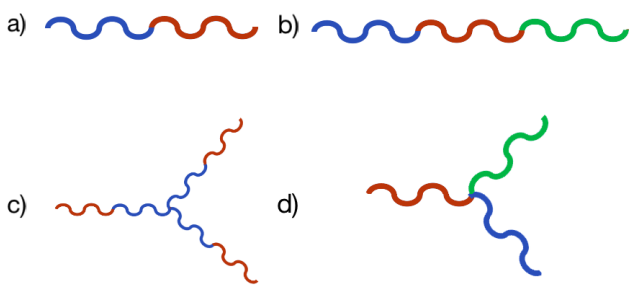

Figure 1.2. a) AB diblock copolymer, b) ABC triblock copolymer, c) AB star block copolymer, d) ABC mixed-star block copolymer

1.2.1 Amphiphilic BCPs and Their Self-Assembly in Solution

BCPs can have multiple distinct segments with similar solubility characteristics, being either polar or non-polar or in reference to water, hydrophilic or hydrophobic. When the

segments have differing solubilities in water, the molecule is called an amphiphilic block copolymer. This property yields the capacity for self-assembly. Aqueous self-assembly is the result of the poor affinity of the non-polar, or hydrophobic, block for the aqueous medium thus inducing the assembly of like blocks into an energetically favourable construct that will hide this part of the polymer. This results in variable, yet very tunable, aggregate morphologies. Self-assembly can occur in the bulk, thin-film or solution phases, each having its own applications.[3] Over that last two decades however, solution phase self-assembly with BCPs has been an area of significant interest and discovery. Studies into morphological variations of assemblies, as shown in Figure 1.3, have revealed the formation of spherical micelles, worm-like micelles, vesicles, and other nanoparticles for drug delivery applications[4, 5, 6] where the resulting morphology of the polymer assembly is largely due to the hydrophilic volume fraction of the polymer.[7]

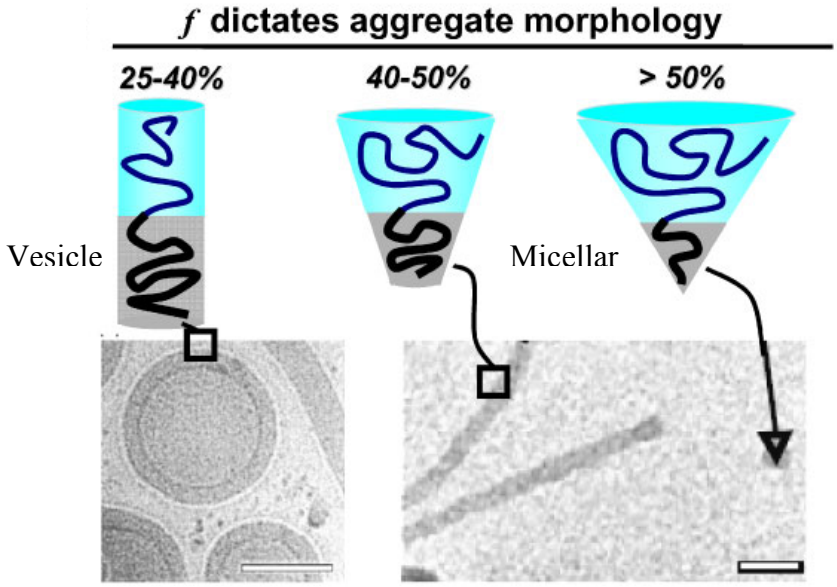

Figure 1.3. Aggregate morphology of block copolymer self-assembly based on ratio of hydrophilic to hydrophobic volume fractions. Observations were made by cryo-TEM. The figure was reproduced with permission of John Wiley and Sons from Ahmed *et al.* (2006).

Polymersomes have proven to be a very interesting system for biomedical applications especially drug delivery. Like liposomes, their architecture comprises an amphiphilic

bilayer, but studies have shown that vesicles assembled from block copolymers have increased strength and stability while maintaining low permeability relative to phospholipid vesicles.[8] Not only do they have desirable structural characteristics when assembled from block copolymers, but the use of poly(ethylene glycol) (PEG) as a hydrophilic block has been shown to increase circulation time *in vivo* as it reduces protein adsorption and macrophage binding to the assembly surface.[9] The size of the assembly has also shown to play a role in circulation time. A particle diameter of approximately 100 nm is the optimal size as the renal threshold for particles in the blood is ~10 nm and particles larger than ~200 nm are actively catabolized and removed through immune system processes.[9] Lastly, what makes polymersomes an ideal drug delivery candidate is their ability to encapsulate both hydrophobic and hydrophilic drugs and release them in a controlled manner while at the same time prolonging their circulation time and protecting them from premature degradation.[10]

1.2.2 Stimuli-Responsive Nanomaterials for Biomedical Applications

In recent years, there has been significant interest in the development of stimuli-responsive smart materials for a wide range of applications including drug delivery, medical imaging, sensors, and microfluidics. Smart materials are small molecules, or macromolecules that have molecular functionalities that in response to an external stimulus or stimuli will change one or more of its properties. Polymers and block copolymers responsive to stimuli including light,[11] mechanical force,[12] changes in pH,[13] redox potential,[14] magnetic field,[15] and CO_2 concentration[16] have been synthesized and studied. A number of photosensitive units have been studied and employed in various systems. Our group most often employs *o*-nitrobenzyl esters[17, 18, 19, 20, 21, 22] in our UV-responsive systems, however other groups have used pyrenylmethyl esters,[23] *p*-methoxyphenacyl esters,[24] and coumarin derivatives[25] as shown in Scheme 1.4.

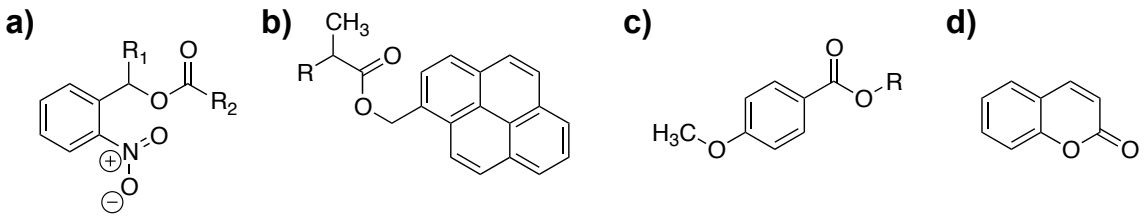

Figure 1.4. Photolabile groups. a) *o*-nitrobenzyl ester, b) pyrenyl methyl ester, c) p-methoxyphenacyl ester, d) coumarin.

The *o*-nitrobenzyl ester group is an attractive system because it is modular and easily synthesized and for these reasons it has been widely used as a photodegradable unit in materials science.[26] This photolabile group decays by way of a radical rearrangement which passes through a nitronic acid intermediate before cleavage into nitroso and carboxylic acid by-products (Scheme 1.5).

Scheme 1.2. Photolabile *o*-nitrobenzyl ester radical mechanism.

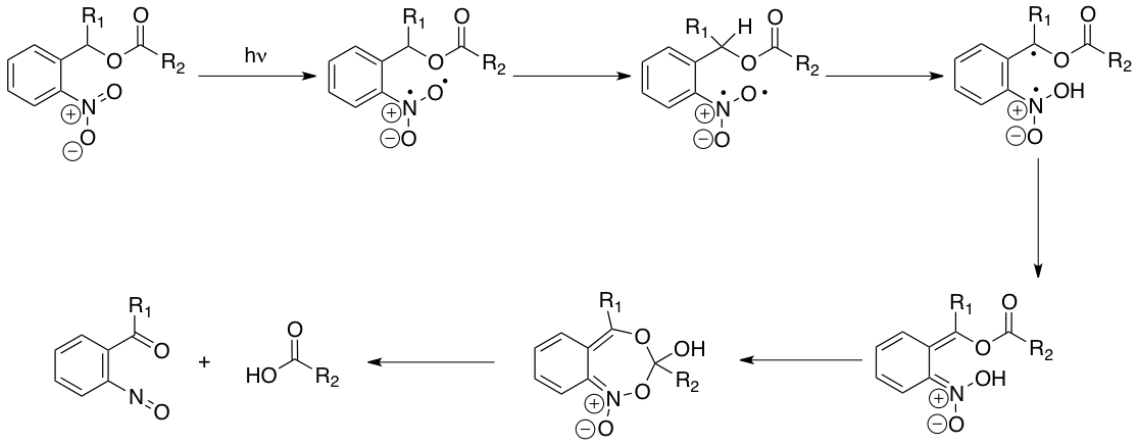

1.3 Dendrons and Dendrimers

Different from linear polymers, and receiving an increasing amount of attention are polymers known as dendrons or dendrimers.[10, 27, 28, 29] These are highly branched, 3-dimensional architectures, grown generation-by-generation. They consist of three regions: the core or focal point, the repeating backbone branches (made up by the monomeric units) and the peripheral functional groups. Dendrimers differ from

hyperbranched polymers, which are synthesized from monomers in a single step, resulting in random branching and polydispersity.

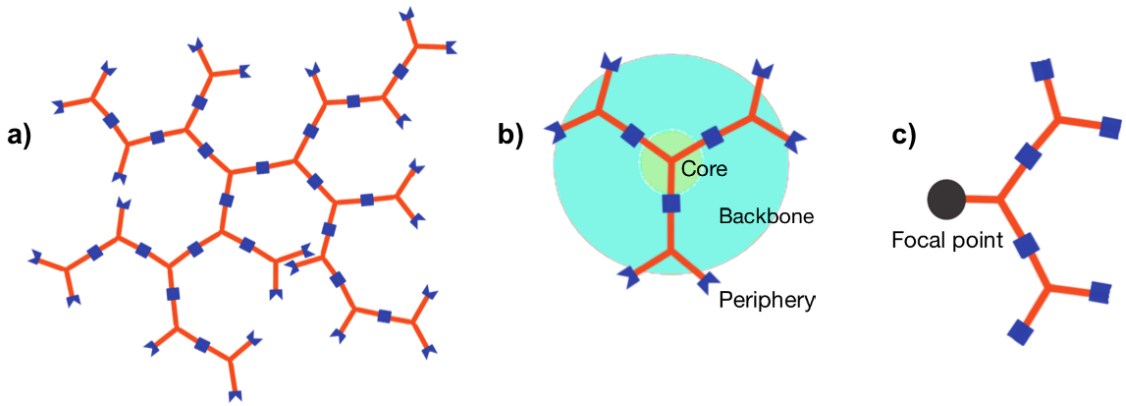

Figure 1.5. a) hyperbranched polymer, b) dendrimer, c) dendron.

Because dendrons and dendrimers are synthesized step-wise, they have very low dispersities and thus well-defined molecular weights. However the synthesis of "perfect" dendrimers is very challenging especially at higher generations. A well-known and successful method of polyester dendrimer growth uses the 2,2-bis(hydroxymethyl) propionic acid (bis-MPA) monomer in either its acid or anhydride forms.[30] The former requires the use of a coupling agent, either *N*,*N*'-dicyclohexylcarbodiimide (DCC) or *N*-(3-dimethylaminopropyl)-*N*'-ethylcarbodiimide (EDC), during reaction with a free dendritic alcohol while the latter requires no coupling agent except in the synthesis of the anhydride itself. This method of growth is effective in that its only limitation is that growth beyond the fourth generation becomes increasingly difficult. Complete reactivity beyond this generation is very challenging. Growth of these molecules can occur divergently, adding monomeric units generationally to a molecular focal point or they can also be grown convergently, combining preformed dendrons to a reactive monomer.

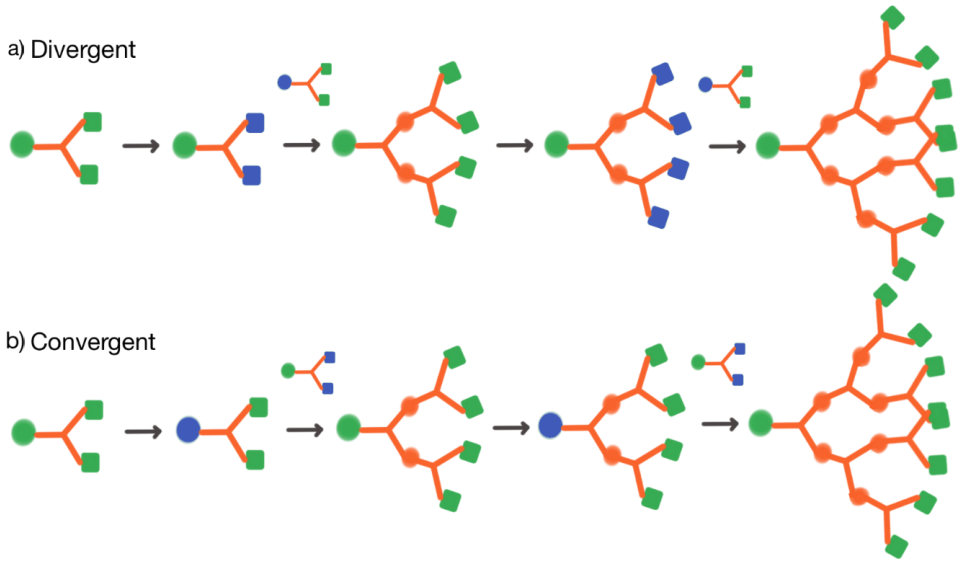

Figure 1.6. a) Divergent growth of generation three dendron, b) convergent growth of generation three dendron, where green represents a protected functional group and blue represents an activated group.

1.3.1 Amphiphilic Janus Dendrimers and Their Self-Assembly

Two dendrons can be linked by a common focal point. When these two dendrons are chemically distinct, the resulting molecule is termed a Janus dendrimer, so named after the two-faced Roman god of new beginnings, Janus. Often the two distinct segments are divergently synthesized and then convergently coupled. Moreover, when Janus-dendrimers are made with two segments of opposite solvophilicity (affinity for a particular solvent), they can be amphiphilic and therefore have the capacity for self-assembly into various aggregate morphologies, much like block copolymers as shown in Figure 1.7.

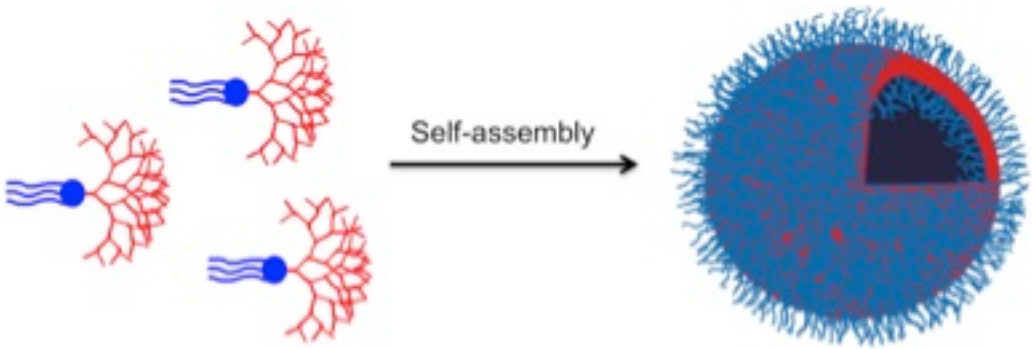

Figure 1.7. Self-assembly of vesicles with amphiphilic Janus dendrimers.

It has been shown, through the preparation and study of a library of amphiphilic Janus dendrimers, that a vast array of morphologies can be formed in water. Percec *et al*. have observed the assembly of vesicles (dendrimersomes), cubosomes, disks, tubular vesicles and helical ribbons.[31] The same group has also shown the assembly of so-called "onion-like dendrimersomes" using a nano-precipitation procedure, thereby mimicking multi-bilayer biological systems. The size and number of bilayers is tunable based on the concentration of the Janus dendrimer species.[32]

Dendrimer assemblies, like polymer ones, have been shown to be able to encapsulate both hydrophobic and hydrophilic cargo molecules and then release them in response to a stimulus.[33] Furthermore, based on their monodisperse nature, high loading capacities, large-scale production and bioconjugation capabilities, dendritic structures have been recognized to be ideal building blocks for biomedical applications.[34] Nazemi and Gillies showed the synthesis of photoresponsive dendrons with an *o*-nitrobenzyl ester-bis-MPA monomer derivative backbone. Synthesis and complete photodegradation of the G1, G2 and G3 dendrons was shown.[35] Using a similar system, they were able to synthesize a Janus dendrimer using the photodegradable dendrons and a tris-tri(ethylene glycol) functionalized gallic acid. The G3 Janus dendrimer self-assembled into dendrimersomes, using a number of nano-precipitation protocols, and these assemblies were shown to be able to encapsulate and release both hydrophilic and hydrophobic payloads when stimulated by a UV-trigger.[33]

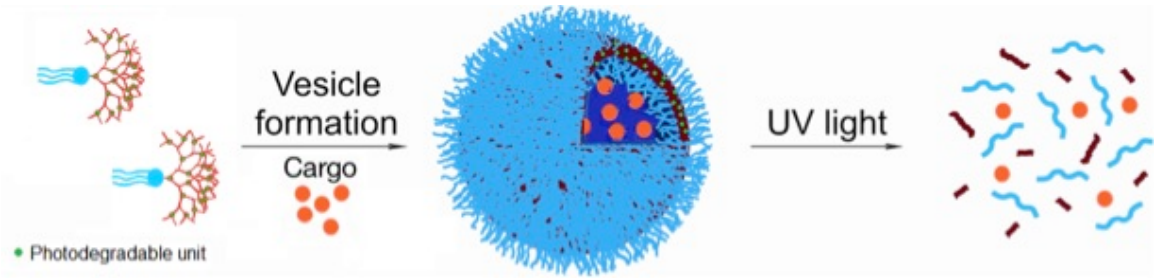

Figure 1.8. Dendrimersomes made from photodegradable Janus dendrimers showing encapsulation and UV-triggered release of cargo molecules.

1.3.2 Surface Functionalization and Dendrimersomes

Dendrimersomes combine the stability and mechanical strength seen in polymersomes with the biological function of stabilized phospholipid vesicles (liposomes), as well as unparalleled uniformity of size, formulation and chemical functionality.[31] These characteristics are a function of the composition of the dendrimer backbone. However the functional groups at the periphery are also critical as they appear at the surface of the assembly and are the first contact with biological targets. Having reactive groups on the surface of the assemblies allows for functionalization and therefore the capacity to impart biological function. Functionalizing the periphery of dendrimers has been a widely studied method for conveying biological functions such as receptor targeting, imaging and drug delivery.[36, 37, 38] Unlike with polymersomes, very little research has been done to study the functionalization of the surface of dendrimersomes and other dendrimer assemblies. Studies have shown the synthesis of glycodendrimers and assembly into structures referred to as "glycodendrimersomes", "glycomicelles" and "glycocubosomes". These were formulated from Janus dendrimers whose peripheries were functionalized with carbohydrates before the self-assembly process. Prior work in the Gillies group has demonstrated that dendron functionalized polymer assemblies could orient reactive groups on the assembly surface for post-assembly functionalization (Figure 1.10). This allowed for a wide array of ligands to be introduced to the dendrimersome surface.[10, 39, 40, 41, 42, 43]

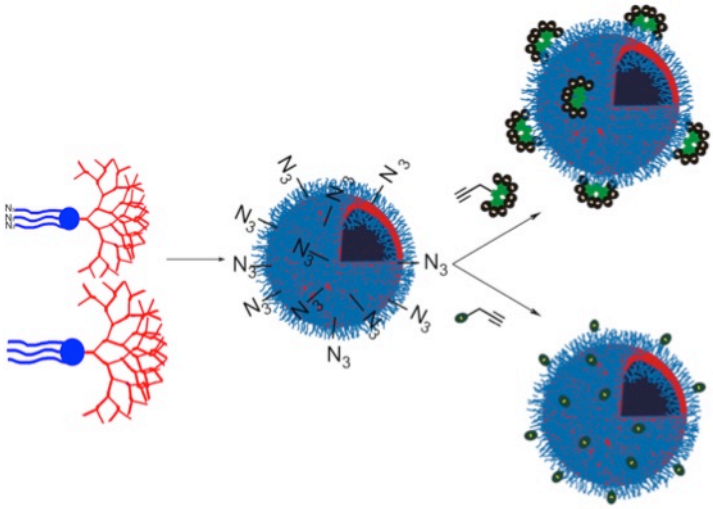

Figure 1.9. Self-assembly and surface functionalization of dendrimersomes.

1.4 Click Chemistry

Click chemistry offers an arsenal of powerful, selective and modular reactions that work reliably in both small- and large-scale applications.[44] This type of chemistry has developed into highly efficient methods for not only synthesis but also polymerization and conjugation. There are six conditions these reactions must realize. They must: 1) be modular, 2) be wide in scope, 3) be very high yielding, 4) generate only inoffensive by-products removable by non-chromatographic methods 5) be stereospecific, and 6) give a product stable under physiological conditions. In terms of the process, these reactions must: 1) include simple reaction conditions (be insensitive to water and oxygen), 2) have readily available starting materials and reagents, and 3) use no solvent, a benign solvent or an easily removed solvent

The most common types of transformations that satisfy these postulates include: 1,3-dipolar cycloadditions, Diels-Alder transformations, ring opening reactions of strained heterocyclic electrophiles, carbonyl chemistry of the "non-aldol" type and additions to carbon-carbon multiple bonds.[44] More specifically, these reactions include the catalyzed and non-catalyzed azide-alkyne coupling,[45] Diels-Alder,[46] thiol-ene,[47, 48] -yne,[48, 49] -

isocyanate[50] and –halo[51] reactions. This thesis will focus on the copper-catalyzed azide-alkyne 1,3-dipolar cycloaddition (CuAAC).

1.4.1 Copper-Catalyzed Azide-Alkyne Cycloaddition (CuAAC)

Over the last decade, the copper(I)-mediated click reaction between azide and alkyne functional groups to form a triazole ring has not only become popular for small molecule synthesis and material functionalization, but has gained much interest for the synthesis of polymers via click polymerization of azide and alkyne monomers. It is highly regarded because of its mild reaction conditions and benign by-products, regioselectivity, high reaction rate, functional group tolerance, and atom economy. In comparison with other polymerization and polymer conjugation techniques, it is one of the most effective in terms of the synthesis of functional polytriazoles with high molecular weight.[52, 53]

Scheme 1.3. Copper(I) catalyzed azide-alkyne click reaction, (Ln= ligand).

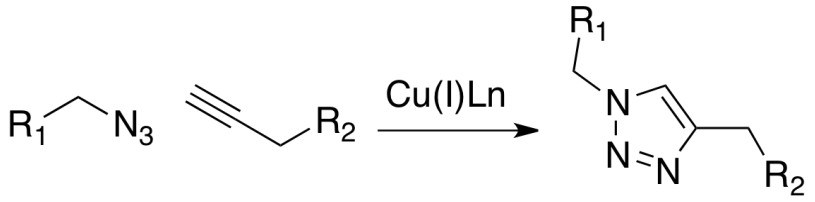

Huisgen was the first to propose the non-catalyzed cycloaddition of azides and alkynes to form triazoles, but it required high temperatures and usually gave variable yields.[52, 53] The reaction proceeded by way of a 1,3-dipolar cycloaddition. Sharpless[54] and Meldal[55] however, independently came to the conclusion that addition of copper(I) affords the same triazole product even at room temperature and in consistently high yields. The original mechanism had been disputed for many years, however in 2013 Worrell *et al*. disproved the original mechanism showing the step-wise nature of the carbon-nitrogen bond-forming events and the equivalence of the two copper atoms within the cycloaddition steps.[56]

Scheme 1.4. Proposed mechanism of the Cu(I)-catalyzed azide-alkyne click reaction.[56]

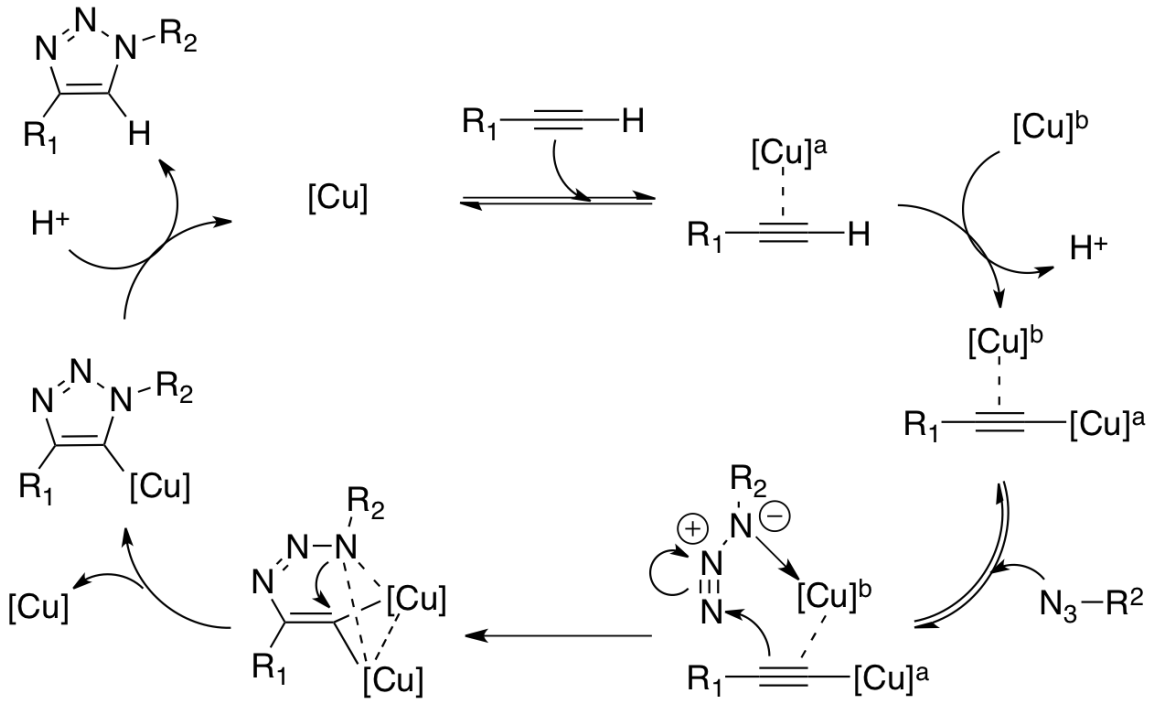

1.5 Thesis Objectives

The main goals of this thesis are to present: the synthesis of novel photoresponsive block copolymers and novel amphiphilic Janus dendrimers, the self-assembly of these polymeric systems into polymersome and dendrimersome structures, respectively, the degradation of the stimuli-responsive polymersomes, and the surface functionalization of the dendrimersomes. This thesis will also describe the relevance of these systems as platforms for biomedical applications, specifically drug delivery.

Chapter 2 describes the first case, to date, of polymersomes assembled from a triblock copolymer with a completely photodegradable hydrophobic block copolymer. This chapter presents this system as a potential stimuli-responsive nanomaterial for drug delivery. The CuAAC click polymerization of the homopolymer with photosensitive *o*-nitrobenzyl ester moieties along its entire length and coupling of the hydrophilic blocks

to form the triblock copolymer is described. The degradation of the copolymer is shown along with the self-assembly and degradation of polymersomes.

Chapter 3 presents the synthesis of various novel amphiphilic Janus dendrimers and their self-assembly. This chapter highlights this type of system as a nanomaterial with potential for targeted drug delivery applications. It shows the formation of various dendrimer assemblies including solid aggregates and dendrimersomes. The synthesis and self-assembly of an azide-terminated analogue to one of the dendrimers is presented and the surface functionalization of the resulting assemblies with 2 kg/mol poly(ethylene oxide) (PEO)-alkyne is shown.

Chapter 4 will summarize the pertinent conclusions drawn from the results and will discuss the future goals and direction of the continuing projects.

1.6 References

1. Hosler, D.; Burkett, S. L.; Tarkanian, M. J., *Science* **1999,** *284* (5422), 1988-1991.
2. Jensen, W. B., *J. Chem. Educ.* **2006,** *83* (6), 838-839.
3. Mastroianni, S. E.; Epps, T. H., *Langmuir* **2013,** *29* (12), 3864-3878.
4. Kamaly, N.; Xiao, Z.; Valencia, P. M.; Radovic-Moreno, A. F.; Farokhzad, O. C., *Chem. Soc. Rev.* **2012,** *41* (7), 2971-3010.
5. Liu, S.; Maheshwari, R.; Kiick, K. L., *Macromolecules* **2009,** *42* (1), 3-13.
6. Rosler, A.; Vandermeulen, G. W. M.; Klok, H.-A., *Adv Drug Deliv Rev* **2012**.
7. Ahmed, F.; Photos, P. J.; Discher, D. E., *Drug Dev. Res.* **2006,** *67* (1), 4-14.
8. Discher, D. E.; Eisenberg, A., *Science* **2002,** *297* (5583), 967-973.
9. Moghimi, S. M.; Porter, C. J. H.; Muir, I. S.; Illum, L.; Davis, S. S., *Biochem. Biophys. Res. Commun.* **1991,** *177* (2), 861-866.
10. Nazemi, A.; Gillies, E. R., *Braz. J. Pharm. Sci.* **2013,** *49* (Spec. Issue), 15-32.
11. Gohy, J.-F.; Zhao, Y., *Chem. Soc. Rev.* **2013,** *42* (17), 7117-7129.
12. Wiggins, K. M.; Brantley, J. N.; Bielawski, C. W., *Chem. Soc. Rev.* **2013,** *42* (17), 7130-7147.
13. Kharkar, P. M.; Kiick, K. L.; Kloxin, A. M., *Chem. Soc. Rev.* **2013,** *42* (17), 7335-7372.
14. Huo, M.; Yuan, J.; Tao, L.; Wei, Y., *Polym. Chem.* **2014,** *5* (5), 1519-1528.
15. Thevenot, J.; Oliveira, H.; Sandre, O.; Lecommandoux, S., *Chem. Soc. Rev.* **2013,** *42* (17), 7099-7116.
16. Schattling, P.; Jochum, F. D.; Theato, P., *Polym. Chem.* **2014,** *5* (1), 25-36.
17. Dispinar, T.; Colard, C. A. L.; Du Prez, F. E., *Polym. Chem.* **2013,** *4* (3), 763-772.
18. Fomina, N.; McFearin, C.; Sermsakdi, M.; Edigin, O.; Almutairi, A., *J. Am. Chem. Soc.* **2010,** *132* (28), 9540-9542.
19. Gu, W.; Zhao, H.; Wei, Q.; Coughlin, E. B.; Theato, P.; Russell, T. P., *Adv. Mater.* **2013,** *25* (34), 4690-4695.
20. Kloxin, A. M.; Kasko, A. M.; Salinas, C. N.; Anseth, K. S., *Science* **2009,** *324* (5923), 59-63.

21. Liu, J.; Burts, A. O.; Li, Y.; Zhukhovitskiy, A. V.; Ottaviani, M. F.; Turro, N. J.; Johnson, J. A., *J. Am. Chem. Soc.* **2012,** *134* (39), 16337-16344.

22. Yan, B.; Boyer, J.-C.; Branda, N. R.; Zhao, Y., *J. Am. Chem. Soc.* **2011,** *133* (49), 19714-19717.

23. Jiang, J.; Tong, X.; Zhao, Y., *J. Am. Chem. Soc.* **2005,** *127* (23), 8290-8291.

24. Bertrand, O.; Gohy, J.-F.; Fustin, C.-A., *Polym. Chem.* **2011,** *2* (10), 2284-2292.

25. Dong, J.; Xun, Z.; Zeng, Y.; Yu, T.; Han, Y.; Chen, J.; Li, Y.-Y.; Yang, G.; Li, Y., *Chem. - Eur. J.* **2013,** *19* (24), 7931-7936.

26. Zhao, H.; Sterner, E. S.; Coughlin, E. B.; Theato, P., *Macromolecules* **2012,** *45* (4), 1723-1736.

27. Carlmark, A.; Malmstroem, E.; Malkoch, M., *Chem. Soc. Rev.* **2013,** *42* (13), 5858-5879.

28. Astruc, D.; Wang, D.; Deraedt, C.; Liang, L.; Ciganda, R.; Ruiz, J., *Synthesis* **2015,** *47* (14), 2017-2031.

29. Liu, Y.; Tee, J. K.; Chiu, G. N. C., *Curr. Pharm. Des.* **2015,** *21* (19), 2629-2642.

30. Gillies, E. R.; Frechet, J. M. J., *J. Am. Chem. Soc.* **2002,** *124* (47), 14137-14146.

31. Percec, V.; Wilson, D. A.; Leowanawat, P.; Wilson, C. J.; Hughes, A. D.; Kaucher, M. S.; Hammer, D. A.; Levine, D. H.; Kim, A. J.; Bates, F. S.; Davis, K. P.; Lodge, T. P.; Klein, M. L.; De Vane, R. H.; Aqad, E.; Rosen, B. M.; Argintaru, A. O.; Sienkowska, M. J.; Rissanen, K.; Nummelin, S.; Ropponen, J., *Science* **2010,** *328* (5981), 1009-1014.

32. Zhang, S.; Sun, H.-J.; Hughes, A. D.; Moussodia, R.-O.; Bertin, A.; Chen, Y.; Pochan, D. J.; Heiney, P. A.; Klein, M. L.; Percec, V., *Proc. Natl. Acad. Sci. U. S. A.* **2014,** *111* (25), 9058-9063.

33. Nazemi, A.; Gillies, E. R., *Chem. Commun.* **2014,** *50* (76), 11122-11125.

34. Gillies, E. R.; Frechet, J. M. J., *Drug Discovery Today* **2005,** *10* (1), 35-43.

35. Nazemi, A.; Schon, T. B.; Gillies, E. R., *Org. Lett.* **2013,** *15* (8), 1830-1833.

36. Zhu, J.; Shi, X., *J. Mater. Chem. B* **2013,** *1* (34), 4199-4211.

37. Majoros, I. J.; Myc, A.; Thomas, T.; Mehta, C. B.; Baker, J. R., Jr., *Biomacromolecules* **2006,** *7* (2), 572-579.

38. Zheng, Y.; Fu, F.; Zhang, M.; Shen, M.; Zhu, M.; Shi, X., *Med. Chem. Comm.* **2014,** *5* (7), 879-885.

39. Amos, R. C.; Nazemi, A.; Bonduelle, C. V.; Gillies, E. R., *Soft Matter* **2012,** *8* (21), 5947-5958.

40. Gillies, E. R.; Li, B.; Martin, A. L., *J. Am. Chem. Soc.* **2008,** *98*, 311-312.

41. Martin, A. L.; Li, B.; Gillies, E. R., *J. Am. Chem. Soc.* **2009,** *131* (2), 734-741.

42. Nazemi, A.; Amos, R. C.; Bonduelle, C. V.; Gillies, E. R., *J. Polym. Sci., Part A: Polym. Chem.* **2011,** *49* (12), 2546-2559.

43. Nazemi, A.; Haeryfar, S. M. M.; Gillies, E. R., *Langmuir* **2013,** *29* (21), 6420-6428.

44. Kolb, H. C.; Finn, M. G.; Sharpless, K. B., *Angew. Chem., Int. Ed.* **2001,** *40* (11), 2004-2021.

45. Dervaux, B.; Du Prez, F. E., *Chem. Sci.* **2012,** *3* (4), 959-966.

46. Tasdelen, M. A., *Polym. Chem.* **2011,** *2* (10), 2133-2145.

47. Lowe, A. B., *Polym. Chem.* **2010,** *1* (1), 17-36.

48. Chan, J. W.; Yu, B.; Hoyle, C. E.; Lowe, A. B., *Polymer* **2009,** *50* (14), 3158-3168.

49. Lowe, A. B.; Hoyle, C. E.; Bowman, C. N., *J. Mater. Chem.* **2010,** *20* (23), 4745-4750.

50. Li, H.; Yu, B.; Matsushima, H.; Hoyle, C. E.; Lowe, A. B., *Macromolecules* **2009,** *42* (17), 6537-6542.

51. Xu, J.; Tao, L.; Boyer, C.; Lowe, A. B.; Davis, T. P., *Macromolecules* **2010,** *43* (1), 20-24.

52. Huisgen, R., *Pure Appl. Chem.* **1989,** *61* (4), 613-628.

53. Huisgen, R.; Szeimies, G.; Moebius, L., *Chem. Ber.* **1967,** *100* (8), 2494-2507.

54. Rostovtsev, V. V.; Green, L. G.; Fokin, V. V.; Sharpless, K. B., *Angew. Chem., Int. Ed.* **2002,** *41* (14), 2596-2599.

55. Tornoe, C. W.; Christensen, C.; Meldal, M., *J. Org. Chem.* **2002,** *67* (9), 3057-3064.

56. Worrell, B. T.; Malik, J. A.; Fokin, V. V., *Science* **2013,** *340* (6131), 457-460.

Chapter 2

2 Photodegradable Polymer Vesicles

2.1 Introduction

In recent years, there has been significant interest in the development of stimuli-responsive materials for a wide range of applications including drug delivery, medical imaging, sensors, and microfluidics. Polymers and block copolymers responsive to stimuli including light,[1] mechanical force,[2] and changes in pH,[3] redox potential,[4] magnetic field,[5] and CO_2 concentration[6] have been synthesized and studied. Among these stimuli, light is particularly attractive because it can be applied with high spatial and temporal resolution and benefits from reasonable control over its wavelength and intensity.[7] While the use of UV light for biomedical applications is limited by the absorption of tissues and DNA damage, recent work has demonstrated that it is possible to use upconverting nanoparticles in conjugation with UV-visible chromophores to obtain photoinduced changes with near-infrared light.[8]

In photoresponsive materials, changes such as cross-linking,[9, 10] *cis-trans* isomerization[11, 12] and bond cleavage,[13, 14, 15] have all been successfully induced by light. In the context of photocleavable materials, various functional groups have been employed, including *o*-nitrobenzyl esters,[8, 16, 17, 18, 19, 20] pyrenylmethyl esters,[21] *p*-methoxyphenacyl esters,[22] and coumarin derivatives.[23] Due to its ease of synthesis and derivatization, the *o*-nitrobenzyl ester group has been widely used as a photodegradable unit in materials science.[24]

Photoinduced changes are of particular interest in the context of amphiphilic block copolymers that assemble in aqueous solution to form spherical micelles, worm-like micelles, vesicles, and other nanoparticles for drug delivery applications.[25, 26, 27] Such assemblies can enhance the properties of drug molecules by increasing their aqueous solubility, increasing their circulation time in vivo, and improving their targeting to the disease site. The integration of a photoresponsive moiety into these materials offers a

possibility to trigger the release of their cargo at a specific time and location in vivo. In photodegradable polymer assemblies, a common approach has involved the placement of the *o*-nitrobenzyl ester group at the junction of copolymer blocks,[13, 18, 28, 29, 30, 31, 32, 33, 34, 35, 36] with their subsequent self-assembly into various morphologies including micelles and vesicles.[13, 28, 29, 31, 33, 35] Upon irradiation with light, these nanostructures decompose into their individual hydrophobic and hydrophilic polymer blocks. In most cases, this has resulted in either rearrangement of the initial morphologies to a secondary structure or the precipitation of the hydrophobic segments in aqueous media.[13, 31] A potential drawback of this approach is that encapsulated hydrophobic molecules may remain in the aggregated hydrophobic core. To address this limitation, an alternative approach is to place photodegradable units along the entire length of the hydrophobic block such that when irradiated, complete decomposition of the hydrophobic block occurs. This strategy has been used to prepare micelles that degrade in response to light.[14, 15, 37] Apart from a recent example employing self-immolative polymers with a photolabile end-cap,[38] which assemble into polymer vesicles, this approach has not been extended to other types of polymer assemblies to the best of our knowledge. We describe here the synthesis of two amphiphilic triblock copolymers composed of 750 g/mol or 2 kg/mol poly(ethylene glycol) (PEG) and a high molecular weight photodegradable hydrophobic block containing *o*-nitrobenzyl esters. The self-assembly of these triblock copolymers using nano-precipitation is investigated, and it is demonstrated that under optimized conditions, vesicles can be obtained. The photodegradation of these vesicles is studied by spectroscopy, light scattering, and electron microscopy (Figure 2.1).

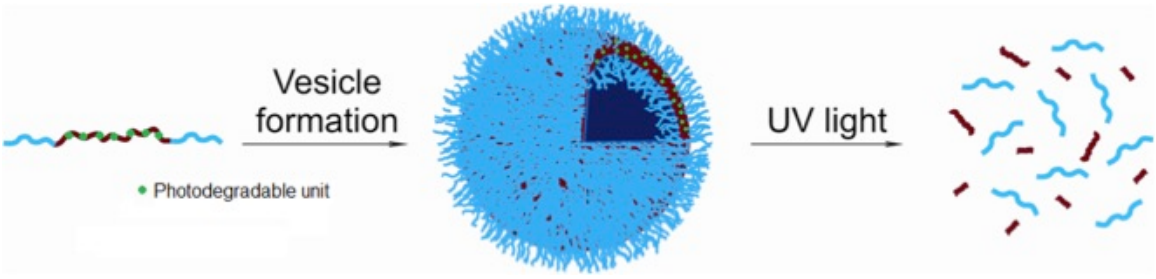

Figure 2.1. Self-assembly of vesicles using a triblock copolymer with photodegradable units along the entire hydrophobic block.

2.2 Results and Discussion

2.2.1 Synthesis

Copper-catalyzed azide-alkyne cycloaddition chemistry (CuAAC) was selected for the synthesis of the photodegradable hydrophobic block as it is an efficient step-growth polymerization method that allows for the incorporation of the photodegradable *o*-nitrobenzyl esters within the polymer backbone.[15, 39, 40] An approach involving the polymerization of A2 and B2 monomers was employed because a small excess of one monomer could be used to prevent polymer cyclization and to allow for the subsequent coupling of the hydrophilic PEG blocks to both polymer termini. As shown in Scheme 2.1, the nitro-functionalized diol **2.1** was reacted with azidoacetic acid **2.2**, in the presence of EDC·HCl, DMAP and pyridine to provide the target diazide monomer **2.3**. Reaction of **2.1** with pentynoic acid **2.4** under the same conditions provided the dialkyne monomer **2.5**.

Scheme 2.1. Synthesis of monomers 2.3 and 2.5.

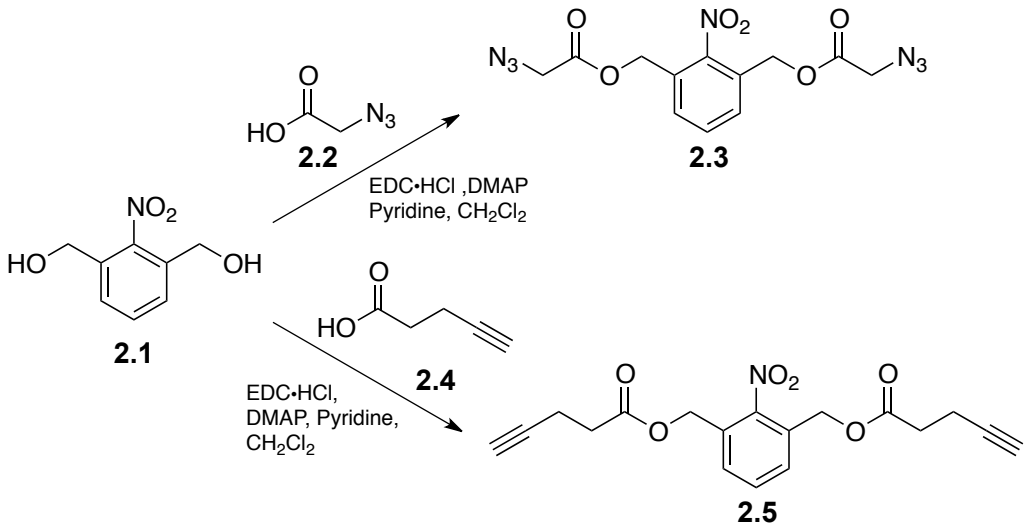

As shown in Scheme 2.2, the hydrophobic block **2.6** was prepared from monomers **2.3** and **2.5** using CuAAC with $Cu(PPh_3)_3Br$ in DMF. This solvent was selected for solubility reasons. Initial polymerization attempts in THF provided poor results as the product polymer is insoluble in THF. A small excess of monomer **2.3** (1.05 equiv. relative to

monomer **2.5**) was used during the initial polymerization, followed by the addition of a large excess of **2.3** at the end of the polymerization to ensure that both ends of the polymer were capped with azide functionalities. Based on integration of the peak at 4.17 ppm corresponding to the methylene groups adjacent to the terminal azides, relative to those of peaks corresponding to the repeat units throughout the polymer backbone, the degree of polymerization of **2.6** was ~55. Based on the repeat unit molar mass of 692 g/mol, this corresponds to an M_n of ~38 kg/mol. A peak at 2110 cm^{-1} in the IR spectrum confirmed the presence of azide groups on the polymer. SEC in DMF suggested an M_n of 24 kg/mol and a dispersity index (*Đ*) of 1.65 relative to polystyrene standards. The differences in these M_ns may arise from the differing hydrodynamic volumes of **6** and the polystyrene calibration standards. In addition, although the polymerization was run very concentrated and in the presence of excess of monomer **2.3**, which should disfavour intramolecular cyclization, the presence of cyclic polymer products cannot be fully excluded. Based on either SEC or NMR measurements, polymer **2.6** has a significantly higher molar mass than the photodegradable hydrophobic blocks synthesized by Zhao and coworkers where M_ns of 14 kg/mol and 4,150 g/mol were obtained using hydroxyl-isocyanate couplings and CuAAC respectively.[14, 15]

Scheme 2.2. Synthesis of the hydrophobic polymer block 2.6.

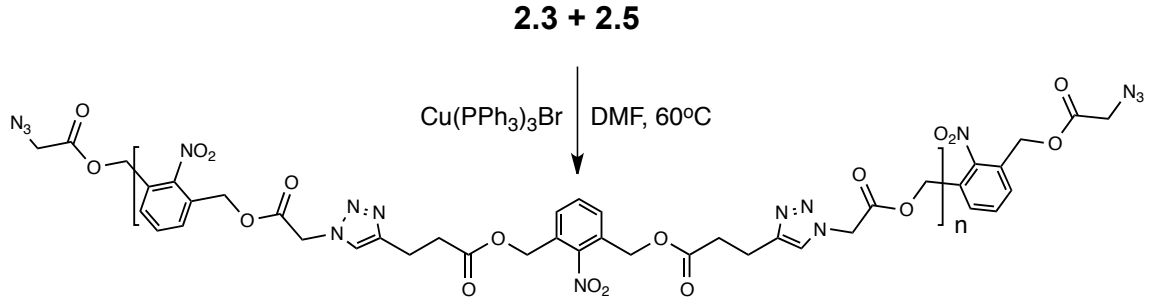

2.6

The next step in the synthesis was to connect the hydrophilic blocks to the hydrophobic main chain (Scheme 2.3). In the work of Zhao and coworkers the coupling of two PEG chains of 2 kg/mol to both termini of a 14 kg/mol hydrophobic photodegradable block

based on *o*-nitrobenzyl esters provided a triblock copolymer with a hydrophilic mass fraction of only ~0.22 that formed micelles in aqueous solution.[14] Therefore we coupled relatively short PEG blocks to polymer **2.6** with the aim of obtaining different morphologies. As shown in Scheme 3, propargyl ether-functionalized PEG 750 g/mol (**2.7**) and 2 kg/mol (**2.8**) were coupled to **2.6** using the same CuAAC conditions described above, to provide triblock copolymers **2.9** and **2.10** respectively. These materials were purified by dialysis to remove any uncoupled PEG. Based on ^{1}H NMR spectroscopy, the degree of functionalization of the terminal alkynes with PEG was quantitative for copolymer **2.9** and ~70% for copolymer **2.10**. IR data was in agreement with these results as the peak at 2110 cm^{-1} corresponding to the azide stretch in polymer **2.6** disappeared in copolymer **2.9**, whereas a small azide peak remained for copolymer **2.10** (chapter 2 supporting info). This data suggests low hydrophilic weight fractions of ~0.04 and ~0.07 for copolymers **2.9** and **2.10** respectively. SEC confirmed the absence of uncoupled PEG in these products. The molecular weights of the polymers based on SEC did not change significantly upon conjugation of the PEG, with polymer **2.9** having an M_n of 23 kg/mol and $Đ$ of 1.76 and **2.10** having an M_n of 25 kg/mol and $Đ$ of 1.62. This was expected based on the low overall PEG content.

Scheme 2.3. Synthesis of amphiphilic triblock copolymers 2.9 and 2.10.

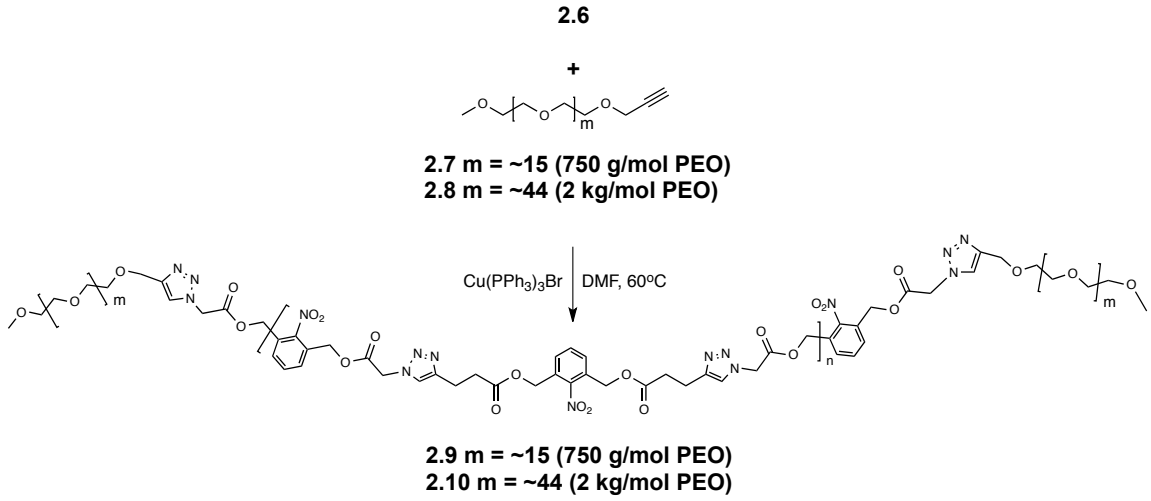

2.2.2 Self-Assembly of Triblock Copolymers 2.9 and 2.10 in Aqueous Solution

The self-assembly of copolymers **2.9** and **2.10** by nano-precipitation was investigated. The copolymers were first dissolved in dimethyl sulfoxide (DMSO) at a concentration of 8 mg/mL. This DMSO solution was then either rapidly injected into water with stirring, providing kinetic trapping of assemblies, or water was gradually added to the DMSO solution with stirring over a period of approximately 1 min. This latter approach allows a more thermodynamically-driven assembly to occur. In each case, the final volume was 0.9 mL H_2O:0.1 mL of DMSO, with a final copolymer concentration of 0.8 mg/mL. The DMSO was then removed via dialysis using a 3500 g/mol MWCO membrane.

A summary of the characterization data for the assemblies is presented in Table 2.1 and representative DLS traces and TEM images are shown in Figures 2.2 and 2.3 respectively. For copolymer **2.9** having the shorter PEG block, DMSO into water led to particles with a Z-average diameter of 110 nm and a polydispersity index (PDI) of 0.17. TEM showed the presence of sub-50 nm particles that may be micelles, but also larger solid aggregates (Figure 2.3a). The addition of water into DMSO for this same polymer led to much larger aggregates with a Z-average diameter of 400 nm and a PDI of 0.27. TEM confirmed that the assemblies were a polydisperse mixture of solid particles along with vesicles (Figure 2.3b). For copolymer **2.10**, DMSO into water provided assemblies with a Z-average hydrodynamic diameter of 90 nm and PDI of 0.25 as measured by DLS. TEM suggested that these assemblies were mainly vesicles with a relatively narrow size distribution, along with a small fraction of solid particles having similar dimensions (Figure 2.3c). The polydispersity of this sample likely arises from a small population of vesicles and particle aggregates. Water into DMSO provided larger assemblies having a Z-average hydrodynamic diameter of 230 nm and a PDI of 0.056. TEM showed that they were a mixture of vesicles and smaller solid particles (Figure 2.3d).

Table 2.1. Summary of self-assembly results for copolymers 2.9 and 2.10.

Copolymer and conditions	Hydrodynamic diameter (DLS)	Polydispersity index (DLS)	Morphology (TEM)
2.9 (DMSO into water)	110 nm	0.17	solid particles
2.9 (water into DMSO)	400 nm	0.27	mixture of vesicles and solid particles
2.10 (DMSO into water)	90 nm	0.25	mostly vesicles
2.10 (water into DMSO)	230 nm	0.056	mixture of vesicles and solid particles

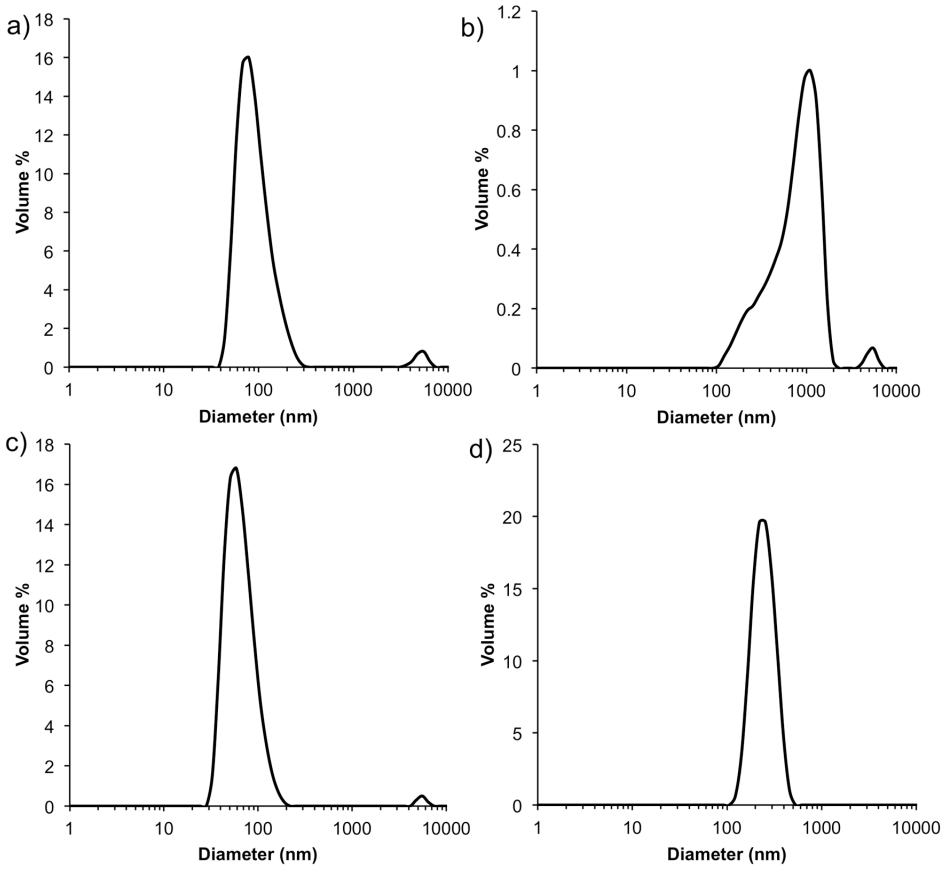

Figure 2.2. DLS traces for assemblies formed by copolymers 2.9 and 2.10 using different procedures: a) Copolymer 2.9, DMSO into water; b) Copolymer 2.9, water into DMSO; c) Copolymer 2.10, DMSO into water; d) Copolymer 2.10, water into DMSO.

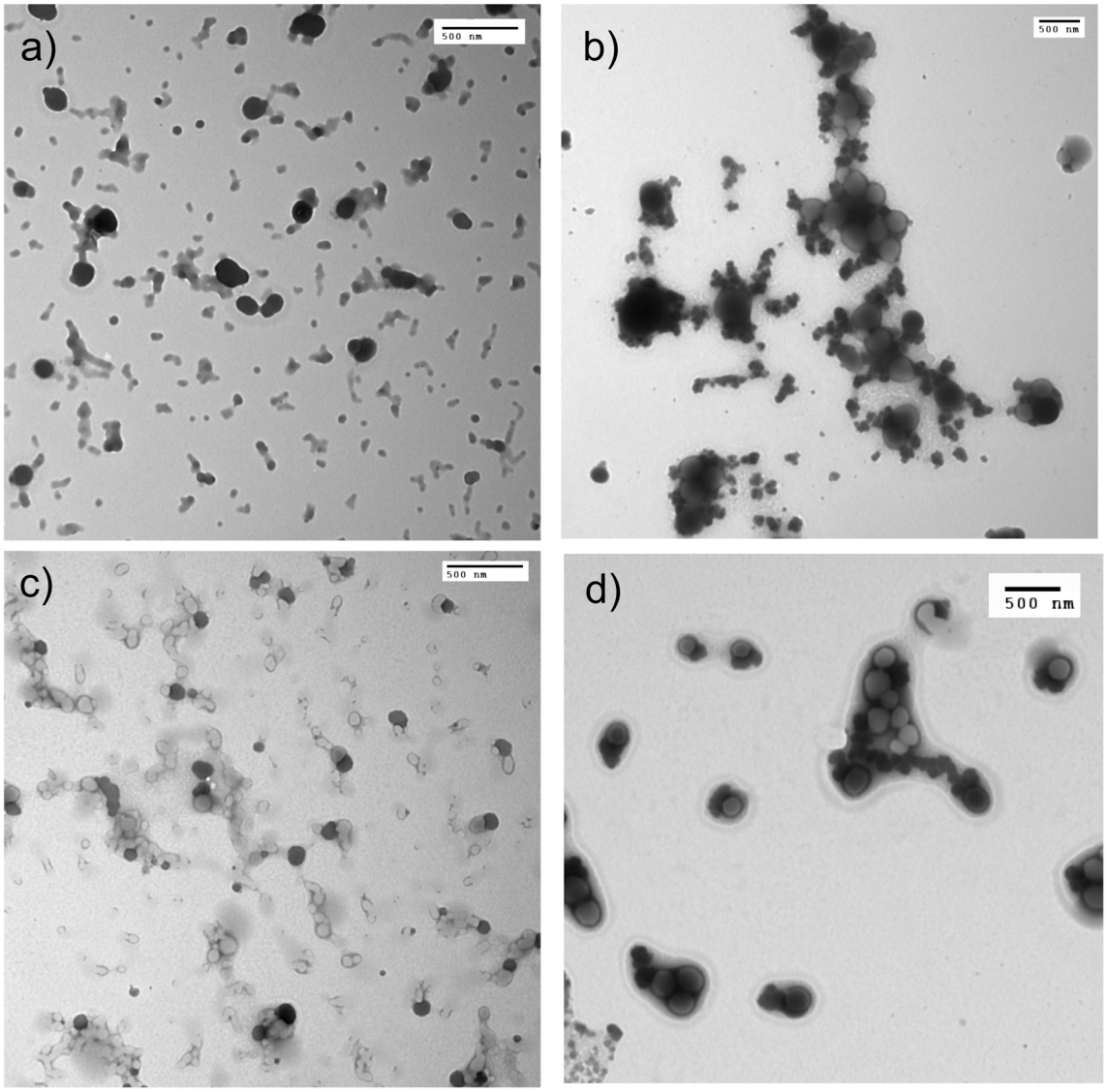

Figure 2.3. TEM images of assemblies formed by copolymers 2.9 and 2.10 using different procedures: a) Copolymer 2.9, DMSO into water; b) Copolymer 2.9, water into DMSO; c) Copolymer 2.10, DMSO into water; d) Copolymer 2.10, water into DMSO.

Overall, these results show that copolymers **2.9** and **2.10** self-assemble into spherical objects in water. As predicted by Discher and Eisenberg, triblock copolymer **2.9**, with the lowest hydrophilic weight fraction (~0.04) favours the formation of polydisperse solid particles that likely have inverted microstructures containing multiple PEG cores within

coronas of polymer **2.6** and with PEG stabilizing the surface of the particle.[41] Increasing the hydrophilic weight fraction to ~0.07 in copolymer **2.10** favours vesicle formation, along with a smaller population of solid particles. It should be noted that the hydrophilic weight fraction in copolymer **2.10** is much lower than the normal range of 0.25 to 0.45, which is expected to lead to vesicle formation.[42] This behaviour might be explained by the fact that although polymer **2.6** is considered to be hydrophobic, the many triazole moieties throughout the backbone may impart some degree of hydrophilicity to this block. However, this is likely not the only factor, as Zhao and coworkers have previously demonstrated that a similar photodegradable polymer lacking triazoles in the polymer backbone self-assembled to form micelles at a hydrophilic weight fraction of only 0.22,[14] well below the hydrophilic weight fraction of > 45%, generally required for micelle formation.[42] By using the method involving the addition of a DMSO solution of the polymer into water, smaller assemblies were generally obtained. This was expected as the rapid change in solvent can kinetically trap smaller aggregates in a non-equilibrium state. The assembly of mainly vesicle morphologies from copolymer **2.10** by this method was of particular interest because of their sub-100 nm diameters which should make them useful for applications such as drug delivery and medical imaging.[43]

2.2.3 Photodegradation Studies

The *o*-nitrobenzyl ester moiety is a known photolabile unit which degrades by way of a radical mechanism[24] when irradiated with UV light. To confirm the photodegradability of the hydrophobic block, a solution of copolymer **2.10** in DMSO-d_6 was irradiated and the degradation was monitored by ^{1}H NMR spectroscopy. As shown in Figure 2.4, peaks corresponding to the aromatic protons labeled B and C, as well as the benzylic protons labeled D and E almost completely disappeared over a period of 600 min. The peak corresponding to protons K - N on the PEG were relatively unchanged, while the peaks corresponding to protons A, E, H and I underwent small changes in chemical shift as would be expected upon their conversion into the dicarboxylic acid product.

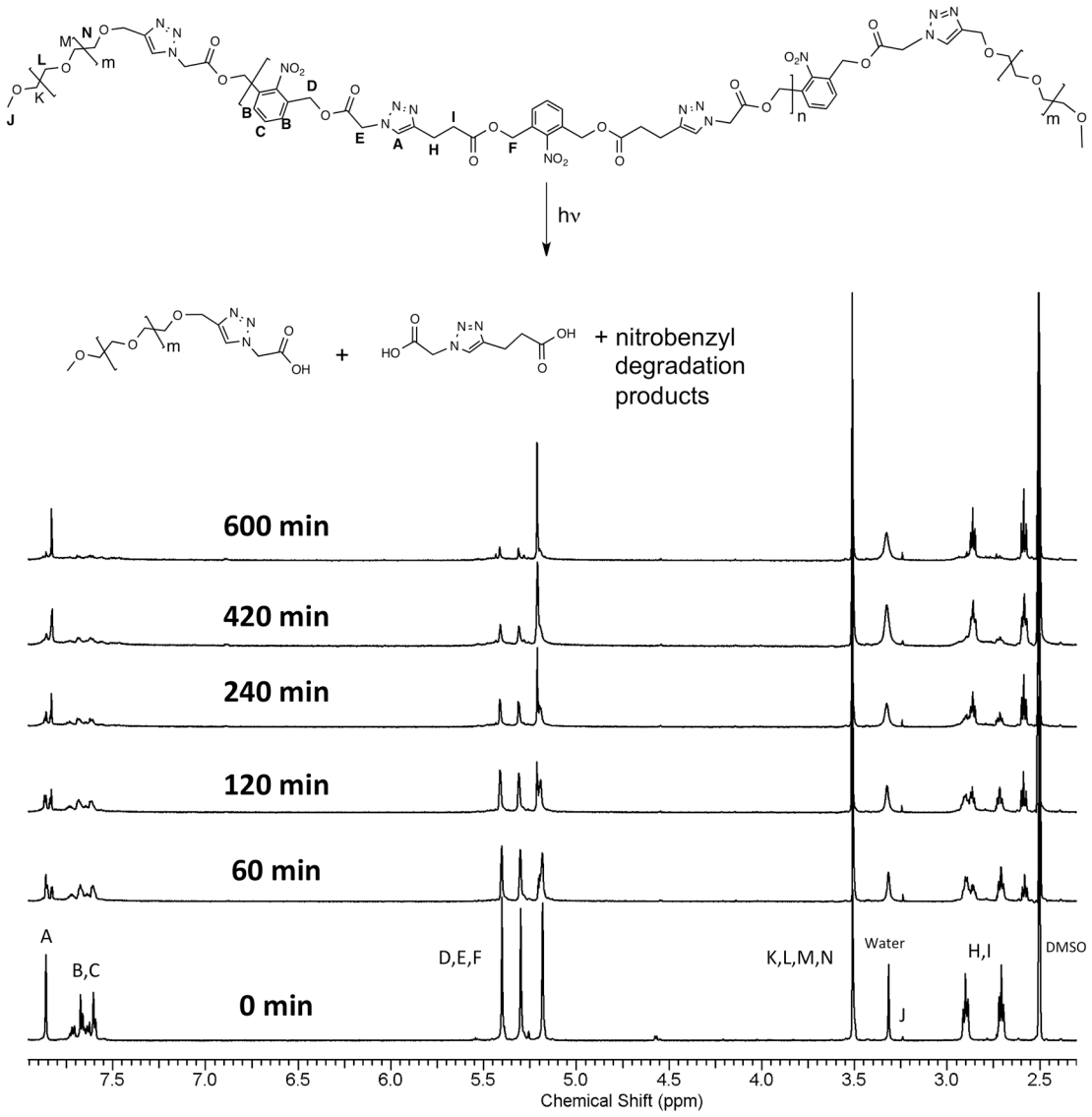

Figure 2.4. ^{1}H NMR spectra of copolymer 2.10 following different time periods of irradiation with UV light. Spectral changes are consistent with conversion into the expected products.

The photodegradation of the aqueous vesicle sample obtained through nano-precipitation of copolymer **2.10** from DMSO into water was also studied. First, the absorption spectrum of the vesicles following photoirradiation was studied. As shown in Figure 2.5, there was a progressive increase in the absorbance at 320 nm. This corresponds to the

photodegradation of the *o*-nitrobenzyl ester unit into the corresponding nitroso benzaldehyde by-products.[13, 15]

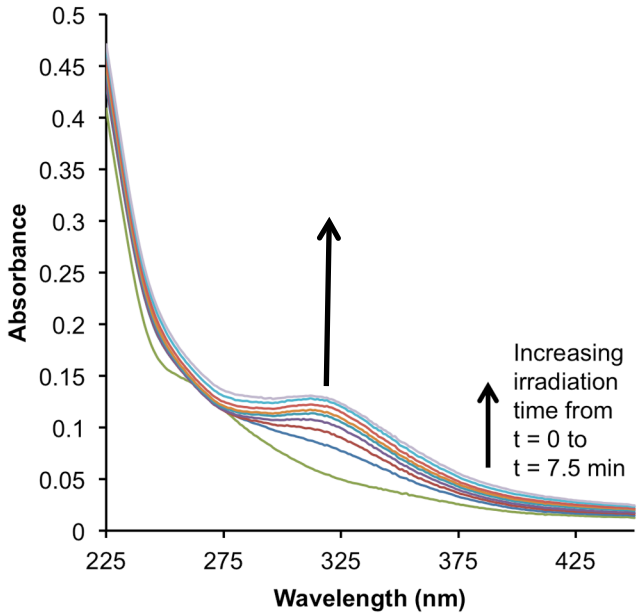

Figure 2.5. Change in absorption spectra of vesicles (0.3 mg/mL) formed from polymer 2.10 following different UV irradiation periods.

The vesicle degradation upon photoirradiation was also studied by DLS and TEM. As shown in Figure 2.6a, over a period of 500 min there was a continual decrease in the count rate measured by DLS. This suggests a decrease in the size and/or number of assemblies in solution, consistent with the expected photodegradation of the vesicles. Over the first 70 min, the diameter of the assemblies rapidly decreased to ~70% the initial size and this size did not further change throughout the experiment. We propose that upon partial cleavage of the photodegradable hydrophobic block over the first 100 min, amphiphilic PEG derivatives were generated, which reassemble from vesicles into micelles. Throughout the remainder of the experiment, as the hydrophobic block continued to degrade, the number of micelles continued decreasing, leading to decreasing count rates. Consistent with this interpretation, some solid spherical particles were still observed by TEM after 500 min. The increased time required for this photodegradation process relative to the UV-vis study described above can be attributed to the increased

concentration of the suspension as well as well as the different light source used for this experiment.

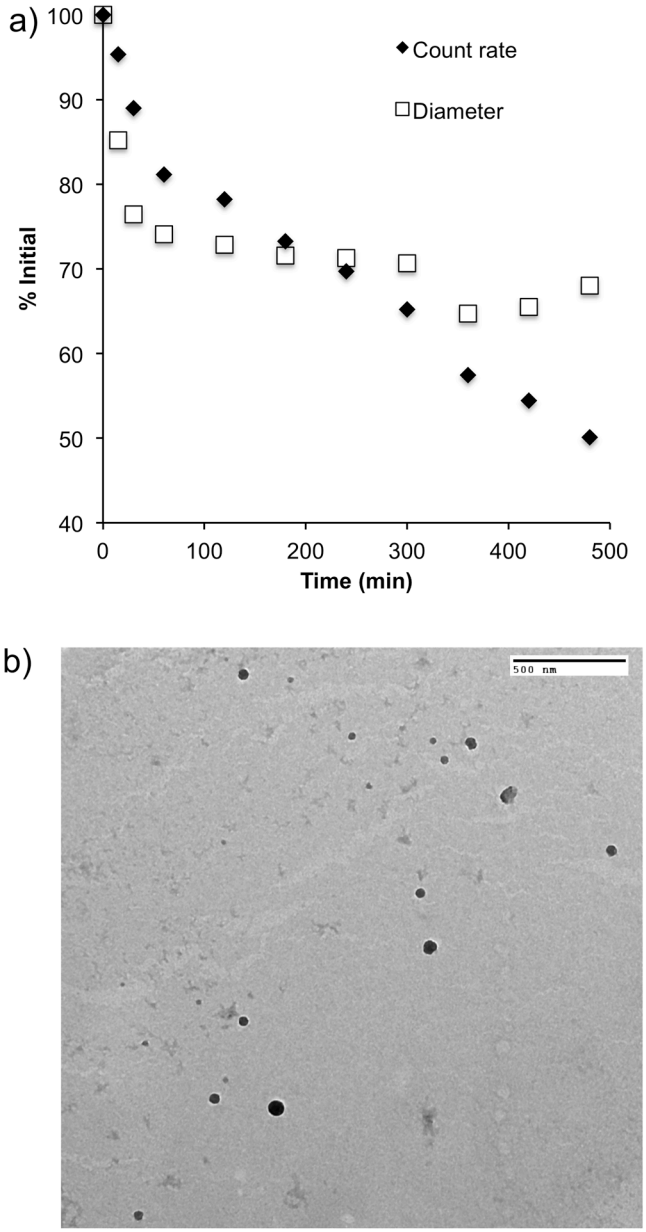

Figure 2.6. a) Photodegradation of vesicles formed from copolymer 2.10 as measured by DLS count rate and diameter; b) TEM of the assemblies following 500 min of photoirradiation (scale bar = 500 nm).

2.3 Experimental

2.3.1 General Procedure and Materials

Compounds **2.1**,[44] **2.2**,[45] **2.7**,[46] and **2.8**[46] were synthesized according to previously reported procedures. Other reagents were purchased from commercial suppliers and used without further purification unless otherwise noted. Anhydrous *N*,*N*-dimethylformamide (DMF) and tetrahydrofuran (THF) were obtained from a solvent purification system using aluminum oxide columns. CH_2Cl_2 and pyridine were distilled over calcium hydride and all dry glassware was oven-dried overnight. Thin layer chromatography (TLC) was run on Macherney-Nagel Polygram SIL G/UV_{254} plates and columns were packed using SiliaFlash P60 silica (40-60 μm, 230-400 mesh). Dialyses were performed using either 12 - 14 or 50 kg/mol molecular weight cut off (MWCO) Spectra/Por regenerated cellulose membranes (Spectrum Laboratories).^{1}H NMR and ^{13}C NMR spectra were obtained at 400 MHz and 100 MHz respectively using a Varian Inova spectrometer. NMR chemical shifts are reported in ppm and are calibrated against residual solvent signals of $CDCl_3$ (δ 7.26, 77.2 ppm) or DMSO-d_6 (δ 2.50, 39.5 ppm). Coupling constants are expressed in hertz (Hz). High-resolution mass spectrometry (HRMS) was performed on a Finnigan MAT 8400 electron impact mass spectrometer. Fourier transform infrared spectroscopy (FT-IR) was performed on a Bruker tensor 27 instrument via thin film drop cast from CH_2Cl_2 on KBr plates for compound **2.3** and **2.5** and via mixture with KBr powder and compressed into a plate for polymers **2.6**, **2.9**, and **2.10**. Size exclusion chromatography (SEC) was performed at a flow rate of 1 mL/min in DMF with 10 mM LiBr and 1% (v/v) triethylamine at 85 °C using a Waters 2695 separations module equipped with a Waters 2414 differential refractometer and two PLgel 5 μm mixed-D (300 mm x 7.5 mm) columns from Polymer Laboratories connected in series. The calibration was performed using polystyrene standards.

Synthesis of monomer 2.3

Diol **2.1**[44] (1.60 g, 8.73 mmol) and acid **2.2**[45] (2.58 g, 26.2 mmol) were dissolved in CH_2Cl_2 (30 mL). *N*-(3-dimethylaminopropyl)-*N*'-ethylcarbodiimide hydrochloride (EDC·HCl) (5.36 g, 27.9 mmol), pyridine (2.26 mL, 27.9 mmol), and 4-(dimethylamino)pyridine (DMAP) (3.41 g, 27.9 mmol) were then sequentially added to

the reaction mixture. The resulting reaction mixture was stirred in the dark for ~24 h. The reaction was monitored by TLC in a 1:1 ethyl acetate (EtOAc)/hexanes system. Upon completion of the reaction, the solution was concentrated *in vacuo*, diluted with ethyl acetate (200 mL), and then washed with $KHSO_4$ (3×50 mL), Na_2CO_3 (3×50 mL), water (3×50 mL) and brine (1×50 mL). The organic phase was then dried over $MgSO_4$, filtered and concentrated in vacuo. The crude product was purified by silica gel chromatography using a 4:1 hexanes/EtOAc as the eluent to provide monomer **2.3** (2.28 g, 74.8%). ^{1}H NMR ($CDCl_3$): δ 7.51-7.63 (m, 3 H), 5.34 (s, 4 H), 3.92 (s, 4 H). ^{13}C NMR ($CDCl_3$): δ 50.0, 63.1, 128.6, 130.7, 131.5, 148.9, 167.7. HRMS calculated $[M + H]^+$ ($C_{12}H_{12}O_6N_8$): 350.0849. Found: 350.0855. IR ν (cm^{-1}): 2920, 2100, 1750, 1540, 1180.

Synthesis of monomer 2.5

Compound **2.1**[44] (1.00 g, 5.46 mmol) and acid **2.4** (1.61 g, 16.4 mmol) were dissolved in CH_2Cl_2 (30 mL). EDC·HCl (3.35 g, 17.5 mmol), pyridine (1.41 mL, 17.5 mmol), and DMAP (2.13 g, 17.5 mmol) were then sequentially added to the reaction mixture and it was stirred for ~24 h in the dark. The reaction was monitored by TLC in a 1:1 ethyl acetate (EtOAc)/hexanes system. Upon completion of the reaction, the solution was concentrated in vacuo and then diluted in ethyl acetate (200 mL), washed with $KHSO_4$ (3×50 mL), Na_2CO_3 (3×50 mL), water (3×50 mL) and brine (1×50 mL). The organic fraction was then dried over $MgSO_4$, filtered and concentrated. The crude product was purified by silica gel chromatography using a 4:1 hexanes/EtOAc as the eluent to provide monomer **2.5** (1.41 g, 75.4 %). ^{1}H NMR ($CDCl_3$): δ 7.50 - 7.54 (m, 3 H), 5.25 (s, 4 H), 2.58-2.62 (m, 4 H), 2.49-2.52 (m, 4 H), 1.98 (t, J = 2.5, 2 H). ^{13}C NMR ($CDCl_3$): δ 14.1, 32.9, 62.2, 69.2, 82.0, 129.2, 130.0, 131.1, 148.7, 170.9. HRMS cald $[M + H]^+$ ($C_{18}H_{17}O_6N$): 344.1134. Found: 344.1132. IR ν (cm^{-1}): 3300, 2120, 1740, 1540, 1370, 1160.

Synthesis of polymer 2.6

Monomers **2.3** (0.539 g, 1.54 mmol) and **2.5** (0.500 g, 1.46 mmol) were combined in a flask with bromotris(triphenylphosphine) copper(I) (54.3 mg, 0.0584 mmol) and dissolved in dry DMF (6 mL). The solution was subjected to three freeze-pump-thaw cycles before being heated in the dark at 60 °C, for 4 h. At this point, excess azide-

terminated monomer **2.3** (51.0 mg, 0.146 mmol) was added. After stirring overnight, the polymerization was cooled to room temperature and the solution was dialyzed using a 50 kg/mol MWCO membrane against DMF. After 8 h the dialysate was changed to water and dialysis was continued for an additional 16 h. Polymer **2.6** was isolated by lyophilization as a white powder (0.95 g, 87.2%). ^{1}H NMR (DMSO-d_6): δ 7.85 (s, 104 H), 7.56 - 7.75 (m, 356 H), 5.39 (s, 215 H), 5.29 (s, 214 H), 5.25 (s, 12 H), 5.18 (s, 236 H), 4.55 - 4.58 (m, 10 H), 4.17 (s, 4 H), 2.86 - 2.93 (m, 234 H), 2.66 - 2.74 (m, 237 H). SEC: M_n = 24 kg/mol, Đ = 1.65. IR ν (cm^{-1}): 3440, 3150, 3090, 2950, 2110, 1760, 1530, 1360, 1190.

Synthesis of triblock copolymer 2.9

Polymer **2.6** (250 mg, ~13 μmol of azide), alkyne-terminated PEG **2.7** (16.9 mg, 21.0 μmol) and bromotris(triphenylphosphine) copper(I) (0.390 mg, 42.0 μmol) were dissolved in DMF (3 mL). Air was removed through three cycles of freeze-pump-thaw and then the reaction mixture was heated at 60 °C in the dark for 24 h. It was then cooled to room temperature and dialyzed against DMF, using a 12 - 14 kg/mol MWCO dialysis membrane for 8 h then against water for 16 h. Lyophilization provided **2.9** as a white solid (250 mg, 96%). ^{1}H NMR (DMSO-d_6): δ 7.87 (s, 103 H), 7.56 - 7.78 (m, 356 H), 5.41 (s, 206 H), 5.31 (s, 206 H), 5.26 (s, 12 H), 5.19 (s, 218 H), 4.56 - 4.59 (m, 11 H), 3.48 - 3.53 (m, 135 H), 3.24 (s, 6 H), 2.85 - 2.95 (m, 213 H), 2.67 - 2.76 (m, 222 H). SEC: M_n = 23 kg/mol, $Đ$ = 1.76. IR ν (cm^{-1}): 3460, 3150, 3090, 2950, 1740, 1530, 1360, 1190.

Synthesis of triblock copolymer 2.10

The same procedure described above for the synthesis of triblock copolymer **2.9** was followed, except that alkyne-functionalized PEG **2.8** (43.4 mg, 21.0 μmol) was used. Copolymer **2.10** was isolated by lyophilization (265 mg, > 99%). ^{1}H NMR (DMSO-d_6) δ: 7.85 (s, 103 H), 7.54 - 7.74 (m, 350 H), 5.39 (s, 209 H), 5.28 (s, 209 H), 5.24 (s, 12 H), 5.16 (s, 221 H), 4.51 - 4.58 (m, 10 H), 3.49 (s, 258 H), 3.20 - 3.23 (m, 4 H), 2.82 - 2.93 (m, 217 H), 2.63 - 2.74 (m, 220 H). SEC: M_n = 25 kg/mol, $Đ$ = 1.62. IR (cm^{-1}) 3460, 3150, 3090, 2950, 1750, 1530, 1360, 1180.

Polymer self-assembly

An 8 mg/mL solution of the polymer was prepared in DMSO and was stirred overnight to ensure complete solubilization. It was then filtered using a Dynagard® polypropylene syringe filter (0.2 μm, surface area 0.8 m^2). Next, either 0.1 mL of the DMSO solution was rapidly injected into 0.9 mL of filtered (Acrodisc® 25 mm syringe filter with 0.1 μm Supor® membrane) deionized water with rapid stirring or 0.9 mL of filtered, deionized water was added to 0.1 mL of the DMSO solution with rapid stirring over a period of ~ 1 minute. The resulting suspension was then dialyzed against deionized water using a 3500 g/mol MWCO membrane.

Dynamic light scattering (DLS)

DLS analysis was run using the 0.8 mg/mL suspensions of polymer assemblies prepared as described above. The measurements were performed in a 1 cm pathlength glass cuvette using a Zetasizer Nano ZS instrument from Malvern. Fifteen repeat diameter measurements were made per run to determine an average particle size and three runs per sample were done.

Transmission electron microscopy (TEM)

The suspension of assemblies (5 μL, 0.1 mg/mL) was placed on a copper Formvar/carbon support film coated grid and was left to stand for 5 min. The excess solution was then blotted off using a piece of filter paper. The resulting sample was dried in air overnight before imaging. Imaging was performed using a Phillips CM10 microscope operating at 80 kV with a 40 μm aperture.

NMR study of photodegradation

Polymer **2.10** (5 mg/mL) was dissolved in DMSO-d_6 and transferred to a quartz NMR tube. Over the course of 600 min, the sample was irradiated with a Hanovia medium pressure mercury lamp (PC 451050/616750, 450 Wage). The sample was placed 10 cm from the lamp with one face of the NMR tube directly facing the lamp. The degradation was monitored by ^{1}H NMR at various time intervals using a 600 MHz Varian Inova spectrometer.

UV-visible (UV-vis) spectroscopy study of photodegradation

Assemblies (0.3 mg/mL) prepared from copolymer **2.10** via the DMSO into water method were used. The measurements were performed in a 1 cm pathlength quartz cuvette, using a Varian Cary 300 Bio UV-visible spectrophotometer, over a wavelength range of 200 - 800 nm. Photoirradiation was performed using a model LZC-4X Luzchem Photoreactor equipped with Luzchem LZC-UVB lamps. The sample as placed in the middle of a rotating platform, 15 cm from the lamps. Multiple lamps were on two walls and the ceiling of the lightbox therefore continuously irradiating the sample from multiple sides. Spectra were obtained at various time points over a period of 7.5 min.

Dynamic light scattering study of photodegradation

Assemblies (0.8 mg/mL) prepared from copolymer **2.10** via the DMSO into water method were placed in a 1 cm pathlength quartz cuvette. The sample was irradiated using a Hanovia medium pressure mercury lamp (PC 451050/616750, 450 Wage). The sample was placed 10 cm from the lamp with one face of the cuvette directly facing the lamp. Measurements were performed at various time points using a Zetasizer Nano ZS instrument from Malvern, keeping all instrument parameters constant throughout the study.

2.4 Conclusions

Photodegradable triblock copolymers with low hydrophilic weight fractions of 0.04 and 0.07 were prepared by a CuAAC polymerization of photodegradable diazide and dialkyne monomers, followed by CuAAC conjugation of PEG. The self-assembly of these materials by nano-precipitation methods was studied. It was found that mixtures of vesicles and polydisperse solid particles probably having inverted microstructures were formed from these materials. The procedure involving the addition of a DMSO solution of polymer into water led to smaller assemblies than the inverse procedure. For the copolymer with the longer PEG blocks, assemblies comprising mainly vesicles were obtained by this procedure. The photodegradation of the triblock copolymer in DMSO was studied by ^{1}H NMR spectroscopy and the expected products were observed. In

addition, the photodegradation of the vesicles was studied by UV-vis, DLS, and TEM. These studies suggested that the vesicles degrade via conversion to micelles, followed by photodegradation of the micelles. This study demonstrates the potential of these new materials for encapsulation and release applications.

2.5 References

1. Gohy, J.-F.; Zhao, Y., *Chem. Soc. Rev.* **2013,** *42* (17), 7117-7129.
2. Wiggins, K. M.; Brantley, J. N.; Bielawski, C. W., *Chem. Soc. Rev.* **2013,** *42* (17), 7130-7147.
3. Kharkar, P. M.; Kiick, K. L.; Kloxin, A. M., *Chem. Soc. Rev.* **2013,** *42* (17), 7335-7372.
4. Huo, M.; Yuan, J.; Tao, L.; Wei, Y., *Polym. Chem.* **2014,** *5* (5), 1519-1528.
5. Thevenot, J.; Oliveira, H.; Sandre, O.; Lecommandoux, S., *Chem. Soc. Rev.* **2013,** *42* (17), 7099-7116.
6. Schattling, P.; Jochum, F. D.; Theato, P., *Polym. Chem.* **2014,** *5* (1), 25-36.
7. Lv, C.; Wang, Z.; Wang, P.; Tang, X., *Langmuir* **2012,** *28* (25), 9387-9394.
8. Yan, B.; Boyer, J.-C.; Branda, N. R.; Zhao, Y., *J. Am. Chem. Soc.* **2011,** *133* (49), 19714-19717.
9. Halim, A.; Reid, T. D.; Ren, J. M.; Fu, Q.; Gurr, P. A.; Blencowe, A.; Kentish, S. E.; Qiao, G. G., *J. Polym. Sci., Part A: Polym. Chem.* **2014**, Ahead of Print.
10. Ding, J.; Liu, G., *Macromolecules* **1998,** *31* (19), 6554-6558.
11. Wang, G.; Tong, X.; Zhao, Y., *Macromolecules* **2004,** *37* (24), 8911-8917.
12. del Barrio, J.; Oriol, L.; Sanchez, C.; Serrano, J. L.; Di Cicco, A.; Keller, P.; Li, M.-H., *J. Am. Chem. Soc.* **2010,** *132* (11), 3762-3769.
13. Cabane, E.; Malinova, V.; Meier, W., *Macromol. Chem. Phys.* **2010,** *211* (17), 1847-1856.
14. Han, D.; Tong, X.; Zhao, Y., *Macromolecules* **2011,** *44* (3), 437-439.
15. Han, D.; Tong, X.; Zhao, Y., *Langmuir* **2012,** *28* (5), 2327-2331.
16. Dispinar, T.; Colard, C. A. L.; Du Prez, F. E., *Polym. Chem.* **2013,** *4* (3), 763-772.
17. Fomina, N.; McFearin, C.; Sermsakdi, M.; Edigin, O.; Almutairi, A., *J. Am. Chem. Soc.* **2010,** *132* (28), 9540-9542.
18. Gu, W.; Zhao, H.; Wei, Q.; Coughlin, E. B.; Theato, P.; Russell, T. P., *Adv. Mater.* **2013,** *25* (34), 4690-4695.

19. Kloxin, A. M.; Kasko, A. M.; Salinas, C. N.; Anseth, K. S., *Science* **2009,** *324* (5923), 59-63.

20. Liu, J.; Burts, A. O.; Li, Y.; Zhukhovitskiy, A. V.; Ottaviani, M. F.; Turro, N. J.; Johnson, J. A., *J. Am. Chem. Soc.* **2012,** *134* (39), 16337-16344.

21. Jiang, J.; Tong, X.; Zhao, Y., *J. Am. Chem. Soc.* **2005,** *127* (23), 8290-8291.

22. Bertrand, O.; Gohy, J.-F.; Fustin, C.-A., *Polym. Chem.* **2011,** *2* (10), 2284-2292.

23. Dong, J.; Xun, Z.; Zeng, Y.; Yu, T.; Han, Y.; Chen, J.; Li, Y.-Y.; Yang, G.; Li, Y., *Chem. - Eur. J.* **2013,** *19* (24), 7931-7936.

24. Zhao, H.; Sterner, E. S.; Coughlin, E. B.; Theato, P., *Macromolecules* **2012,** *45* (4), 1723-1736.

25. Kamaly, N.; Xiao, Z.; Valencia, P. M.; Radovic-Moreno, A. F.; Farokhzad, O. C., *Chem. Soc. Rev.* **2012,** *41* (7), 2971-3010.

26. Liu, S.; Maheshwari, R.; Kiick, K. L., *Macromolecules* **2009,** *42* (1), 3-13.

27. Rosler, A.; Vandermeulen, G. W. M.; Klok, H.-A., *Adv Drug Deliv Rev* **2012**.

28. Bertrand, O.; Poggi, E.; Gohy, J.-F.; Fustin, C.-A., *Macromolecules* **2014,** *47* (1), 183-190.

29. Cabane, E.; Malinova, V.; Menon, S.; Palivan, C. G.; Meier, W., *Soft Matter* **2011,** *7* (19), 9167-9176.

30. Kang, M.; Moon, B., *Macromolecules* **2009,** *42* (1), 455-458.

31. Katz, J. S.; Zhong, S.; Ricart, B. G.; Pochan, D. J.; Hammer, D. A.; Burdick, J. A., *J. Am. Chem. Soc.* **2010,** *132* (11), 3654-3655.

32. Li, H.; Rathi, S.; Sterner, E. S.; Zhao, H.; Hsu, S. L.; Theato, P.; Zhang, Y.; Coughlin, E. B., *J. Polym. Sci., Part A: Polym. Chem.* **2013,** *51* (20), 4309-4316.

33. Rabnawaz, M.; Liu, G., *Macromolecules* **2012,** *45* (13), 5586-5595.

34. Schumers, J.-M.; Gohy, J.-F.; Fustin, C.-A., *Polym. Chem.* **2010,** *1* (2), 161-163.

35. Xuan, J.; Han, D.; Xia, H.; Zhao, Y., *Langmuir* **2014,** *30* (1), 410-417.

36. Zhao, H.; Gu, W.; Sterner, E.; Russell, T. P.; Coughlin, E. B.; Theato, P., *Macromolecules* **2011,** *44* (16), 6433-6440.

37. Lee, H.; Kim, Y.; Schweickert, P. G.; Konieczny, S. F.; Won, Y.-Y., *Biomaterials* **2014,** *35* (3), 1040-1049.

38. Liu, G.; Wang, X.; Hu, J.; Zhang, G.; Liu, S., *J. Am. Chem. Soc.* **2014,** *136* (20), 7492-7497.

39. Sheng, X.; Mauldin, T. C.; Kessler, M. R., *J. Polym. Sci., Part A: Polym. Chem.* **2010,** *48* (18), 4093-4102.

40. Li, H.-k.; Sun, J.-z.; Qin, A.-j.; Tang, B. Z., *Chin. J. Polym. Sci.* **2012,** *30* (1), 1-15.

41. Zhang, L.; Eisenberg, A., *Science* **1995,** *268* (5218), 1728-1731.

42. Discher, D. E.; Eisenberg, A., *Science* **2002,** *297* (5583), 967-973.

43. Perrault, S. P.; Chan, W. C. W., *Proc. Natl. Acad. Sci. U. S. A.* **2010,** *107* (25), 11194-11199, S11194/11191-S11194/11194.

44. Griffin, D. R.; Kasko, A. M., *J. Am. Chem. Soc.* **2012,** *134* (31), 13103-13107.

45. Choi, I.; Kim, Y.-K.; Min, D.-H.; Lee, S.; Yeo, W.-S., *J Am Chem Soc* **2011,** *133* (42), 16718-16721.

46. Lussis, P.; Svaldo-Lanero, T.; Bertocco, A.; Fustin, C.-A.; Leigh, D. A.; Duwez, A.-S., *Nat. Nanotechnol.* **2011,** *6* (9), 553-557.

Chapter 3

3 Surface Functionalization of Dendrimersomes

3.1 Introduction

Polymer assembly has been an area of significant interest for many years.[1, 2, 3, 4] The desire to understand all that contributes to variation in aggregate morphology as well as exploiting different morphologies for application purposes has fueled the fire for this research. Polymersomes in particular have seen much interest as they share many structural and physical characteristics with biological membranes making them promising candidates for drug delivery applications.[2, 5, 6, 7, 8, 9, 10, 11, 12] They are similar to biological membranes as they have a hydrophilic core, hydrophobic membrane and outer membrane surface, but can also have various groups decorating their surfaces.[8, 13, 14, 15] By functionalizing the outer surface, biological functions can be imparted yielding another dynamic avenue of versatility and application.

Combining both dendritic and linear polymer architectures, Gillies *et al*. have shown the surface functionalization of polymersomes with dendritic groups.[6, 7, 8, 15] Dendrimers with a number of peripheral functional groups, such as hydroxyls, amines, guanidines, carbohydrates and Gd(III) chelates were synthesized. By functionalizing the polymersomes' surface with each of these dendritic species they could tune characteristics such as toxicity, cell uptake, protein binding and contrast agent efficiency. To compliment this, they were also able to show comparable release rates of encapsulated rhodamine B and rhodamine B-labeled protein, among the different functionalized polymersomes.[16] The group has also shown the potential for surface functionalized poly(ethylene oxide)-polycaprolactone polymersomes to interact with and inhibit the influenza virus from binding host cells.[9] Through surface functionalization with sialic acid (*N*-acetylneuraminic acid), binding to a sialic acid-binding lectin was observed serving as a model for the binding of a sialic acid-binding protein on the surface of the virus. Encapsulated within the polymersomes' core was the neuraminidase inhibitor

zanamivir which prevents the release of progeny virus from the host cell thereby inhibiting viral replication.[9]

Using only amphiphilic dendrimers to provide surface functionalized assemblies, Percec *et al*. have also shown the first synthesis and self-assembly of what they termed "Janus glycodendrimers" made with D-mannose, D-galactose or D-lactose. These dendrimers were shown to assemble into "glycodendrimersomes", "glycomicelles" and "glycocubosomes" whose carbohydrate multivalency yielded promising properties as new mimics of biological membranes with programmable glycan ligand presentations. These glycol-architectures yield the potential to serve as supramolecular lectin blockers, vaccines and targeted delivery devices.[17, 18] They used lauryl chains as the hydrophobic block and acetonide-deprotected, bis-MPA polyester dendrons as the hydrophilic block, finding an inverse proportionality between size, stability, mechanical properties of dendrimersomes and the thickness of their membrane.[19, 20]

Rather than needing to pre-synthesize amphiphilic dendrons with functional peripheral moieties such as carbohydrates, the goal of the current work is to provide a platform based on amphiphilic dendrons onto which specific groups can be "clicked" post-assembly. Specifically the goal of this chapter is to describe the synthesis of a novel Janus dendrimer having surface azide groups. The Janus dendrimer will be subjected to self-assembly with the aim of obtaining dendrimersomes having surface azide groups. Having surface functionalized dendrimersomes will yield the capacity for cellular targeting. For example, studies have shown the functionalization of certain dendrimers with tumor targeting ligands such as folic acid,[21] arginine-glycine-aspartic acid peptide,[22] and lactobionic acid can lead to more effective tumor targeting drug deliver vehicles.[23]

3.2 Results and Discussions

3.2.1 Synthesis of Janus Dendrimers 3.7 and 3.12

Dendrimer synthesis can occur convergently, divergently or by way of a combination of the two. Likewise, Janus dendrimers can be synthesized in the same fashion with a final coupling step to link the two blocks. Our group has had much success in polyester dendrimer synthesis by using the bis-MPA monomer anhydride along with DMAP and pyridine.[24] This method is very effective growing to the fourth generation dendron, however it has also been shown to be able to grow up to the sixth generation.[25] Growth becomes increasingly difficult at higher generations due to steric bulk as well as the size and reactivity of the anhydride. To prepare dendrons with acetonide peripheral groups, third and fourth generation dendrons, **3.1**[24] and **3.8** [24] (Figure 3.1), were prepared using a previously reported procedure.[24]

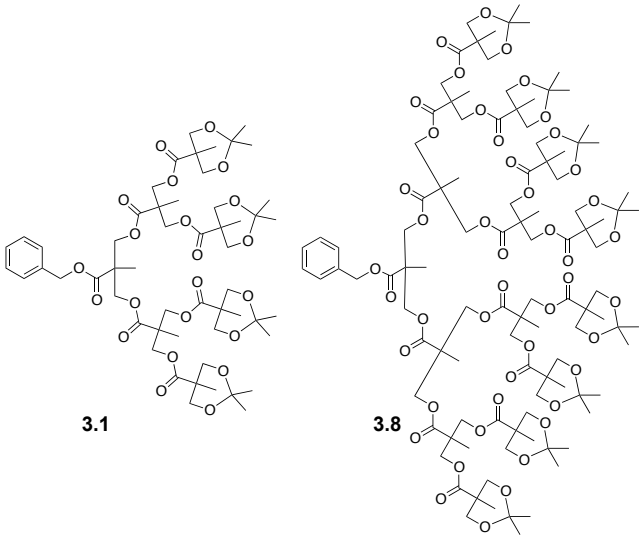

Figure 3.1. Third and fourth generation dendrons, 3.1 and 3.8 respectively, prepared by previously reported procedures.[24]

As shown in Scheme 3.1, the focal point benzyl ester **3.1**[24] was then cleaved by hydrogenolysis in EtOAc and MeOH, providing **3.2**. 4-Aminobutyric acid (**3.3**[26]) was then coupled to the focal point acid using *o*-(6-chlorobenzotriazol-1-yl)-*N*,*N*,*N*',*N*'-tetramethyluronium hexafluorophosphate (HCTU) and N, N-diisopropylethylamine (DIPEA) to afford **3.4**. It acts as a tether between the hydrophobic and hydrophilic

blocks, providing enough space between the two that they may be effectively coupled without hindrance of the reactive site. Untethered dendrons were unable to be coupled with the hydrophilic block, presumably because of the steric crowding from the dendritic backbones. After attaching the tether, the benzyl ester was cleaved by hydrogenolysis using the method described above to provide **3.5** and then the hydrophilic block **3.6**[27], prepared as previously reported,[27] was subsequently coupled using EDC·HCl, DMAP and pyridine, forming the amphiphilic Janus dendrimers **3.7**. As shown in Scheme 3.2, the fourth generation dendron **3.8**[24] was converted to the corresponding amphiphilic Janus dendrimer **3.12** using the same methods as described for the third generation dendron. Both of the resulting Janus dendrimers **3.7** and **3.12** were characterized by ^{1}H NMR spectroscopy.

Scheme 3.1. Synthesis of Janus dendrimer 3.7.

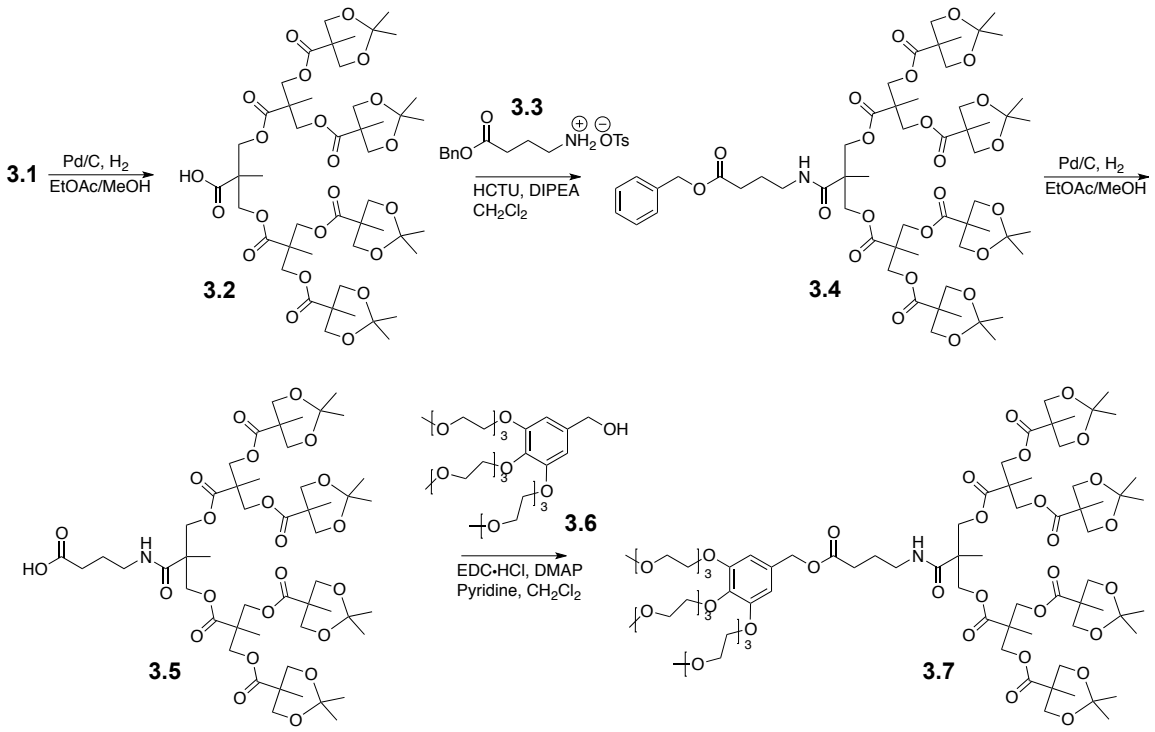

Scheme 3.2. Synthesis of Janus dendrimer 3.12.

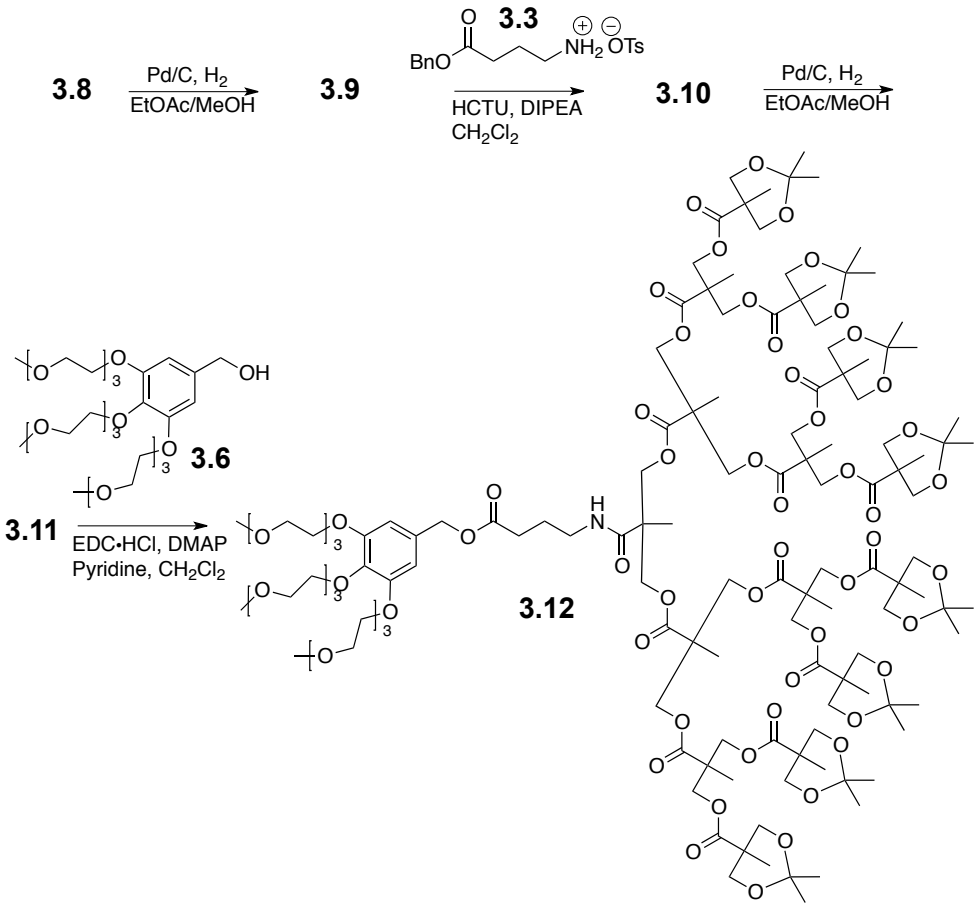

3.2.2 Self-Assembly of Janus Dendrimers 3.7 and 3.12 in Aqueous Solution

Aggregate morphology is largely dictated by hydrophilic volume fraction,[2] but the hydrophilic to hydrophobic weight ratio can give an adequate estimation of the volume fraction and therefore be a guide to predicting morphologies. Janus dendrimers **3.7** and **3.12** were prepared for this study and their hydrophilic mass fractions are summarized in Table 3.1. Considering the preparation of these Janus dendrimers was performed via coupling of the hydrophilic gallic acid moiety and the hydrophobic tethered dendron moiety, the hydrophilic mass ratios were calculated by considering these components as the hydrophilic and hydrophobic fractions respectively.

Table 3.1. Hydrophilic weight fraction of Janus dendrimers 3.7 and 3.12.

	Total MW (g/mol)	Hydrophilic mass fraction
Dendrimer **3.7**	1653	0.36
Dendrimer **3.12**	2742	0.22

The self-assembly of each of these dendrimers was studied using the nano-precipitation method. Janus dendrimers were dissolved in either DMSO or THF and this organic solution was added to water, or water was added to the organic solution of the dendrimer. The organic solvent was then removed via dialysis and the assemblies were characterized by DLS and TEM. Table 3.2 and Figure 3.2 summarize these results.

Table 3.2. Summary of self-assembly results for Janus dendrimers 3.7 and 3.12.

Dendrimer and conditions	Hydrodynamic diameter (DLS)	Polydispersity index (DLS)	Morphology (TEM)
Dendrimer **3.7** (DMSO into water)	230	0.19	solid aggregates
Dendrimer **3.7** (water into DMSO)	250	0.22	solid aggregates
Dendrimer **3.12** (DMSO into water)	1070	0.48	solid aggregates
Dendrimer **3.12** (water into DMSO)	610	0.36	solid aggregates
Dendrimer **3.12** (THF into water)	320	0.32	solid aggregates
Dendrimer **3.12** (water into THF)	400	0.26	solid aggregates

a)

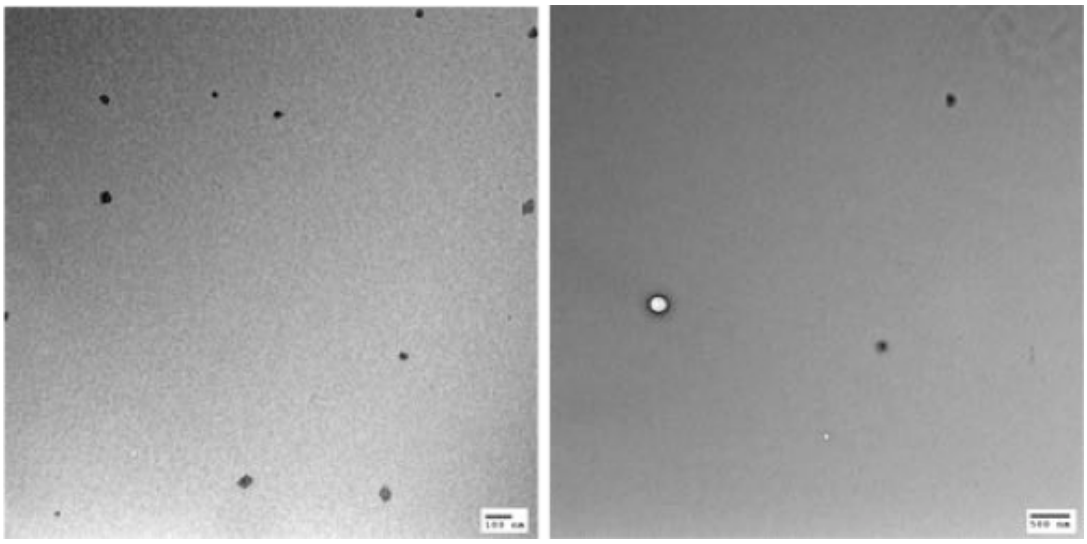

b)

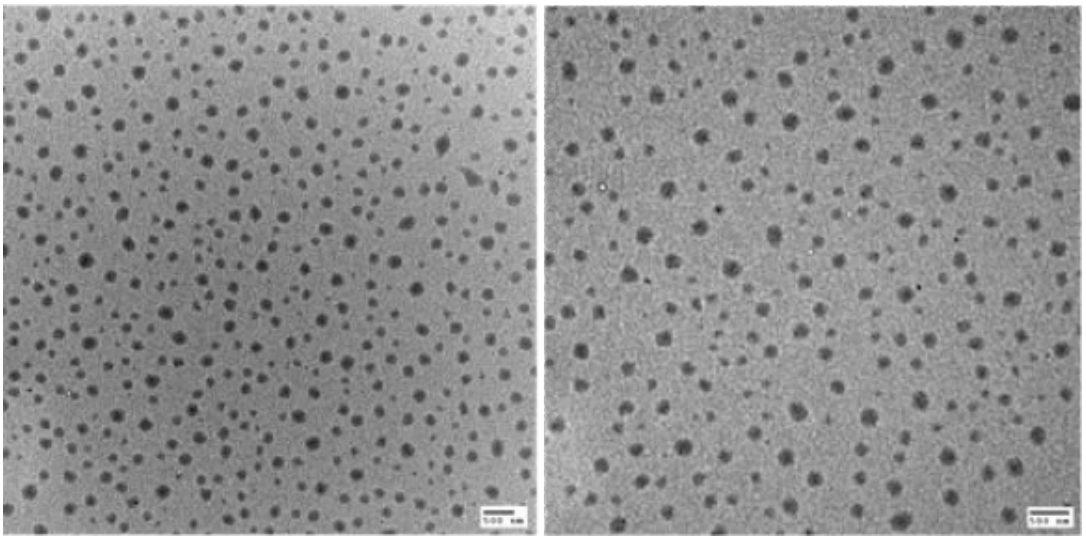

c)

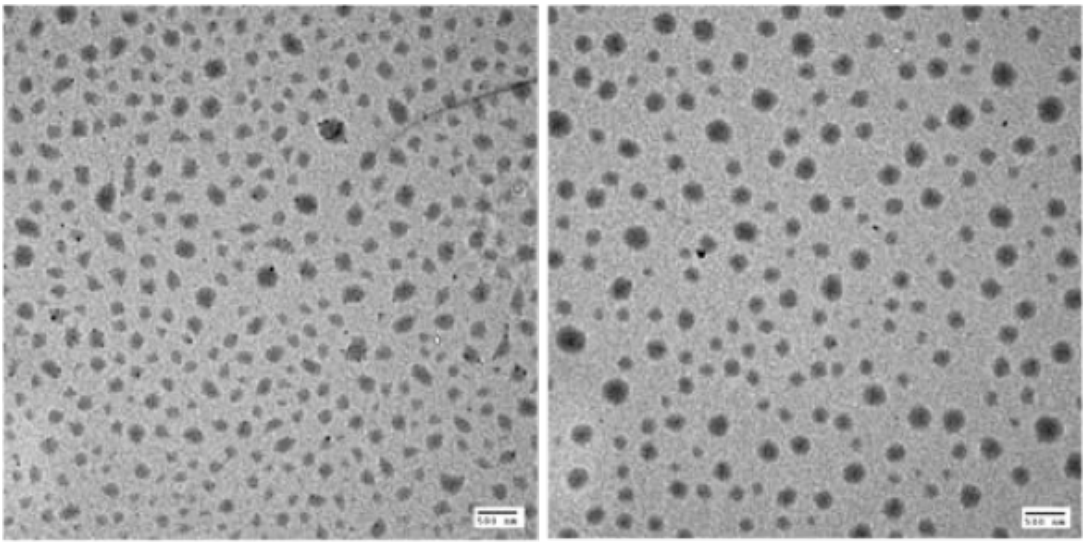

Figure 3.2. TEM images of assemblies formed by Janus dendrimers 3.7 and 3.12 using different procedures: a) Janus dendrimer 3.7, DMSO into water (left) and water into DMSO (right); b) Janus dendrimer 3.12, DMSO into water (left) and water into DMSO (right); c) Janus dendrimer 3.12, THF into water (left) and water into THF (right).

Most assemblies of the Janus dendrimers were solid aggregates as indicated by TEM imaging (Figure 3.2), however the sizes of these particles, measured by DLS, were much too large to be true micelles. Based on the hydrophilic mass fractions for **3.7** (0.36) and **3.12** (0.22), it is feasible that micelles and even vesicles may have formed in solution. This suggests that micelles or vesicles may form, but are unstable due to the molecular architecture of the dendrimers, resulting in aggregation or other undesirable drying effects during TEM grid preparation. This has been previously observed for the lower generations of our previously reported photodegradable amphiphilic Janus dendrimers.[28]

3.2.3 Synthesis of Janus Dendrimers 3.18 and 3.22

After having seen the assembly results of Janus dendrimers **3.7** and **3.12**, it was clear, if dendrimersomes were to form, that the hydrophobic content provided by terminal acetonide groups was not sufficient. It was hypothesized that the hydrophobic content needed to be increased while maintaining a fluid and malleable hydrophobic membrane. Based on previous work by Percec and coworkers[20, 29] the proposed solution was an amphiphilic dendrimer with peripheral acyl chains instead of growing to the fifth generation with the terminal acetone groups.

As shown in Scheme 3.3, to prepare dendrons with terminal acyl groups, the second generation acetonide-deprotected dendron **3.13**[24] was prepared from previously reported procedures and acylated using lauroyl chloride in pyridine. Acylated dendron **3.14** was carried through similar synthetic steps to those described above for the preparation of Janus dendrimers **3.7** and **3.12** to yield Janus dendrimer **3.18**.

Scheme 3.3. Synthesis of Janus dendrimer 3.18.

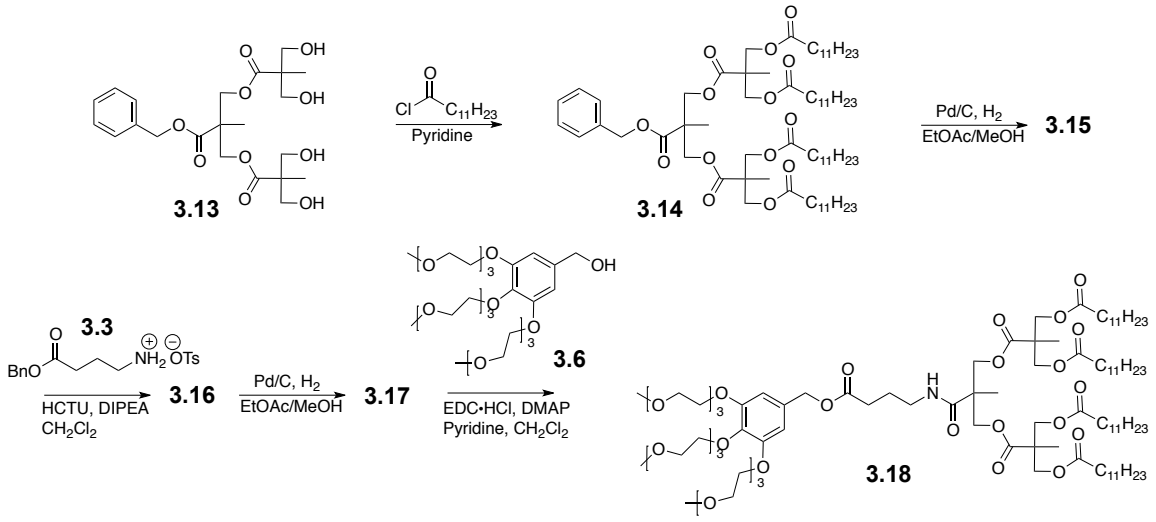

A third generation acyl-terminated dendron was synthesized as shown in Scheme 3.4. The acetonide protecting groups of dendron **3.4**, prepared as described in Scheme 3.1, were removed using H_2SO_4 in MeOH and the resulting dendron **3.19** was acylated yielding dendron **3.20**. The benzyl protecting group was then cleaved through hydrogenolysis and the resulting dendron **3.21** was coupled to the hydrophilic block **3.6**[27] using EDC·HCl, DMAP and pyridine to yield Janus dendrimer **3.22**. Janus dendrimers **3.18** and **3.22** were characterized by ^{1}H NMR, ^{13}C NMR and IR spectroscopy, as well as SEC and mass spectrometry.

Scheme 3.4. Synthesis of Janus dendrimer 3.22.

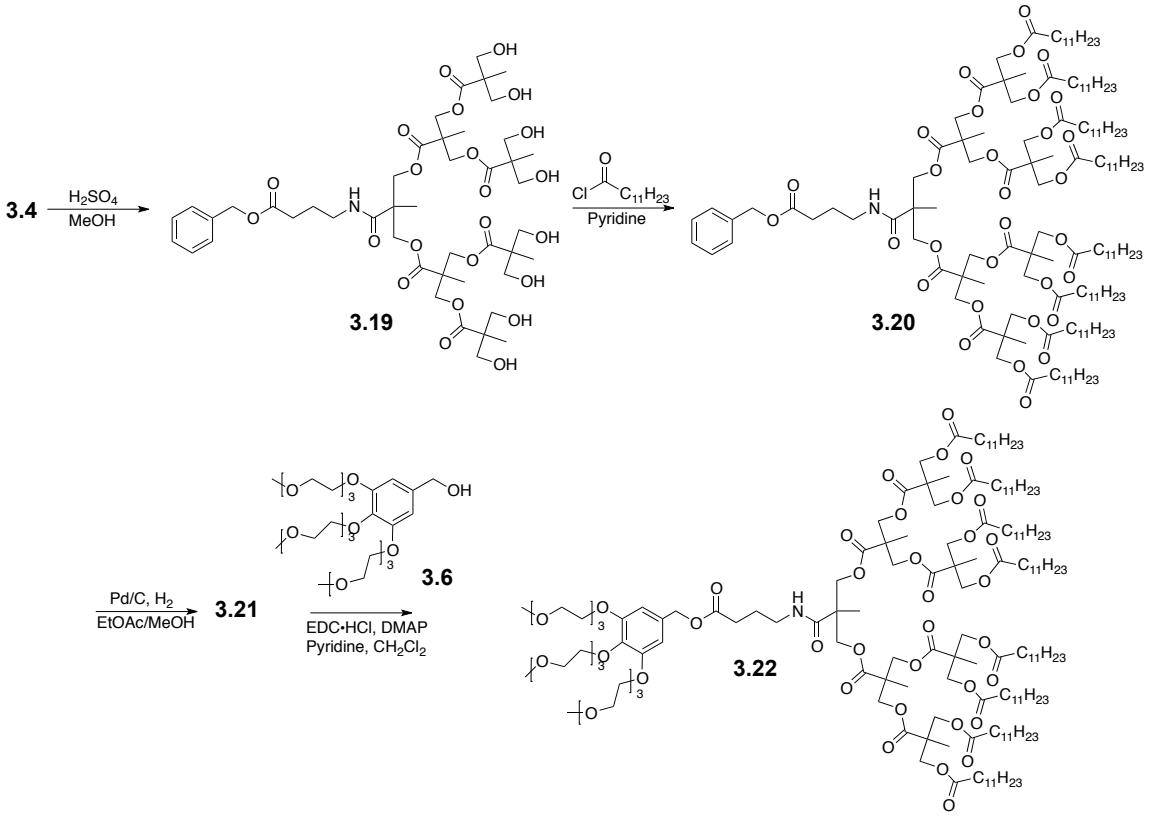

3.2.4 Self-Assembly of Janus Dendrimers 3.18 and 3.22 in Aqueous Solution

Janus dendrimers **3.18** and **3.22** were prepared for this study and their hydrophilic mass fractions summarized in Table 3.3. The hydrophilic mass fractions were calculated in the same way as Janus dendrimers **3.7** and **3.12**. By adding acyl groups to the periphery of the dendrons instead of another bis-MPA monomer, the hydrophilic mass fractions of each Janus dendrimer decreased by 2%.

Table 3.3. Hydrophilic weight fraction of Janus dendrimers 3.18 and 3.22.

	Total MW (g/mol)	Hydrophilic mass fraction
Dendrimer **3.18**	1757.35	0.34
Dendrimer **3.22**	2951.02	0.20

The self-assembly of each of these dendrimers was studied using the nano-precipitation method. Janus dendrimers were dissolved in either DMSO or THF and this organic solution was added to water, or water was added to the organic solution of the dendrimer. The organic solvent was removed via dialysis from dendrimer **3.18** assembliess while dendrimer **3.22** was allowed to stir open, overnight, to allow THF to evaporate. The assemblies were characterized by DLS and TEM. Table 3.4 and Figure 3.3 summarize these results.

Table 3.4. Summary of self-assembly results for Janus dendrimers 3.18 and 3.22.

Dendrimer and conditions	Hydrodynamic diameter (DLS)	Polydispersity index (DLS)	Morphology (TEM)
Dendrimer **3.18** (DMSO into water)	140	0.09	solid aggregates
Dendrimer **3.18** (water into DMSO)	490	0.06	solid aggregates
Dendrimer **3.18** (THF into water)	1030	0.22	solid aggregates
Dendrimer **3.18** (water into THF)	850	0.74	solid aggregates
Dendrimer **3.22** (THF into water)	230	0.04	solid aggregates
Dendrimer **3.22** (water into THF)	260	0.29	vesicles and solid particles

a)

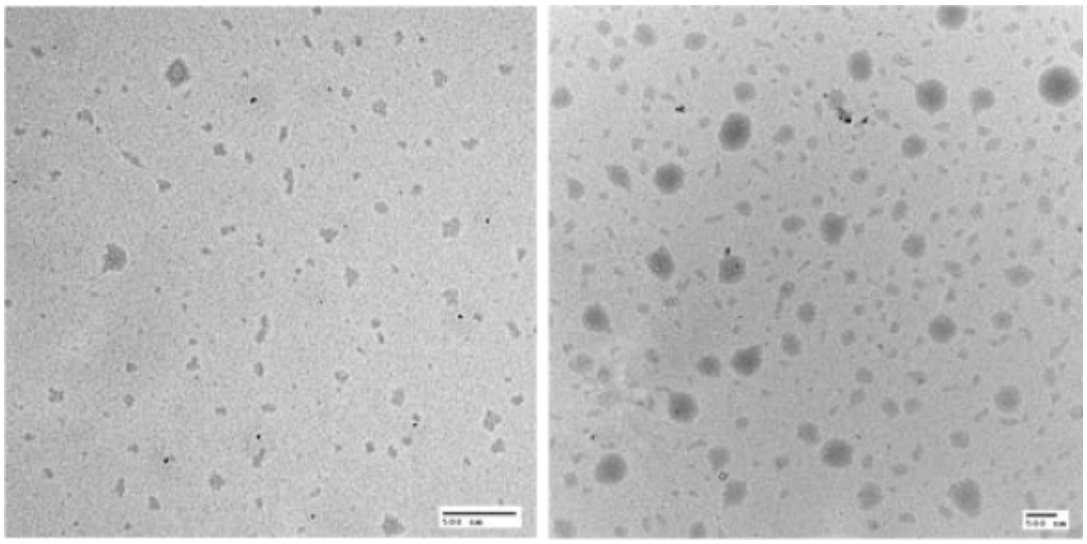

b)

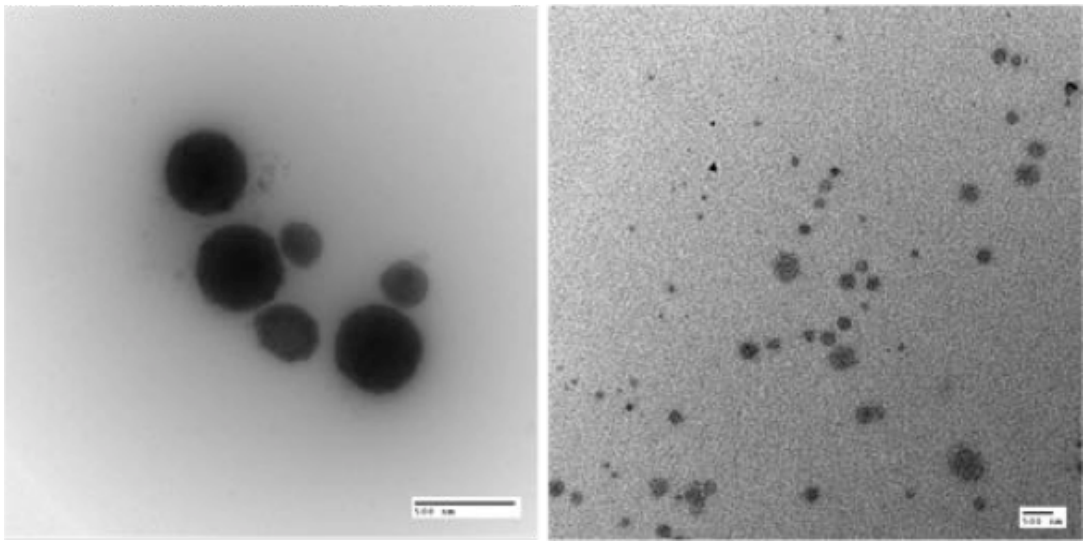

c)

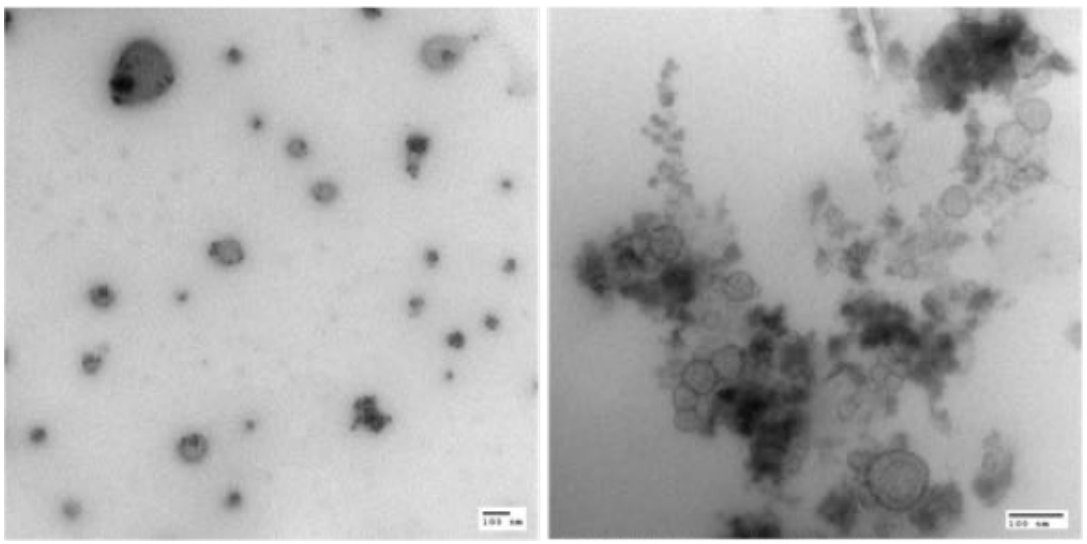

Figure 3.3. TEM images of assemblies formed by Janus dendrimers 3.18 and 3.22 using different procedures: a) Janus dendrimer 3.18, DMSO into water (left) and water into DMSO (right); b) Janus dendrimer 3.18, THF into water (left) and water into THF (right); c) Janus dendrimer 3.22, THF into water (left) and water into THF (right).

Self-assembly of Janus dendrimer **3.18** resulted in solid aggregates in each of the particle formation procedures. In the case where DMSO was used as solvent, the DLS results matched the size of the particles seen by TEM whereas when THF was used as solvent, the particles appeared much larger by DLS compared to the TEM images. The cause of this may be due to aggregation of the particles at higher concentrations during DLS.

Janus dendrimer **3.22** was not soluble in DMSO so self-assembly was performed exclusively with THF. As observed by TEM, when water was added to the THF/dendrimer solution, the assemblies appeared to be dendrimersomes <100 nm in diameter while the DLS showed particles approximately 250 nm in diameter. The reason for the discrepancy may be from swelling in solution and then shrinkage when drying on the TEM grid. With this in mind, the result of adding the THF solution to water appears to give solid aggregates, as observed by TEM, however at a closer look, it seems that there is some clustering around the periphery of the aggregates which may indicate that disruption of the dendrimersome bilayer occurred as a result of drying on the TEM grid.

3.2.5 Synthesis of Azide-Terminated Janus Dendrimer 3.25

While the above dendrons would enable studies of the self-assembly, the ultimate goal was to be able to perform surface functionalization. This required access to an amphiphilic dendrimer having functional groups on the hydrophilic block. To accomplish this, an azide-terminated, methyl gallate analogue **3.23**[30] of hydrophilic block **3.6**[27] was synthesized based on previously recorded procedures[30] and then reduced using LiCl and $NaBH_4$ in THF and ethanol (Scheme 3.5) to give the azide-terminated hydrophilic block **3.24**.

Scheme 3.5. Synthesis of azide-terminated hydrophilic block 3.24.

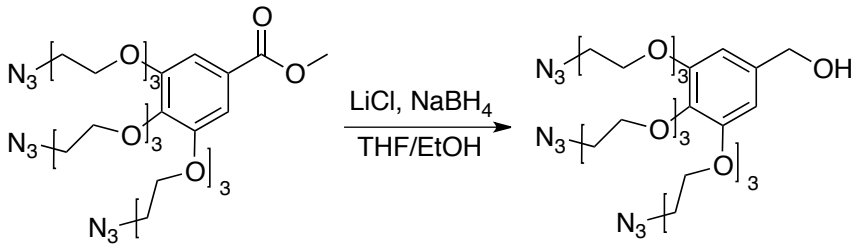

3.23 **3.24**

The same synthetic strategy for preparing Janus dendrimer **3.22** was used to synthesize its azide analogue, **3.25** (Scheme 3.6).

Scheme 3.6. Synthesis of azide-terminated Janus dendrimer 3.25.

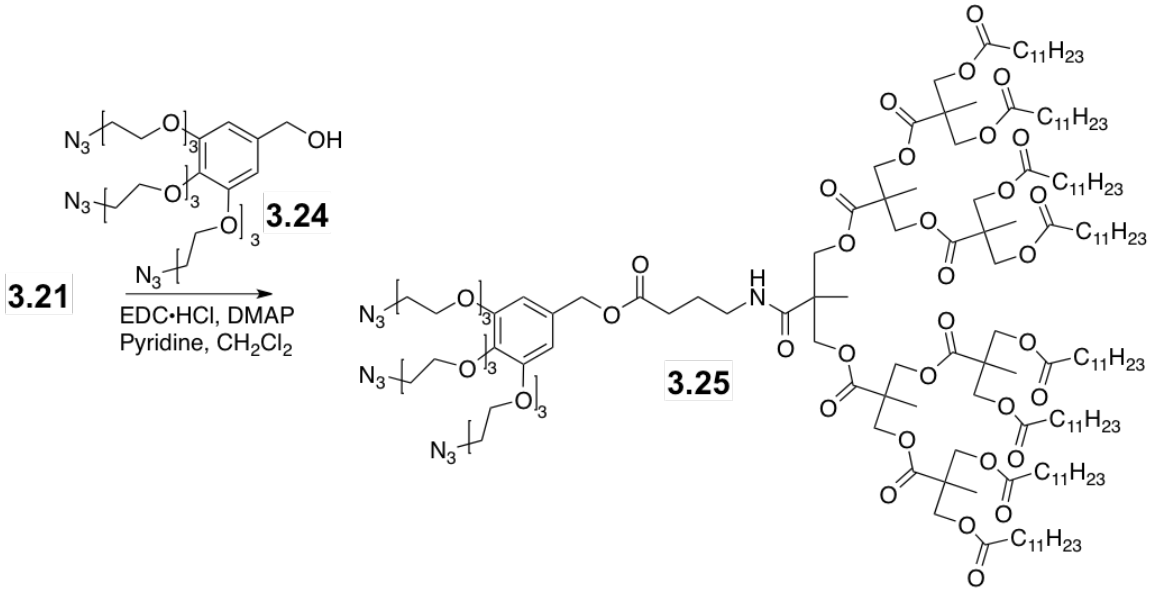

Hydrophilic block **3.24** was characterized by ^{1}H NMR, ^{13}C NMR and IR spectroscopy, as well as mass spectrometry, while Janus dendrimer **3.25** was characterized by the same methods including SEC.

3.2.6 Self-Assembly of Janus Dendrimer 3.25 in Aqueous Solution

The self-assembly of the azide-terminated analogue, **3.25**, was studied as summarized in Table 3.5 and Figure 3.4. No dendrimersomes were detected during these studies. It was

hypothesized that the introduction of the azide groups somehow disrupts the hydrophilic/hydrophobic balance of these molecules. Knowing that the non-azide dendrimer **3.22** had formed vesicles, self-assembly was also performed with mixtures of the two analogues using either 20% or 5% of Janus dendrimer **3.25** with the remainder being Janus dendrimer **3.22**. Unfortunately, this yielded large micellar aggregates in both cases.

Table 3.5. Summary of self-assembly results for Janus dendrimer 3.25 and mixtures of 3.22 and 3.25.

Dendrimer and conditions	Hydrodynamic diameter (DLS)	Polydispersity index (DLS)	Morphology (TEM)
Dendrimer **3.25**	280	0.31	solid aggregates
20% **3.25**:80% **3.22** (water into THF)	250	0.12	solid aggregates
20% **3.25**:80% **3.22** (water into THF) -2 kg/mol PEO functionalized	190	0.15	solid aggregates
5% **3.25**:95% **3.22** (water into THF)	360	0.33	solid aggregates

a)

b)

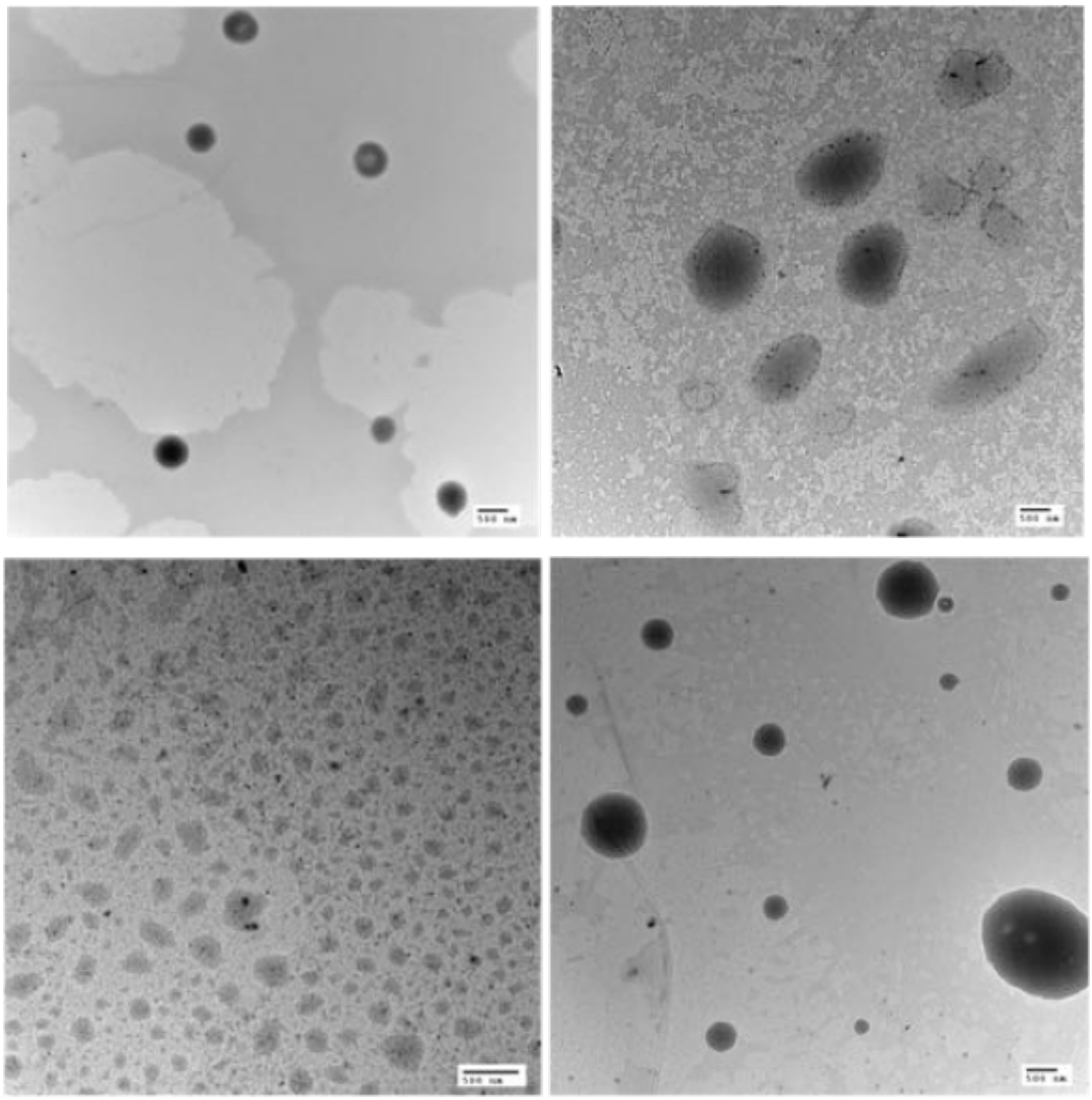

Figure 3.4. TEM images of assemblies formed by Janus dendrimer 3.25 and mixtures of 3.22 and 3.25: a) Janus dendrimer 3.25, water into THF; b)20% 3.25:80% 3.22 (left) and 5% 3.25:95% 3.22 (right), water into THF.

3.2.7 Surface Functionalization of Dendrimer Assemblies

Despite the lack of success in obtaining dendrimersomes with surface azide groups, the reactivity of the azide groups on the assemblies was studied. To achieve this, Janus dendrimers **3.22** and **3.25** were combined in an 80:20 ratio. The dendrimer mixture was dissolved in THF (0.1 mL) and while stirring, water (0.9 mL) was added dropwise. The

resulting particles were characterized with DLS and TEM (Table 3.5 and Figure 3.4) and functionalized via CuAAC chemistry by adding $CuCl_2$, sodium ascorbate and a 2 kg/mol PEO-pentynoic ester to the particles. They were then dialyzed against water to remove excess PEG and the other reagents. The functionalized particles were characterized using DLS, TEM (Table 3.5 and Figure 3.5) and IR (Figure 3.6).

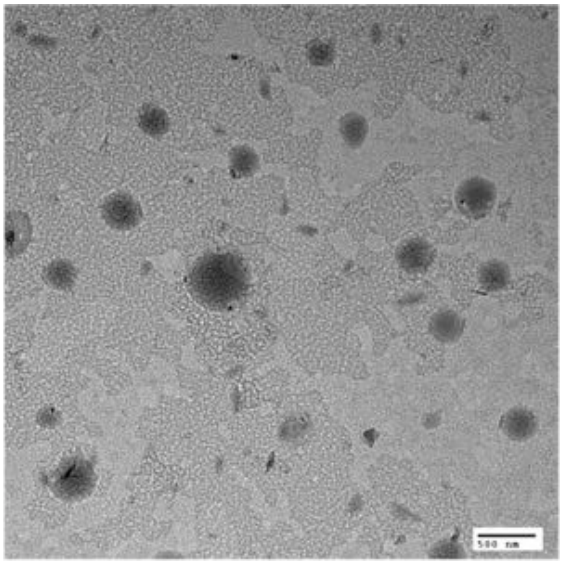

Figure 3.5. TEM images of 2 kg/mol PEO functionalized assemblies formed by 20% 3.25:80% 3.22.

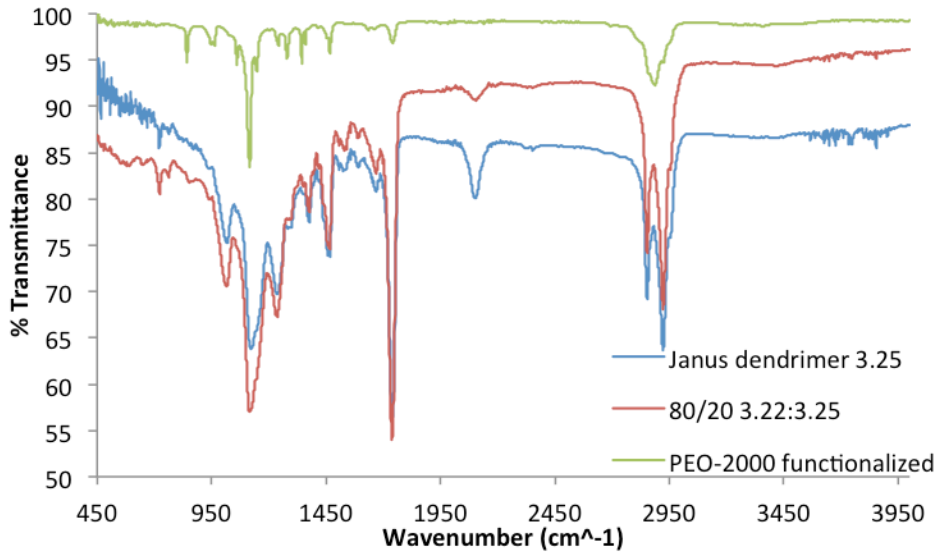

Figure 3.6. FTIR spectra of Janus dendrimer 29, 20% 29:80% 25 dendrimer assemblies, and 20% 29:80% 25 dendrimer assemblies functionalized with 2 kg/mol PEO-pentynoic ester.

Figure 3.6 shows the IR spectra of Janus dendrimer **3.25**, the assemblies formed by the 80/20 mixture of **3.22** and **3.25** and the 2 kg/mol PEO functionalized versions of those particles. Evidence of the success of the reaction is observed through the disappearance of the azide stretch at 2100 cm^{-1}. It does not provide quantification of the yield of the reaction, but indicates that it was successful and therefore yielded surface functionalized dendrimer assemblies.

3.3 Experimental

3.3.1 General Procedure and Materials

Compounds **3.1**,[24] **3.3**,[26] **3.8**,[24] **3.13**,[24] **3.6**,[27] and **3.23**[30] were synthesized using previously reported procedures. Other reagents were purchased from commercial suppliers and used without further purification unless otherwise noted. Tetrahydrofuran (THF) was obtained from a solvent purification system using aluminum oxide columns. CH_2Cl_2 and pyridine were distilled over calcium hydride and all dry glassware was oven-dried overnight. Thin layer chromatography (TLC) was run on Macherney-Nagel Polygram SIL G/UV_{254} plates

and columns were packed using SiliaFlash P60 silica (40-60 μm, 230-400 mesh). Dialyses were performed using either 3.5 or 10 kg/mol molecular weight cut off (MWCO) Spectra/Por regenerated cellulose membranes (Spectrum Laboratories). ^{1}H NMR and ^{13}C NMR spectra were obtained at 400/600 MHz and 100/151 MHz respectively using a Varian Inova spectrometer. NMR chemical shifts are reported in ppm and are calibrated against residual solvent signals of $CDCl_3$ (δ 7.26, 77.2 ppm) or DMSO-d_6 (δ 2.50, 39.5 ppm). Coupling constants are expressed in Hertz (Hz). High-resolution mass spectrometry (HRMS) was performed on a Finnigan MAT 8400 electron impact mass spectrometer. Attenuated total reflection-fourier transform infrared spectroscopy (ATR-FTIR) was performed on a Perkin Elmer Spectrum Two™ FT-IR spectrometer using thin film drop cast from $CHCl_3$. The GPC instrument was equipped with a Viscotek GPC Max VE2001 solvent module. Samples were analyzed using the viscotek VE3580 RI detector operating at 30 °C. The separation technique employed two Agilent Polypore (300x7.5mm) columns connected in series and to a Polypore guard column (50x7.5mm). Samples were dissolved in THF (glass distilled grade) in approximately 5 mg/mL concentrations and filtered through 0.22 μm syringe filters. Samples were injected using a 100 μL loop. The THF eluent was filtered and eluted at 1 mL/min for a total of 30 minutes. A calibration curve was obtained from polystyrene samples with molecular weight ranges of 1540-1,126,000 g/mol. DLS data were obtained using a Zetasizer Nano ZS instrument from Malvern Instruments.

Synthesis of benzyl-deprotected G3 dendron 3.2

Dendron **3.1**[24] (660 mg) was dissolved in an EtOAc/MeOH mixture (60 mL, 4:1) and the solution was purged with argon for 5 minutes. Pd/C (10% wt) was then added and the resulting mixture was purged with and placed under H_2 for 4 hours. It was then filtered through celite and concentrated *in vacuo* to yield a quantitative amount of compound **3.2**, which was taken to the next step without further purification. Complete removal of the benzyl ester was confirmed by ^{1}H NMR spectroscopy. ^{1}H NMR (599 MHz, $CDCl_3$) δ 4.25 - 4.42 (m, 12H), 4.20 – 4.18 (m, 8H), 3.62 - 3.66 (m, 8H), 1.44 (s, 12H), 1.36 - 1.40 (m, 12H), 1.28 - 1.33 (m, 9H), 1.08 - 1.14 (m, 12H).

Synthesis of tethered G3 dendron 3.4

Dendron **3.2** (220 mg, 0.222 mmol) was dissolved in dry CH_2Cl_2 (15 mL) and stirred for 2 hours with HCTU (101 mg, 0.266 mmol) and DIPEA (0.191 mL, 1.11 mmol). Compound **3.3**[26] (80.0 mg, 0.222 mmol) was then added to the reaction mixture and stirred for 48 hours. It was diluted in CH_2Cl_2 and washed with $KHSO_4$ and Na_2CO_3 twice each, and brine once before being dried with $MgSO_4$ and concentrated *in vacuo*. The crude mixture was purified via column chromatography with a 40% EtOAc/hexanes solvent system yielding 100 mg (39%) of compound **3.4**. ^{1}H NMR ($CDCl_3$): δ 7.31 - 7.39 (m, 5 H), 6.53 - 6.57 (m, 1 H), 5.13 (s, 2 H), 4.27 - 4.37 (m, 12 H), 4.14 - 4.16 (m, 8 H), 3.62 (d, *J*=11.7 Hz, 8 H), 3.30 - 3.35 (m, 2 H), 2.43 - 2.48 (m, 2 H), 1.85 - 1.91 (m, 2 H), 1.42 (s, 12 H), 1.35 (s, 12 H), 1.28 (s, 6 H), 1.25 (s, 3 H), 1.14 (s, 12 H). ^{13}C NMR ($CDCl_3$): δ 173.5, 173.3, 171.7, 171.6, 135.7, 128.5, 128.2, 128.1, 98.0, 67.1, 66.4, 65.8, 64.9, 60.2, 46.8, 46.2, 42.0, 39.4, 31.7, 25.3, 24.1, 21.7, 18.4, 18.3, 17.6, 17.5, 14.1 ppm. ($C_{58}H_{87}NO_{23}$) calculated=1165.5669. HRMS cald $[M+Na]^+$=1188.5561. Obs=1188.5567. SEC: M_n=945 g/mol, $Đ$=1.01. IR ν (cm^{-1}): 3418, 2924, 2854, 1740.

Synthesis of benzyl-deprotected tethered G3 dendron 3.5

Compound **3.4** (100 mg, 85.9 μmol) was dissolved in 4:1 EtOAc/MeOH (15 mL) mixture and purged with nitrogen. Palladium on carbon (10% by wt.) (10 mg) was then added before the reaction was purged with hydrogen and stirred under a hydrogen balloon for four hours. The reaction was then filtered through celite and concentrated *in vacuo* to yield 90 mg (98%) of compound **3.5**, which was taken to the next step without further purification. Complete removal of the benzyl ester was confirmed by ^{1}H NMR spectroscopy. ^{1}H NMR ($CDCl_3$) δ 7.02 - 7.07 (m, 1H), 4.28 - 4.35 (m, 8H), 4.21 - 4.27 (m, 4H), 4.15 - 4.19 (m, 8H), 3.61 - 3.65 (m, 8H), 3.35 - 3.41 (m, 2H), 2.45 - 2.51 (m, 2H), 1.86 - 1.92 (m, 2H), 1.42 (s, 12H), 1.35 (s, 12H), 1.28 (s, 6H), 1.26 (s, 3H), 1.13 (s, 12H).

Synthesis of G3 Janus dendrimer 3.7

Compound **3.5** (90.0 mg, 83.8 μmol) was dissolved in CH_2Cl_2 along with EDC·HCl (15.0 mg, 83.8 μmol), DMAP (10.0 mg, 83.8 μmol) and pyridine (8 μL, 105 μmol). The reaction mixture was stirred for 20 minutes before having hydrophilic block **3.6**[27] (41.0

mg, 69.8 μmol) added to it and being left for 48 hours. At this point the reaction was diluted in CH_2Cl_2 and washed with $KHSO_4$ and Na_2CO_3 twice each, and brine once before being dried with $MgSO_4$ and concentrated *in vacuo*. The residue was purified via prep TLC using a 10% MeOH in EtOAc solvent system. This yielded 30 mg of the desired product. ^{1}H NMR ($CDCl_3$): δ 6.58 (s, 2 H), 6.52 (t, J=5.3 Hz, 1 H), 4.99 (s, 2 H), 4.28 - 4.39 (m, 8 H), 4.20 - 4.28 (m, 6 H), 4.12 - 4.20 (m, 14 H), 3.83 - 3.88 (m, 4 H), 3.77 - 3.81 (m, 2 H), 3.71 - 3.76 (m, 6 H), 3.60 - 3.69 (m, 18 H), 3.53 - 3.58 (m, 6 H), 3.38 (s, 9 H), 3.29 - 3.36 (m, 2 H), 2.44 (t, J=7.0 Hz, 2 H), 1.84 - 1.92 (m, 2 H), 1.39 - 1.45 (m, 12 H), 1.33 - 1.39 (m, 12 H), 1.29 (s, 6 H), 1.27 (m, 3 H), 1.11 - 1.17 (m, 12 H).

Synthesis of benzyl-deprotected G4 dendron 3.9

Dendron **3.8**[24] (600 mg) was dissolved in an EtOAc/MeOH mixture (60 mL, 4:1) and purged with argon for 5 minutes. Pd/C (10% wt) was then added and the resulting mixture was purged with and placed under H_2 for 4 hours. It was then filtered through celite and concentrated *in vacuo* to yield a quantitative amount of compound **3.9**, which was taken to the next step without further purification. Complete removal of the benzyl ester was confirmed by ^{1}H NMR spectroscopy. ^{1}H NMR ($CDCl_3$) δ 4.19 - 4.38 (m, 28H), 4.13 - 4.19 (m, 16H), 3.59 - 3.67 (m, 16H), 1.42 (s, 24H), 1.36 (s, 24H), 1.32 (s, 3H), 1.28 - 1.30 (m, 18H), 1.15 (s, 24H).

Synthesis of tethered G4 dendron 3.10

Dendron **3.9** (550 mg, 0.265 mmol) was dissolved in dry CH_2Cl_2 (15 mL) and stirred for 2 hours with HCTU (120 mg, 0.317 mmol) and DIPEA (0.230 mL, 1.32 mmol). Compound **3.3**[26] (116 mg, 0.317 mmol) was then added to the reaction mixture and stirred for 48 hours. It was diluted in CH_2Cl_2 and washed with $KHSO_4$ and Na_2CO_3 twice each, and brine once before being dried with $MgSO_4$ and concentrated *in vacuo*. The crude mixture was purified via column chromatography with a 40% EtOAc/hexanes solvent system yielding 400 mg (65%) of compound **3.10**. ^{1}H NMR ($CDCl_3$) δ 7.31 - 7.39 (m, 5H), 6.58 - 6.64 (m, 1H), 5.12 (s, 2H), 4.19 - 4.37 (m, 28H), 4.12 - 4.17 (m, 16H), 3.58 - 3.66 (m, 16H), 3.26 - 3.35 (m, 2H), 2.40 - 2.48 (m, 2H), 1.84 - 1.91 (m, 2H), 1.41 (s, 24H), 1.35 (s, 24H), 1.24 - 1.30 (m, 21H), 1.14 (s, 24H).

Synthesis of benzyl-deprotected tethered G4 dendron 3.11

Compound **3.10** (400 mg) was dissolved in 4:1 EtOAc/MeOH (40 mL) mixture and purged with nitrogen. Palladium on carbon (10% by wt.) (40 mg) was then added before the reaction was purged with hydrogen and stirred under a hydrogen balloon for four hours. The reaction was then filtered through celite and concentrated *in vacuo* to a quantitative yield of compound **3.11**, which was taken to the next step without further purification. Complete removal of the benzyl ester was confirmed by ^{1}H NMR spectroscopy. ^{1}H NMR ($CDCl_3$) δ 6.90 - 6.94 (m, 1H), 4.21 - 4.38 (m, 28H), 4.13 - 4.19 (m, 16H), 3.59 - 3.68 (m, 16H), 3.33 - 3.38 (m, 2H), 2.43 - 2.48 (m, 2H), 1.85 - 1.92 (m, 2H), 1.42 (s, 24H), 1.36 (s, 24H), 1.27 - 1.31 (m, 21H), 1.15 (s, 24H).

Synthesis of G4 Janus dendrimer 3.12

Compound **3.11** (73.5 mg, 33.6 μmol) was dissolved in CH_2Cl_2 along with EDC·HCl (9.68 mg, 50.5 μmol), DMAP (6.16 mg, 50.5 μmol) and pyridine (4.07 μL, 50.5 μmol). The reaction mixture was stirred for 20 minutes before having hydrophilic block **3.6**[27] (30.0 mg, 50.5 μmol) added to it and being left for 48 hours. At this point the reaction was diluted in CH_2Cl_2 and washed with $KHSO_4$ and Na_2CO_3 twice each, and brine once before being dried with $MgSO_4$ and concentrated *in vacuo*. The residue was purified via prep TLC using a 20% MeOH in EtOAc solvent system. This yielded 70 mg (75%) of the desired product. ^{1}H NMR ($CDCl_3$) δ 6.88 - 6.94 (m, 1H), 6.58 (s, 2H), 4.98 (s, 2H), 4.20 - 4.36 (m, 40H), 4.12 - 4.18 (m, 28H), 3.83 - 3.87 (m, 3H), 3.77 - 3.81 (m, 2H), 3.70 - 3.76 (m, 5H), 3.59 - 3.69 (m, 33H), 3.51 - 3.59 (m, 6H), 3.37 (s, 9H), 3.27 - 3.34 (m, 2H), 2.39 - 2.48 (m, 2H), 1.82 - 1.90 (m, 2H), 1.41 - 1.42 (m, 24H), 1.34 - 1.36 (m, 24H), 1.27 - 1.30 (m, 21H), 1.14 (s, 24H).

Synthesis of lauryl G2 dendron 3.14

Compound **3.13**[24] (250 mg, 0.565 mmol) was dissolved in pyridine (5 mL) and placed in an ice bath. After stirring on ice for five minutes, lauroyl chloride (507 mg, 2.32 mmol) was added dropwise and left to stir at room temperature overnight. The reaction mixture was diluted in CH_2Cl_2 and washed twice with $KHSO_4$ and once with brine. The organic fraction was dried with $MgSO_4$ and concentrated *in vacuo* to give a quantitative yield of compound **3.14**. ^{1}H NMR ($CDCl_3$): δ 7.32 - 7.39 (m, 5 H), 5.16 (s, 2 H), 4.28 (q, *J*=11.1

Hz, 4 H), 4.10 - 4.20 (m, 8 H), 2.28 (t, *J*=7.6 Hz, 8 H), 1.52 - 1.62 (m, 16 H), 1.20 - 1.35 (m, 56 H), 1.17 (s, 6 H), 0.89 (t, *J*=7.0 Hz, 12 H). ^{13}C NMR ($CDCl_3$): δ 173.1, 172.0, 171.9, 135.3, 128.6, 128.4, 128.3, 67.1, 65.7, 64.9, 46.7, 46.3, 41.8, 34.0, 31.9, 31.5, 30.2, 29.6, 29.4, 29.3, 29.2, 29.1, 24.8, 22.6, 17.7, 17.5, 14.1 ppm. ($C_{70}H_{120}O_{14}$) calculated=1184.8678. HRMS $[M+Na]^+$ cald=1207.8570. Obs=1207.8576. SEC: M_n=1450 g/mol, *Đ*=1.10. IR ν (cm^{-1}): 2923, 2853, 1741.

Synthesis of benzyl-deprotected lauryl G2 dendron 3.15

Dendron **3.14** (1.00 g) was dissolved in an EtOAc/MeOH mixture (100 mL, 4:1) and purged with argon for 5 minutes. Pd/C (10% wt) was then added and the resulting mixture was purged with and placed under H_2 for 4 hours. It was then filtered through celite and concentrated *in vacuo* to yield a quantitative amount of compound **3.15**, which was taken to the next step without further purification. Complete removal of the benzyl ester was confirmed by ^{1}H NMR spectroscopy. ^{1}H NMR ($CDCl_3$) δ 4.16 - 4.32 (m, 12H), 2.30 (t, *J* = 7.62 Hz, 8H), 1.53 - 1.64 (m, 16H), 1.18 - 1.36 (m, 62H), 0.84 - 0.93 (m, 12H).

Synthesis of tethered lauryl G2 dendron 3.16

Dendron **3.15** (760 mg, 0.694 mmol) was dissolved in dry CH_2Cl_2 (50 mL) and stirred for 2 hours with HCTU (316 mg, 0.832 mmol) and DIPEA (0.604 mL, 3.47 mmol). Compound **3.3**[26] (304 mg, 0.832 mmol) was then added to the reaction mixture and stirred for 48 hours. It was diluted in CH_2Cl_2 and washed with $KHSO_4$ and Na_2CO_3 twice each, and brine once before being dried with $MgSO_4$ and concentrated *in vacuo*. The crude mixture was purified via column chromatography with a 10% EtOAc/hexanes solvent system yielding 400 mg (45%) of compound **3.16**. ^{1}H NMR ($CDCl_3$): δ 7.31 - 7.40 (m, 5 H), 6.48 - 6.54 (m, 1 H), 5.13 (s, 2 H), 4.13 - 4.29 (m, 12 H), 3.28 - 3.37 (m, 2 H), 2.41 - 2.49 (m, 2 H), 2.25 - 2.34 (m, 8 H), 1.83 - 1.93 (m, 2 H), 1.52 - 1.67 (m, 16 H), 1.15 - 1.37 (m, 62 H), 0.83 - 0.94 (m, 12 H). ^{13}C NMR ($CDCl_3$): δ 173.3, 173.2, 172.1, 171.7, 135.7, 128.5, 128.3, 128.2, 66.9, 66.5, 65.0, 56.6, 46.5, 46.3, 39.4, 34.0, 31.9, 29.6, 29.5, 29.5, 29.3, 29.3, 29.1, 24.8, 24.3, 22.7, 17.7, 14.1 ppm. ($C_{74}H_{127}NO_{15}$) calculated=1269.9206. HRMS $[M+Na]^+$=1292.9098. Obs=1292.9103. SEC: M_n=2175 g/mol, *Đ*=1.36. IR ν (cm^{-1}): 3410, 2924, 2854, 1740.

Synthesis of benzyl-deprotected tethered lauryl G2 dendron 3.17

Compound **3.16** (100 mg) was dissolved in 4:1 EtOAc/MeOH (15 mL) mixture and purged with nitrogen. Palladium on carbon (10% by wt.) (10 mg) was then added before the reaction was purged with hydrogen and stirred under a hydrogen balloon for four hours. The reaction was then filtered through celite and concentrated in vacuo to yield 90 mg (98%) of compound **3.17**, which was taken to the next step without further purification. Complete removal of the benzyl ester was confirmed by ^{1}H NMR spectroscopy. ^{1}H NMR ($CDCl_3$) δ 6.73 - 6.84 (m, 1H), 4.10 - 4.27 (m, 12H), 3.24 - 3.42 (m, 2H), 2.39 - 2.53 (m, 2H), 2.25 - 2.39 (m, 8H), 1.77 - 1.94 (m, 2H), 1.54 - 1.70 (m, 16H), 1.18 - 1.34 (m, 62H), 0.89 (t, J = 7.04 Hz, 12H).

Synthesis of lauryl G2 Janus dendrimer 3.18

Compound **3.17** (50.0 mg, 42.4 μmol) was dissolved in CH_2Cl_2 along with EDC·HCl (12.2 mg, 63.5 μmol), DMAP (7.75 mg, 63.5 μmol) and pyridine (4.90 μL, 63.5 μmol). The reaction mixture was stirred for 20 minutes before having hydrophilic block **3.6**[27] (37.8 mg, 63.5 μmol) added to it and being left for 48 hours. At this point the reaction was diluted in CH_2Cl_2 and washed with $KHSO_4$ and Na_2CO_3 twice each, and brine once before being dried with $MgSO_4$ and concentrated in vacuo. The residue was purified via prep TLC using a 10% MeOH in EtOAc solvent system. This yielded 60 mg (81%) of the desired product. ^{1}H NMR ($CDCl_3$): δ 6.58 (s, 2 H), 6.47 - 6.50 (m, 1 H), 5.00 (s, 2 H), 4.13 - 4.26 (m, 18 H), 3.83 - 3.88 (m, 4 H), 3.77 - 3.82 (m, 2 H), 3.71 - 3.76 (m, 6 H), 3.63 - 3.70 (m, 12 H), 3.53 - 3.58 (m, 6 H), 3.38 (s, 9 H), 3.30 - 3.34 (m, 2 H), 2.42 - 2.47 (m, 2 H), 2.30 (t, J=7.6 Hz, 8 H), 1.85 - 1.90 (m, 2 H), 1.55 - 1.64 (m, 16 H), 1.20 - 1.34 (m, 62 H), 0.89 (t, J=6.7 Hz, 12 H). ^{13}C NMR ($CDCl_3$): δ 173.2, 173.2, 173.1, 172.1, 171.7, 152.7, 131.6, 131.0, 110.0, 72.3, 71.9, 70.8, 70.7, 70.5, 70.5, 69.7, 68.9, 66.8, 65.0, 59.0, 46.5, 46.3, 34.0, 31.9, 31.8, 29.6, 29.5, 29.3, 29.2, 29.1, 24.8, 22.6, 17.7, 14.1 ppm. ($C_{95}H_{169}NO_{27}$) calculated=1756.1882. HRMS $[M+Na]^+$=1779.1774. Obs=1779.1780. SEC: M_n=2355 g/mol, $Đ$=1.01. IR ν (cm^{-1}): 3366, 2925, 2855, 1742.

Synthesis of acetonide-deprotected tethered G3 dendron 3.19

Compound **3.4** (720 mg, 0.675 mmol) was dissolved in MeOH (70mL) and concentrated sulfuric acid (0.7 mL). The mixture was stirred at room temperature for 2 h before being

concentrated *in vacuo* to remove most of the methanol. It was then diluted with EtOAc and washed with $NaHCO_3$ (1M) once, dried with Mg_2SO_4, filtered and concentrated *in vacuo* to yield 99.7% of compound **3.19** (610 mg). Complete removal of acetonide groups was confirmed by ^{1}H NMR spectroscopy and compound **3.19** was carried through without any further purification. ^{1}H NMR ($CDCl_3$) δ 7.30 - 7.38 (m, 5H), 7.01 - 7.06 (m, 1H), 5.11 (s, 2H), 4.19 - 4.34 (m, 12H), 3.73 - 3.81 (m, 8H), 3.66 - 3.73 (m, 8H), 3.23 - 3.29 (m, 2H), 2.40 - 2.45 (m, 2H), 1.82 - 1.88 (m, 2H), 1.29 (s, 6H), 1.25 (s, 3H), 1.07 (s, 9H).

Synthesis of tethered lauryl G3 dendron 3.20

Dendron **3.19** (329 mg, 0.327 mmol) was dissolved in pyridine (5 mL) and placed in an ice bath. After stirring on ice for five minutes, lauroyl chloride (579 mg, 2.65 mmol) was added dropwise and left to stir at room temperature overnight. The reaction mixture was diluted in CH_2Cl_2 and washed twice with $KHSO_4$ and once with brine. The organic fraction was dried with $MgSO_4$ and concentrated *in vacuo* to give a quantitative yield of compound **3.19**. ^{1}H NMR ($CDCl_3$): δ 7.31 - 7.39 (m, 5 H), 6.63 - 6.70 (m, 1 H), 5.12 (s, 2 H), 4.12 - 4.31 (m, 28 H), 3.27 - 3.36 (m, 2 H), 2.41 - 2.47 (m, 2 H), 2.23 - 2.33 (m, 16 H), 1.83 - 1.92 (m, 2 H), 1.50 - 1.66 (m, 32 H), 1.16 - 1.36 (m, 133 H), 0.82 - 0.94 (m, 24 H). ^{13}C NMR ($CDCl_3$, 101MHz): δ 173.0, 171.9, 171.4, 171.3, 149.8, 135.7, 128.4, 128.1, 128.0, 77.3, 76.7, 66.2, 65.2, 64.7, 46.6, 46.2, 46.2, 33.8, 31.7, 31.6, 29.5, 29.3, 29.2, 29.1, 29.0, 24.7, 24.3, 22.5, 17.6, 17.3, 13.9 ppm. ($C_{142}H_{247}NO_{31}$) calculated=2462.7782. HRMS $[M+Na]^+$=2485.7674. Obs=2485.7674. SEC: M_n=3336 g/mol, $Đ$=1.03. IR ν (cm^{-1}): 3425, 2923, 2854, 1739.

Synthesis of benzyl-deprotected tethered lauryl G3 dendron 3.21

Compound **3.20** (256 mg) was dissolved in 4:1 EtOAc/MeOH (25 mL) mixture and purged with nitrogen. Palladium on carbon (10% by wt.) (25.6 mg) was then added before the reaction was purged with hydrogen and stirred under a hydrogen balloon for four hours. The reaction was then filtered through celite and concentrated in vacuo to quantitatively yield 200 mg of compound **3.21**, which was taken to the next step without further purification. Complete removal of the benzyl ester was confirmed by ^{1}H NMR spectroscopy. ^{1}H NMR ($CDCl_3$) δ 6.86 - 6.91 (m, 1H), 4.15 - 4.30 (m, 28H), 3.34 - 3.41

(m, 2H), 2.45 - 2.50 (m, 2H), 2.27 - 2.33 (m, 16H), 1.89 - 1.94 (m, 2H), 1.55 - 1.63 (m, 32H), 1.19 - 1.34 (m, 133H), 0.89 (t, J = 7.04 Hz, 24H).

Synthesis of lauryl G3 Janus dendrimer 3.22

Compound **3.21** (50.0 mg, 21.1 μmol) was dissolved in CH_2Cl_2 along with EDC·HCl (6.06 mg, 31.6 μmol), DMAP (3.85 mg, 31.6 μmol) and pyridine (2.55 μL, 31.6 μmol). The reaction mixture was stirred for 20 minutes before having hydrophilic block **3.6**[27] (18.8 mg, 31.6 μmol) added to it and being left for 48 hours. At this point the reaction was diluted in CH_2Cl_2 and washed with $KHSO_4$ and Na_2CO_3 twice each, and brine once before being dried with $MgSO_4$ and concentrated in vacuo. The residue was purified via prep TLC using a 10% MeOH in EtOAc solvent system. This yielded 30 mg of the desired product. ^{1}H NMR ($CDCl_3$): δ 6.62 - 6.65 (m, 1 H), 6.58 (s, 2 H), 4.98 (s, 2 H), 4.19 - 4.30 (m, 28 H), 4.13 - 4.19 (m, 6 H), 3.84 - 3.87 (m, 4 H), 3.78 - 3.81 (m, 2 H), 3.72 - 3.75 (m, 6 H), 3.64 - 3.68 (m, 12 H), 3.54 - 3.56 (m, 6 H), 3.38 (s, 9 H), 3.29 - 3.34 (m, 2 H), 2.40 - 2.45 (m, 2 H), 2.30 (t, J=7.6 Hz, 16 H), 1.85 - 1.89 (m, 2 H), 1.55 - 1.64 (m, 32 H), 1.21 - 1.33 (m, 133 H), 0.88 (t, J=7.0 Hz, 24 H). ^{13}C NMR ($CDCl_3$): δ 173.2, 173.2, 173.1, 172.9, 172.0, 171.5, 152.7, 151.4, 151.2, 110.0, 77.2, 76.8, 71.9, 70.8, 69.7, 68.9, 64.8, 59.0, 46.7, 46.3, 34.0, 31.9, 29.6, 29.5, 29.3, 29.3, 29.1, 24.8, 22.7, 17.8, 14.1 ppm. ($C_{163}H_{289}NO_{43}$) calculated=2949.0458. HRMS $[M+Na]^+$=2972.0351. Obs=2972.0356. SEC: M_n=4038 g/mol, $Đ$=1.09. IR ν (cm^{-1}): 3419, 2924, 2854, 1741.

Synthesis of azide-terminated hydrophilic block 3.24

Compound **3.23**[30] (300 mg, 0.458 mmol) was combined in dry THF (1 mL) with LiCl (38.8 mg, 0.915 mmol) and $NaBH_4$ (34.6 mg, 0.915 mmol). Ethanol (1 mL) was then added and the mixture was left to stir overnight at room temperature. The reaction was subsequently diluted in 0.5 M HCl and extracted with three times with EtOAc. The organic fractions were combined, dried with $MgSO_4$ and concentrated *in vacuo*. The resulting oil was purified via column chromatography using EtOAc as the eluent to give compound **3.24** (29.5 mg) in 10% yield. ^{1}H NMR ($CDCl_3$): δ 6.63 (s, 2 H), 4.60 (s, 2 H), 4.17 - 4.20 (m, 4 H), 4.14 - 4.17 (m, 2 H), 3.85 - 3.88 (m, 4 H), 3.80 - 3.83 (m, 2 H), 3.73 - 3.76 (m, 6 H), 3.66 - 3.70 (m, 12 H), 3.39 (t, J=5.0 Hz, 6 H). ^{13}C NMR ($CDCl_3$): δ 152.4, 137.2, 136.7, 106.0, 72.1, 70.4, 69.7, 68.5, 64.8, 50.5 ppm. ($C_{25}H_{41}N_9O_{10}$)

calculated=627.2976. HRMS $[M+Na]^+$ cald=650.2869. Obs=650.2874. IR ν (cm^{-1}): 3455, 2869, 2097.

Synthesis of azide-terminated lauryl G3 Janus dendrimer 3.25

Compound **3.21** (69.4 mg, 29.2 μmol) was dissolved in CH_2Cl_2 along with EDC·HCl (8.40 mg, 43.8 μmol), DMAP (5.34 mg, 43.8 μmol) and pyridine (3.5 μL, 43.8 μmol). The reaction mixture was stirred for 20 minutes before having hydrophilic block **3.24** (27.5 mg, 43.8 μmol) added to it and being left for 48 hours. At this point the reaction was diluted in CH_2Cl_2 and washed with $KHSO_4$ and Na_2CO_3 twice each, and brine once before being dried with $MgSO_4$ and concentrated in vacuo. The residue was purified via dialysis using a 1:1 MeOH/EtOAc solvent system. This yielded 55 mg, 63% of the desired product. ^1H NMR ($CDCl_3$): δ 6.57 - 6.62 (m, 3 H), 5.36 (s, 2 H), 4.15 - 4.31 (m, 34 H), 3.84 - 3.87 (m, 4 H), 3.80 - 3.83 (m, 2 H), 3.71 - 3.76 (m, 4 H), 3.65 - 3.71 (m, 14 H), 3.39 (t, *J*=5.1 Hz, 6 H), 3.29 - 3.34 (m, 2 H), 2.39 - 2.43 (m, 2 H), 2.30 (t, *J*=7.6 Hz, 16 H), 1.85 - 1.90 (m, 2 H), 1.56 - 1.64 (m, 32 H), 1.22 - 1.34 (m, 133 H), 0.86 - 0.92 (m, 24 H). ^{13}C NMR ($CDCl_3$): δ 173.2, 173.2, 173.0, 172.0, 171.6, 171.5, 152.7, 131.1, 125.5, 107.9, 77.2, 76.8, 72.3, 70.9, 70.7, 70.6, 70.5, 70.1, 70.0, 69.8, 68.9, 68.0, 67.1, 66.5, 65.3, 64.9, 50.7, 46.7, 46.4, 46.3, 39.4, 34.2, 34.0, 31.9, 31.8, 31.7, 30.3, 29.7, 29.6, 29.5, 29.3, 29.3, 29.1, 25.6, 24.9, 24.6, 22.7, 22.5, 21.2, 17.8, 17.5, 14.2, 14.1 ppm. ($C_{160}H_{280}N_{10}O_{40}$) calculated=2982.0183. HRMS $[M+Na]^+$ cald=3005.0076. Obs=3005.0081. LRMS $[(M+2K)/2]^+$ cald=1529.0869. Obs=1532.0. SEC: M_n=4329 g/mol, *Đ*=1.06. IR ν (cm^{-1}): 3502, 2922, 2853, 2100, 1740.

2 kg/mol PEO surface functionalization of dendrimer assemblies

Assemblies were made as described above, however using 80% Janus dendrimer **3.22** (0.8 mg, 0.067 μmol) and 20% Janus dendrimer **3.25** (0.2 mg, 0.067 μmol). After stirring 30 minutes, 2 kg/mol PEO-pentynoic ester (1.67 mg, 0.8 μmol), $CuCl_2$ (4.57 μg, 0.0268 μmol) and sodium ascorbate (5.31 μg, 0.0268 μmol) were added and stirred overnight. The reaction mixture was dialyzed against water in a 10 kg/mol MWCO membrane overnight to yield 2 kg/mol PEO surface functionalized dendrimer assemblies.

Janus dendrimer self-assembly

An 8 mg/mL solution of the dendrimer was prepared in DMSO or THF and was stirred overnight to ensure complete solubilization. It was then filtered using a Dynagard® polypropylene syringe filter (0.2 μm, surface area 0.8 m^2). Next, either 0.1 mL of the DMSO or THF solution was rapidly injected into 0.9 mL of filtered (Acrodisc® 25 mm syringe filter with 0.1 μm Supor® membrane) deionized water with rapid stirring or 0.9 mL of filtered, deionized water was added to 0.1 mL of the DMSO solution with rapid stirring over a period of ~ 1 minute. The resulting suspension was then dialyzed against deionized water using a 3500 g/mol MWCO membrane. Note, Janus dendrimers **3.22** and **3.25** were studied only in THF due to insolubility in DMSO. In addition, they were not dialyzed as this caused them to oil out. Instead they were stirred overnight, uncapped to remove THF.

Dynamic light scattering (DLS)

DLS analysis was run using the 0.8 mg/mL suspensions of polymer assemblies prepared as described above. The measurements were performed in a 1 cm pathlength glass cuvette using a Zetasizer Nano ZS instrument from Malvern. Fifteen repeat diameter measurements were made per run to determine an average particle diameter and three runs per sample were done.

Transmission electron microscopy (TEM)

The suspension of assemblies (10 μL, 0.08 mg/mL) was placed on a copper Formvar/carbon support film coated grid and was left to dry overnight. Imaging was performed using a Phillips CM10 microscope operating at 80 kV with a 40 μm aperture.

3.4 Conclusions

A library of Janus dendrimers was synthesized and their self-assembly in water was studied using nano-precipitation particle assembly procedures. Most of these dendrimers formed solid aggregates of varying sizes; however Janus dendrimer **3.22** formed polydisperse dendrimersomes as indicated by TEM imaging. The azide analogue of this Janus dendrimer **3.25** did not form dendrimersomes nor did a mix of this dendrimer with the vesicle-forming dendrimer **3.22**, suggesting that the azide moieties may upset the

hydrophilic-hydrophobic balance of the system. Despite this, a surface functionalization reaction was performed on the assemblies formed by the 80/20 mixture of **3.22** and **3.25**. IR spectroscopy suggested that this reaction was successful and that if it is possible to prepare dendrimersomes from these dendrimers, it should be possible to functionalize their surfaces.

3.5 References

1. Discher, D. E.; Eisenberg, A., *Science* **2002,** *297* (5583), 967-973.
2. Ahmed, F.; Photos, P. J.; Discher, D. E., *Drug Dev. Res.* **2006,** *67* (1), 4-14.
3. Soo, P. L.; Eisenberg, A., *J. Polym. Sci., Part B: Polym. Phys.* **2004,** *42* (6), 923-938.
4. Zhang, L.; Eisenberg, A., *Science* **1995,** *268* (5218), 1728-1731.
5. Gillies, E. R.; Frechet, J. M. J., *Drug Discovery Today* **2005,** *10* (1), 35-43.
6. Gillies, E. R.; Li, B.; Martin, A. L., *J. Am. Chem. Soc.* **2008,** *98*, 311-312.
7. Martin, A. L.; Li, B.; Gillies, E. R., *J. Am. Chem. Soc.* **2009,** *131* (2), 734-741.
8. Nazemi, A.; Gillies, E. R., *Braz. J. Pharm. Sci.* **2013,** *49* (Spec. Issue), 15-32.
9. Nazemi, A.; Haeryfar, S. M. M.; Gillies, E. R., *Langmuir* **2013,** *29* (21), 6420-6428.
10. Cabane, E.; Malinova, V.; Menon, S.; Palivan, C. G.; Meier, W., *Soft Matter* **2011,** *7* (19), 9167-9176.
11. Perrault, S. P.; Chan, W. C. W., *Proc. Natl. Acad. Sci. U. S. A.* **2010,** *107* (25), 11194-11199, S11194/11191-S11194/11194.
12. Liu, S.; Maheshwari, R.; Kiick, K. L., *Macromolecules* **2009,** *42* (1), 3-13.
13. Elsabahy, M.; Wooley, K. L., *Chem. Soc. Rev.* **2012,** *41* (7), 2545-2561.
14. Egli, S.; Schlaad, H.; Bruns, N.; Meier, W., *Polymers* **2011,** *3* (1), 252-280.
15. Nazemi, A.; Amos, R. C.; Bonduelle, C. V.; Gillies, E. R., *J. Polym. Sci., Part A: Polym. Chem.* **2011,** *49* (12), 2546-2559.
16. Amos, R. C.; Nazemi, A.; Bonduelle, C. V.; Gillies, E. R., *Soft Matter* **2012,** *8* (21), 5947-5958.
17. Percec, V.; Leowanawat, P.; Sun, H.-J.; Kulikov, O.; Nusbaum, C. D.; Tran, T. M.; Bertin, A.; Wilson, D. A.; Peterca, M.; Zhang, S.; Kamat, N. P.; Vargo, K.; Moock, D.; Johnston, E. D.; Hammer, D. A.; Pochan, D. J.; Chen, Y.; Chabre, Y. M.; Shiao, T. C.; Bergeron-Brlek, M.; Andre, S.; Roy, R.; Gabius, H.-J.; Heiney, P. A., *J. Am. Chem. Soc.* **2013,** *135* (24), 9055-9077.

18. Zhang, S.; Moussodia, R.-O.; Sun, H.-J.; Leowanawat, P.; Muncan, A.; Nusbaum, C. D.; Chelling, K. M.; Heiney, P. A.; Klein, M. L.; Andre, S.; Roy, R.; Gabius, H.-J.; Percec, V., *Angew. Chem., Int. Ed.* **2014,** *53* (41), 10899-10903.

19. Peterca, M.; Percec, V.; Leowanawat, P.; Bertin, A., *J. Am. Chem. Soc.* **2011,** *133* (50), 20507-20520.

20. Percec, V.; Wilson, D. A.; Leowanawat, P.; Wilson, C. J.; Hughes, A. D.; Kaucher, M. S.; Hammer, D. A.; Levine, D. H.; Kim, A. J.; Bates, F. S.; Davis, K. P.; Lodge, T. P.; Klein, M. L.; De Vane, R. H.; Aqad, E.; Rosen, B. M.; Argintaru, A. O.; Sienkowska, M. J.; Rissanen, K.; Nummelin, S.; Ropponen, J., *Science* **2010,** *328* (5981), 1009-1014.

21. Shi, X.; Wang, S. H.; Van Antwerp, M. E.; Chen, X.; Baker, J. R., Jr., *Analyst* **2009,** *134* (7), 1373-1379.

22. Hill, E.; Shukla, R.; Park, S. S.; Baker, J. R., *Bioconjugate Chem.* **2007,** *18* (6), 1756-1762.

23. Guo, R.; Yao, Y.; Cheng, G.; Wang, S. H.; Li, Y.; Shen, M.; Zhang, Y.; Baker, J. R.; Wang, J.; Shi, X., *RSC Adv.* **2012,** *2* (1), 99-102.

24. Gillies, E. R.; Frechet, J. M. J., *J. Am. Chem. Soc.* **2002,** *124* (47), 14137-14146.

25. Ihre, H.; Padilla de Jesus, O. L.; Frechet, J. M. J., *J. Am. Chem. Soc.* **2001,** *123* (25), 5908-5917.

26. Hada, N.; Shida, Y.; Negishi, N.; Schweizer, F.; Takeda, T., *Chem. Pharm. Bull.* **2009,** *57* (10), 1081-1088.

27. Torres de Pinedo, A.; Penalver, P.; Morales, J. C., *Food Chem.* **2007,** *103* (1), 55-61.

28. Nazemi, A.; Gillies, E. R., *Chem. Commun.* **2014,** *50* (76), 11122-11125.

29. Zhang, S.; Sun, H.-J.; Hughes, A. D.; Draghici, B.; Lejnieks, J.; Leowanawat, P.; Bertin, A.; Otero De Leon, L.; Kulikov, O. V.; Chen, Y.; Pochan, D. J.; Heiney, P. A.; Percec, V., *ACS Nano* **2014,** *8* (2), 1554-1565.

30. Song, H.-O.; Lee, B.; Bhusal, R. P.; Park, B.; Yu, K.; Chong, C.-K.; Cho, P.; Kim, S. Y.; Kim, H. S.; Park, H., *PLoS One* **2012,** *7* (11), e48459.

Chapter 4

4.1 Conclusions and Future Work

The work described in this thesis presented the synthesis of novel polymeric and dendritic systems as well as studies toward their potential utility for various biomedical applications, specifically drug delivery. The formulation of smart materials is always a highly sought after pursuit for it is the future of biological applications. Shown herein is a novel photoresponsive triblock copolymer which self-assembles into polymersomes, the first to date which has been synthesized with a completely photodegradable hydrophobic block. Its self-assembly into polymersomes and subsequent photoinduced degradation showcased its capacity for encapsulation and release of both hydrophilic and hydrophobic cargo molecules. Herein lies the future work involving this system. Although the goal of synthesizing a completely photodegradable hydrophobic block was achieved, the polymerization process yielded a homopolymer that was relatively polydisperse. For use in drug delivery applications, a low polymer dispersity is necessary so that the presence of comparatively high molecular weight polymers does not prolong the degradation process and result in large polymer degradation products being left in the body. By optimizing the reaction conditions such as time and monomer ratio, this can be mitigated. Another option however, is to use a more inherently monodisperse polymer system such as Janus dendrimers. Also, further studies to show the encapsulation and release of hydrophilic and hydrophobic molecules will be able to elaborate the potential of a stimuli-responsive polymersome system. For example the encapsulation and release of fluorescein as a hydrophilic drug model and nile red as a hydrophobic drug model will be able to show the capacity for polymersomes to load cargo in their hydrophilic core and hydrophobic bilayer membrane. This sort of study would elucidate the potential for applications, especially drug delivery.

Also described in this thesis was a novel Janus dendrimer system which was studied and shown to assemble into dendrimersomes. After assembly of a number of Janus

dendrimers, an acylated G3 bis-MPA polyester dendron coupled with a tris-tri(ethylene glycol) gallic alcohol had a suitable hydrophilic weight fraction and membrane properties to form vesicles when self-assembled by adding a THF solution of the Janus dendrimer into water. When the same dendron was coupled to an azide-terminated analogue of the same hydrophilic block it did not yield a vesicle morphology but rather solid aggregates. Despite this, these aggregates were still able to undergo surface functionalization with 2 kg/mol PEO-alkyne via CuAAC chemistry. By doing so, it showed the potential for functionalizing this system with other ligands such as carbohydrates, imaging agents, targeting moieties or even other dendritic systems. Therefore future work for this project includes tuning the chemical structure and/or optimizing the particle assembly protocols to form vesicles with the azide-terminated Janus dendrimer either on its own or as a mixture with the non-azide Janus dendrimer. Perhaps by augmenting the length of the acyl chains, shorter or longer, or changing the generation of polyester dendron backbone, G1 or G2, an optimal hydrophobic unit will be found. The ideal hydrophobic block would combine the right hydrophilic volume fraction with adequately flexible and malleable hydrophobic blocks that can interact with each other, such that when vesicles are formed the membrane will be robust enough that introduction of a small percentage of azide units will not disrupt the assembly process and to survive the drying process during TEM sample preparation. That being said, many research groups characterize their assemblies using cryo-TEM, where instead of dehydrating the assemblies for imaging, they are preserved in their original aqueous environment, thus eliminating the drying step completely. Perhaps outsourcing the imaging to a facility with cryo-TEM would be worthwhile. Following the optimization of the assemblies, they can then be functionalized with those other moieties in order to impart various biological functions to the dendrimersomes such as macromolecule binding, receptor targeting or metal chelating. The effectiveness of coupling these ligands using CuAAC chemistry can then be quantified using infrared spectroscopy by comparing the transmittance percentages of the azide stretch at 2100 cm^{-1} before and after the reaction and relating that value to the concentration using Beer's Law.

4.2 Appendix 1: Permission to Reuse Copyrighted Material

JOHN WILEY AND SONS LICENSE

TERMS AND CONDITIONS

Jul 20, 2015

This Agreement between James T McIntosh ("You") and John Wiley and Sons ("John Wiley and Sons") consists of your license details and the terms and conditions provided by John Wiley and Sons and Copyright Clearance Center.

License Number	3673190416991
License date	Jul 20, 2015
Licensed Content Publisher	John Wiley and Sons
Licensed Content Publication	Drug Development Research
Licensed Content Title	Polymersomes as viral capsid mimics
Licensed Content Author	Fariyal Ahmed,Peter J. Photos,Dennis E. Discher
Licensed Content Date	May 11, 2006
Pages	11
Type of use	Dissertation/Thesis
Requestor type	University/Academic
Format	Print and electronic
Portion	Figure/table
Number of Figures/tables	1
Original Wiley Figure/table number(s)	Figure 2a
Will you be translating?	No
Title of your thesis / dissertation	Stimuli-Responsive Polymersomes and Surface-Functionalized Dendrimersomes: Platforms for Biomedical Applications
Expected completion date	Aug 2015
Expected size (number of pages)	115

TERMS AND CONDITIONS

This copyrighted material is owned by or exclusively licensed to John Wiley & Sons, Inc. or one of its group companies (each a"Wiley Company") or handled on behalf of a society with which a Wiley Company has exclusive publishing rights in relation to a particular work (collectively "WILEY"). By clicking □accept□ in connection with completing this licensing transaction, you agree that the following terms and conditions apply to this transaction (along with the billing and payment terms and conditions established by the Copyright Clearance Center Inc., ("CCC's Billing and Payment terms and conditions"), at the time that you opened your Rightslink account (these are available at any time at http://myaccount.copyright.com).

Terms and Conditions

- The materials you have requested permission to reproduce or reuse (the "Wiley Materials") are protected by copyright.
- You are hereby granted a personal, non-exclusive, non-sub licensable (on a stand-alone basis), non-transferable, worldwide, limited license to reproduce the Wiley Materials for the purpose specified in the licensing process. This license is for a one-time use only and limited to any maximum distribution number specified in the license. The first instance of republication or reuse granted by this licence must be completed within two years of the date of the grant of this licence (although copies prepared before the end date may be distributed thereafter). The Wiley Materials shall not be used in any other manner or for any other purpose, beyond what is granted in the license. Permission is granted subject to an appropriate acknowledgement given to the author, title of the material/book/journal and the publisher. You shall also duplicate the copyright notice that appears in the Wiley publication in your use of the Wiley Material. Permission is also granted on the understanding that nowhere in the text is a previously published source acknowledged for all or part of this Wiley Material. Any third party content is expressly excluded from this permission.
- With respect to the Wiley Materials, all rights are reserved. Except as expressly granted by the terms of the license, no part of the Wiley Materials may be copied, modified, adapted (except for minor reformatting required by the new Publication), translated, reproduced, transferred or distributed, in any form or by any means, and no derivative works may be made based on the Wiley Materials without the prior permission of the respective copyright owner. You may not alter, remove or suppress in any manner any copyright, trademark or other notices displayed by the Wiley Materials. You may not license, rent, sell, loan, lease, pledge, offer as security, transfer or assign the Wiley Materials on a stand-alone basis, or any of the rights granted to you hereunder to any other person.
- The Wiley Materials and all of the intellectual property rights therein shall at all times remain the exclusive property of John Wiley & Sons Inc, the Wiley Companies, or their respective licensors, and your interest therein is only that of having possession of and the right to reproduce the Wiley Materials pursuant to Section 2 herein during the continuance of this Agreement. You agree that you own no right, title or interest in or to the Wiley Materials or any of the intellectual property rights therein. You shall have no rights hereunder other than the license as provided for above in Section 2. No right, license or interest to any trademark, trade name, service mark or other branding ("Marks") of WILEY or its licensors is granted hereunder, and you agree that you shall not assert any such right, license or interest with respect thereto.
- NEITHER WILEY NOR ITS LICENSORS MAKES ANY WARRANTY OR REPRESENTATION OF ANY KIND TO YOU OR ANY THIRD PARTY, EXPRESS, IMPLIED OR STATUTORY, WITH RESPECT TO THE MATERIALS OR THE ACCURACY OF ANY INFORMATION CONTAINED IN THE MATERIALS, INCLUDING, WITHOUT LIMITATION, ANY IMPLIED WARRANTY OF MERCHANTABILITY, ACCURACY, SATISFACTORY QUALITY, FITNESS FOR A PARTICULAR PURPOSE, USABILITY, INTEGRATION OR NON-INFRINGEMENT AND ALL SUCH WARRANTIES ARE HEREBY EXCLUDED BY WILEY AND ITS LICENSORS AND WAIVED BY YOU
- WILEY shall have the right to terminate this Agreement immediately upon breach of this Agreement by you.
- You shall indemnify, defend and hold harmless WILEY, its Licensors and their respective directors, officers, agents and employees, from and against any actual or threatened claims, demands, causes of action or proceedings arising from any breach of this Agreement by you.
- IN NO EVENT SHALL WILEY OR ITS LICENSORS BE LIABLE TO YOU OR ANY OTHER PARTY OR ANY OTHER PERSON OR ENTITY FOR ANY SPECIAL, CONSEQUENTIAL, INCIDENTAL, INDIRECT, EXEMPLARY OR PUNITIVE DAMAGES, HOWEVER CAUSED, ARISING OUT OF OR IN CONNECTION WITH THE DOWNLOADING, PROVISIONING, VIEWING OR USE OF THE MATERIALS REGARDLESS OF THE FORM OF ACTION, WHETHER FOR BREACH OF CONTRACT, BREACH OF WARRANTY, TORT, NEGLIGENCE, INFRINGEMENT OR OTHERWISE (INCLUDING, WITHOUT LIMITATION, DAMAGES BASED ON LOSS OF PROFITS, DATA, FILES, USE, BUSINESS OPPORTUNITY OR CLAIMS OF THIRD PARTIES), AND WHETHER

OR NOT THE PARTY HAS BEEN ADVISED OF THE POSSIBILITY OF SUCH DAMAGES. THIS LIMITATION SHALL APPLY NOTWITHSTANDING ANY FAILURE OF ESSENTIAL PURPOSE OF ANY LIMITED REMEDY PROVIDED HEREIN.

- Should any provision of this Agreement be held by a court of competent jurisdiction to be illegal, invalid, or unenforceable, that provision shall be deemed amended to achieve as nearly as possible the same economic effect as the original provision, and the legality, validity and enforceability of the remaining provisions of this Agreement shall not be affected or impaired thereby.
- The failure of either party to enforce any term or condition of this Agreement shall not constitute a waiver of either party's right to enforce each and every term and condition of this Agreement. No breach under this agreement shall be deemed waived or excused by either party unless such waiver or consent is in writing signed by the party granting such waiver or consent. The waiver by or consent of a party to a breach of any provision of this Agreement shall not operate or be construed as a waiver of or consent to any other or subsequent breach by such other party.
- This Agreement may not be assigned (including by operation of law or otherwise) by you without WILEY's prior written consent.
- Any fee required for this permission shall be non-refundable after thirty (30) days from receipt by the CCC.
- These terms and conditions together with CCC□s Billing and Payment terms and conditions (which are incorporated herein) form the entire agreement between you and WILEY concerning this licensing transaction and (in the absence of fraud) supersedes all prior agreements and representations of the parties, oral or written. This Agreement may not be amended except in writing signed by both parties. This Agreement shall be binding upon and inure to the benefit of the parties' successors, legal representatives, and authorized assigns.
- In the event of any conflict between your obligations established by these terms and conditions and those established by CCC□s Billing and Payment terms and conditions, these terms and conditions shall prevail.
- WILEY expressly reserves all rights not specifically granted in the combination of (i) the license details provided by you and accepted in the course of this licensing transaction, (ii) these terms and conditions and (iii) CCC□s Billing and Payment terms and conditions.
- This Agreement will be void if the Type of Use, Format, Circulation, or Requestor Type was misrepresented during the licensing process.
- This Agreement shall be governed by and construed in accordance with the laws of the State of New York, USA, without regards to such state□s conflict of law rules. Any legal action, suit or proceeding arising out of or relating to these Terms and Conditions or the breach thereof shall be instituted in a court of competent jurisdiction in New York County in the State of New York in the United States of America and each party hereby consents and submits to the personal jurisdiction of such court, waives any objection to venue in such court and consents to service of process by registered or certified mail, return receipt requested, at the last known address of such party.

WILEY OPEN ACCESS TERMS AND CONDITIONS

Wiley Publishes Open Access Articles in fully Open Access Journals and in Subscription journals offering Online Open. Although most of the fully Open Access journals publish open access articles under the terms of the Creative Commons Attribution (CC BY) License only, the subscription journals and a few of the Open Access Journals offer a choice of Creative Commons Licenses:: Creative Commons Attribution (CC-BY) license Creative Commons Attribution Non-Commercial (CC-BY-NC) license and Creative Commons Attribution Non-Commercial-NoDerivs (CC-BY-NC-ND) License. The license type is clearly identified on the article. Copyright in any research article in a journal published as Open Access under a Creative Commons License is retained by the author(s). Authors grant Wiley a license to publish the article and identify itself as the original publisher. Authors also grant any third party the right to use the article freely as long as its integrity is maintained and its original authors, citation details and publisher are identified as follows: [Title of Article/Author/Journal Title and Volume/Issue. Copyright (c) [year] [copyright owner as specified in the Journal]. Links to the final article on Wiley□s website are encouraged where applicable.

The Creative Commons Attribution License

4.3 Appendix 2: Supporting Information for Chapter 2

^{1}H NMR, ^{13}C NMR and IR Spectra

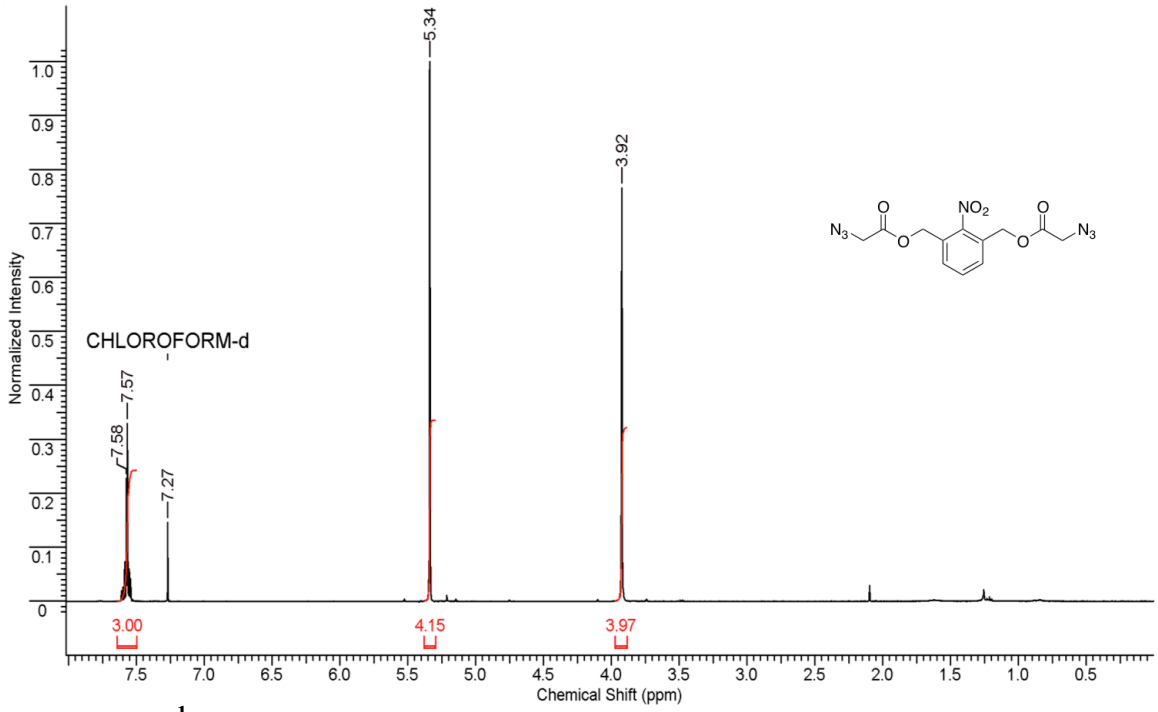

Figure S4.1. ^{1}H NMR spectrum (400MHz, $CDCl_3$) of monomer 2.3.

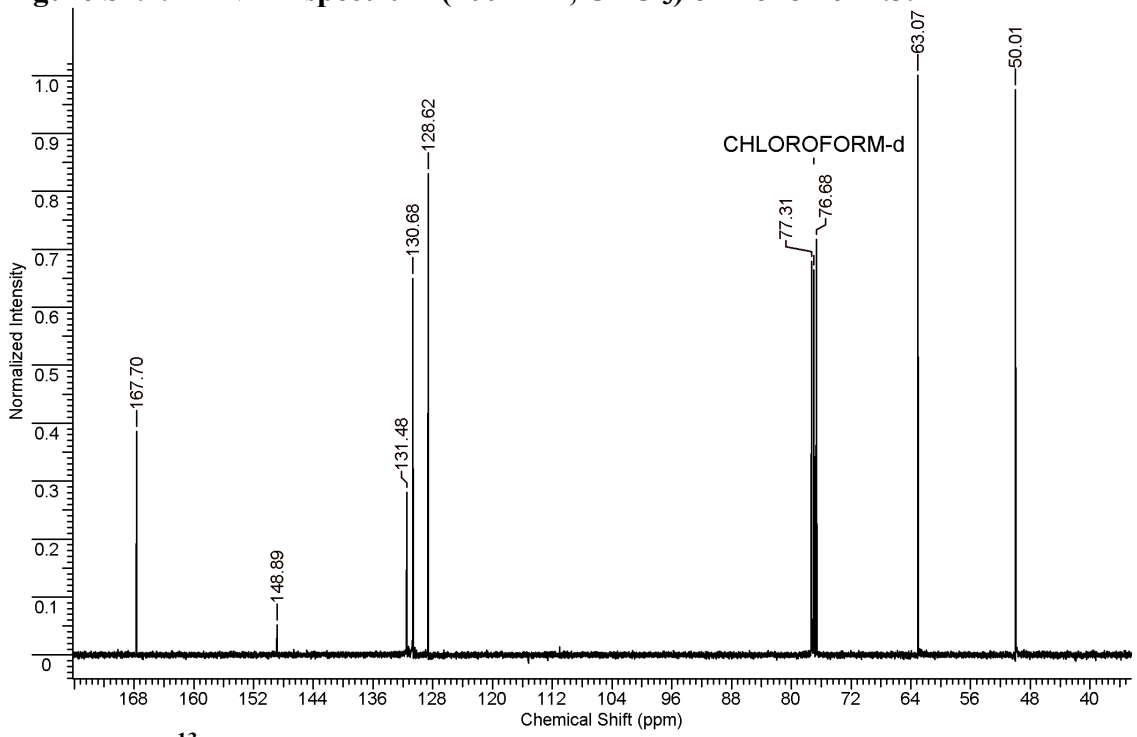

Figure S4.2. ^{13}C NMR spectrum (100MHz, $CDCl_3$) of monomer 2.3

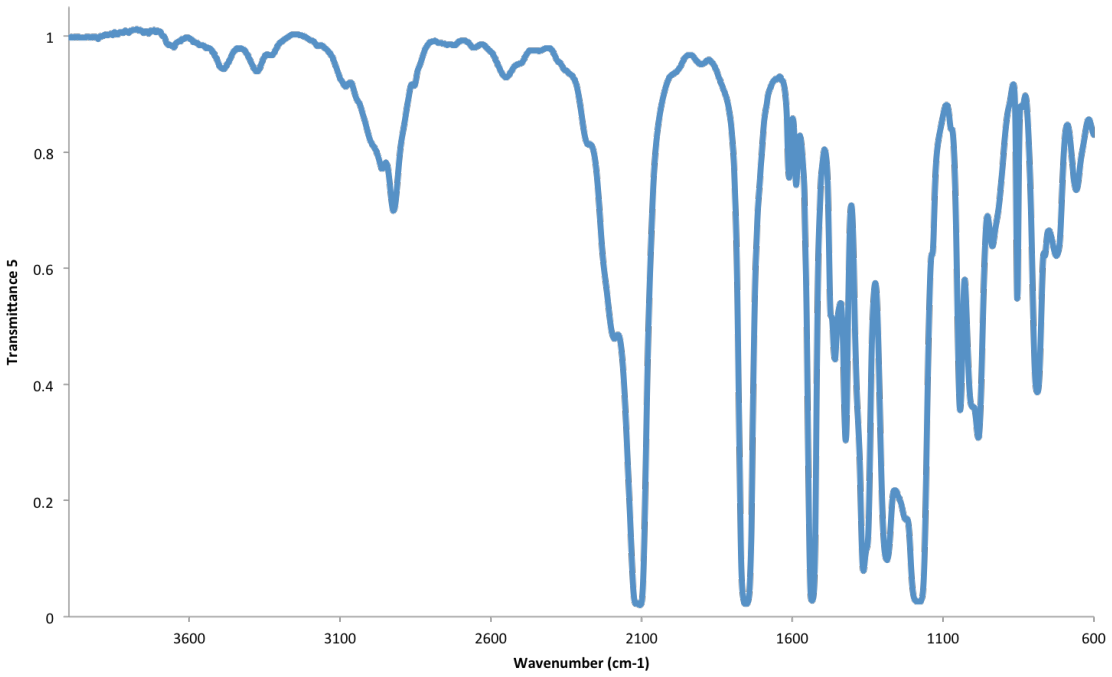

Figure S4.3. IR spectrum of monomer 2.3.

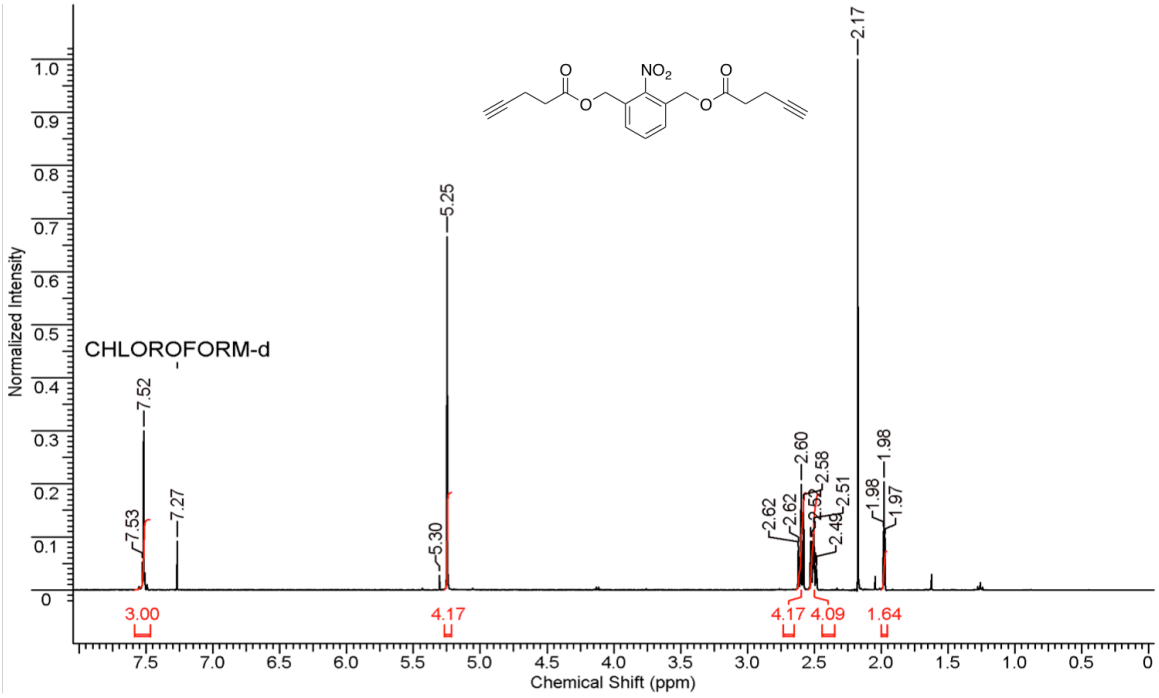

Figure S4.4. ^{1}H NMR spectrum (400MHz, $CDCl_3$) of monomer 2.5.

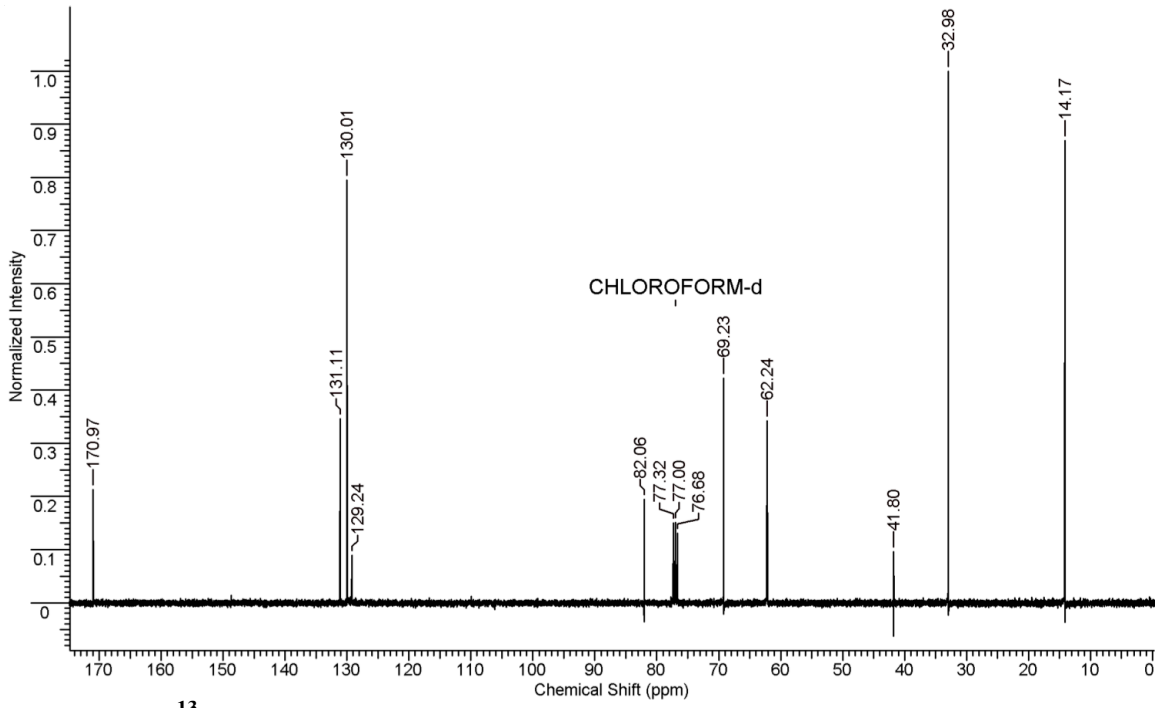

Figure S4.5. ^{13}C NMR spectrum (100MHz, $CDCl_3$) of monomer 2.5.

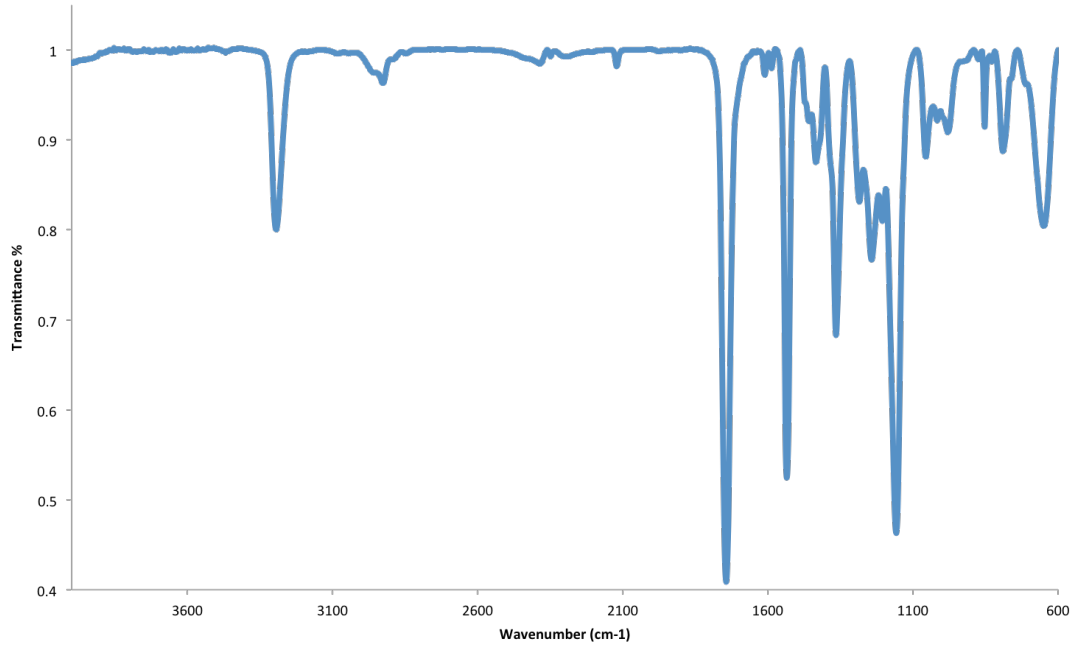

Figure S4.6. IR spectrum of monomer 2.5.

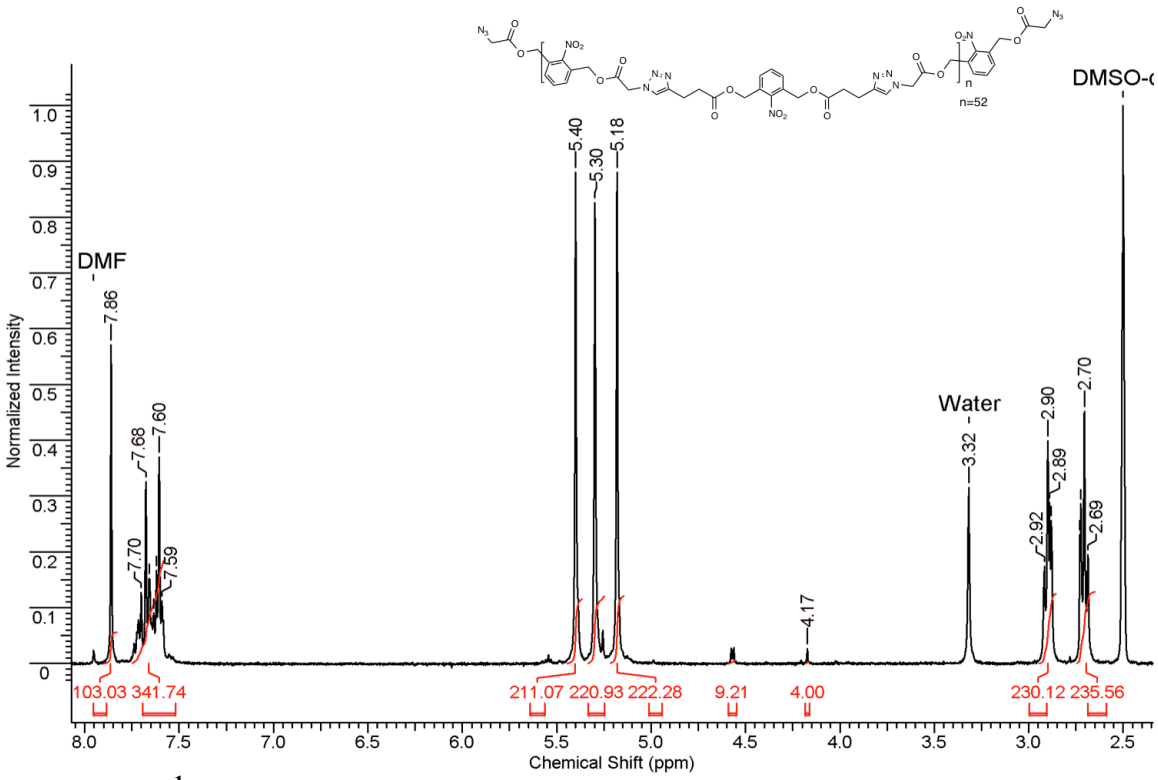

Figure S4.7. ^{1}H NMR spectrum (400MHz, DMSO-d_6) of polymer 2.6.

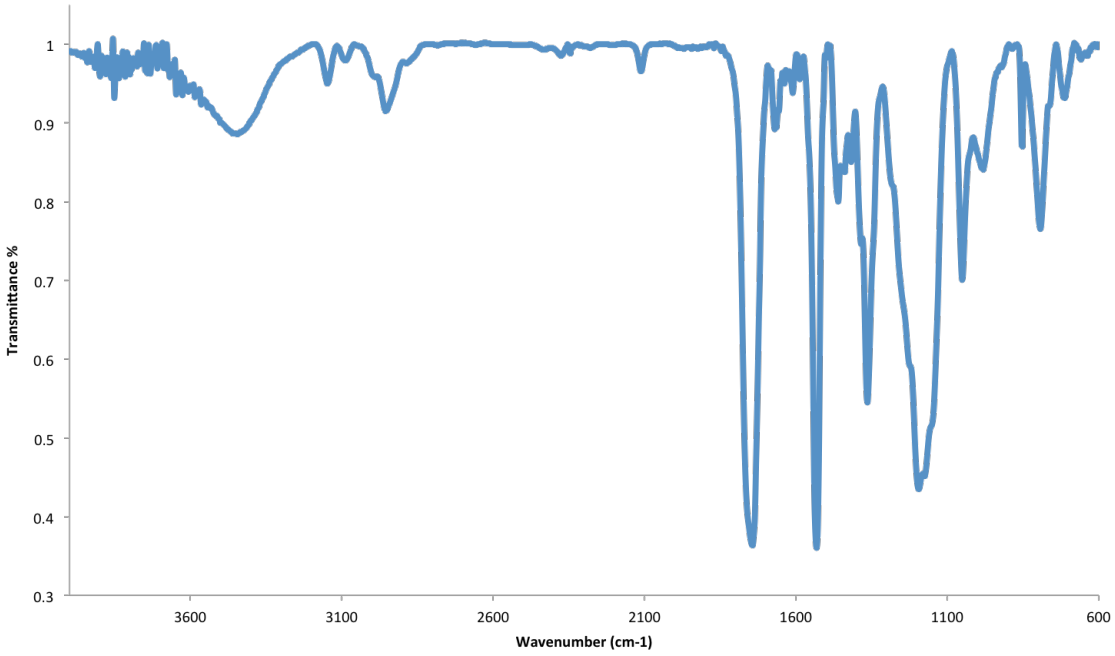

Figure S4.8. IR spectrum of polymer 2.6.

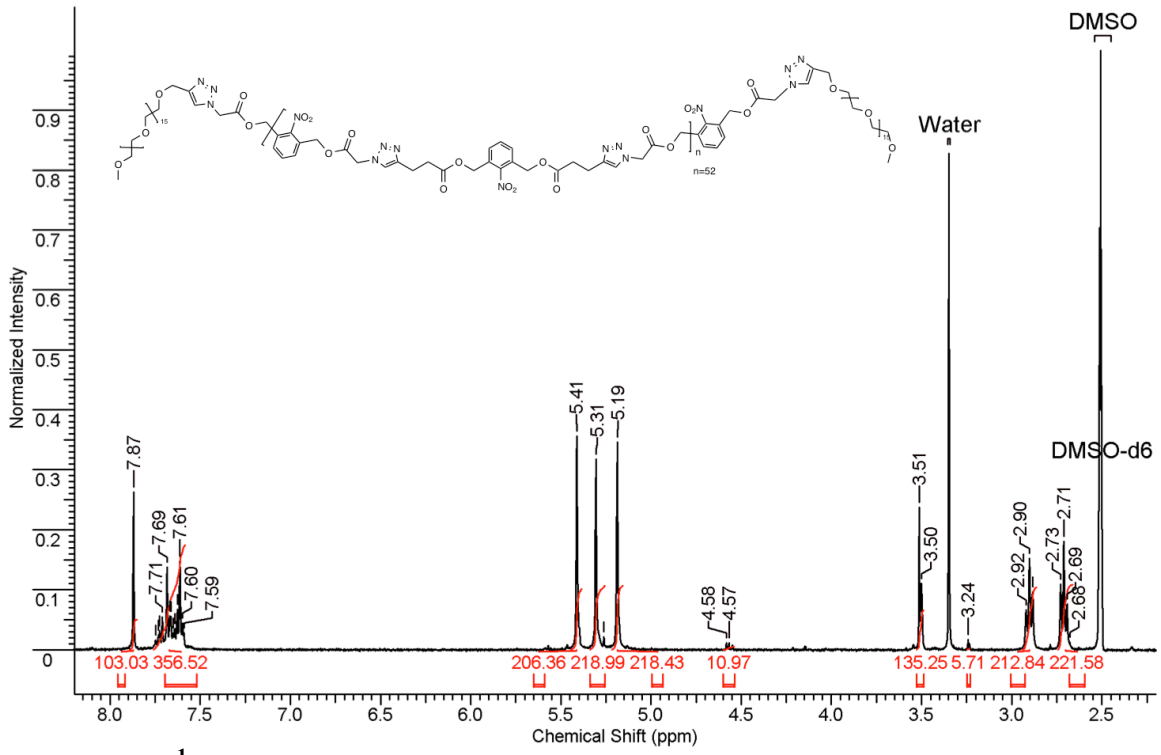

Figure S4.9. ^{1}H NMR spectrum (400MHz, DMSO-d_6) of polymer 2.9.

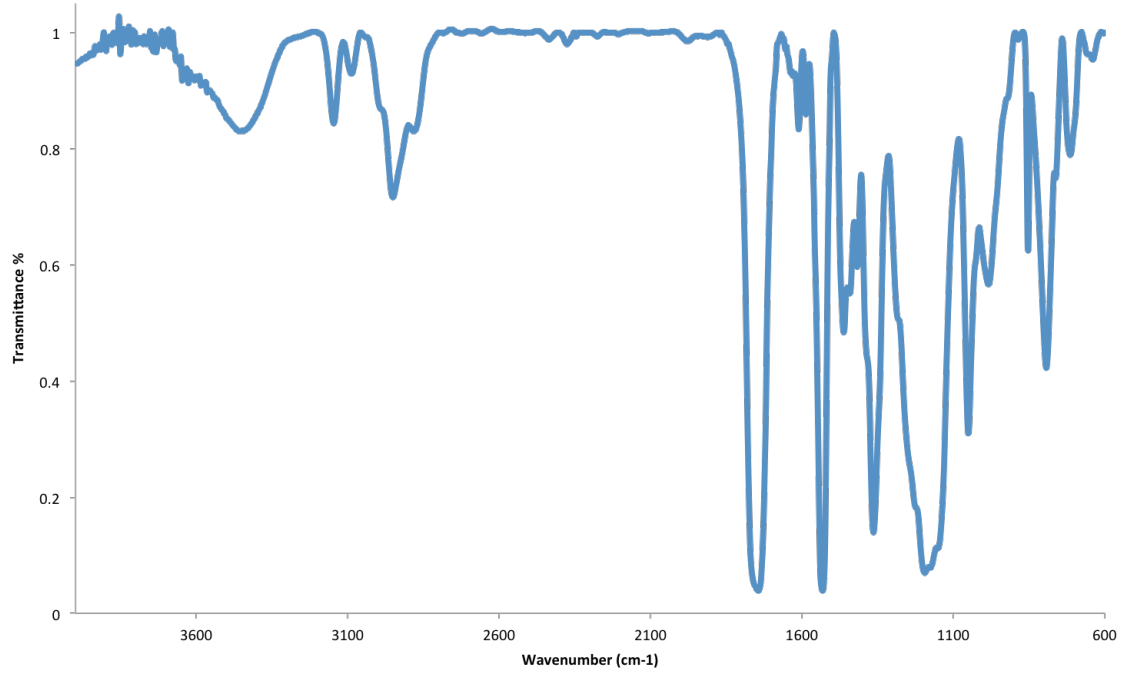

Figure S4.10. IR spectrum of polymer 2.9.

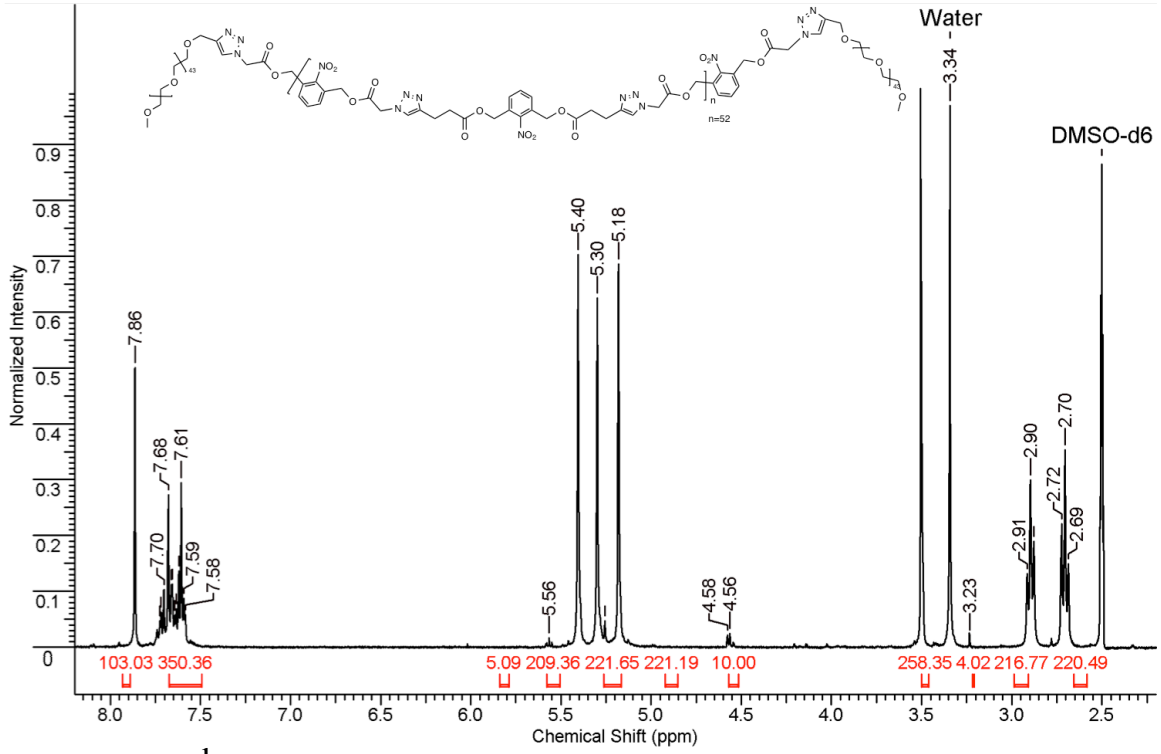

Figure S4.11. ^{1}**H NMR spectrum (400MHz, DMSO-d$_6$) of polymer 2.10.**

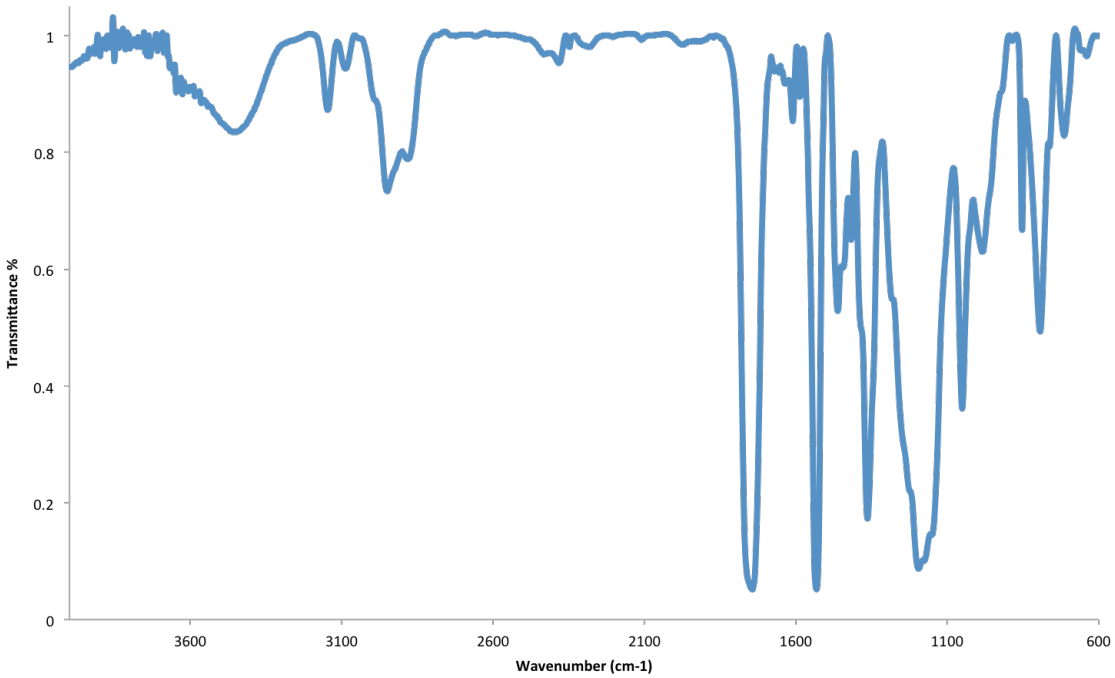

Figure S4.12. IR spectrum of polymer 2.10.

UV-vis Spectra

Small molecule solutions (0.03 mg/3 mL) and polymer solutions (0.2 mg/3 mL) in spectroscopic grade DMSO were used for UV-vis spectrometry. The solutions were housed in a 1 cm quartz cuvette and all measurements were taken in a Varian Cary 300 Bio UV-visible spectrophotometer.

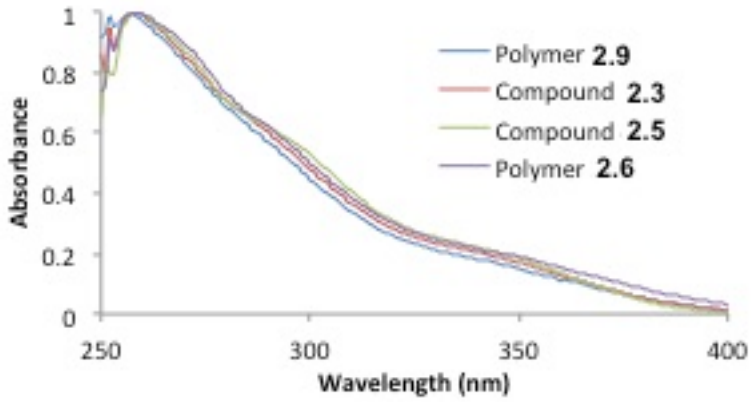

Figure S4.13. UV-vis spectra for monomers 2.3 and 2.5, and polymers 2.6 and 2.9.

Size Exclusion Chromatography

Polymer size was elucidated using size exclusion chromatography. The polymers were run using DMF as eluent and calibrated against polystyrene standards.

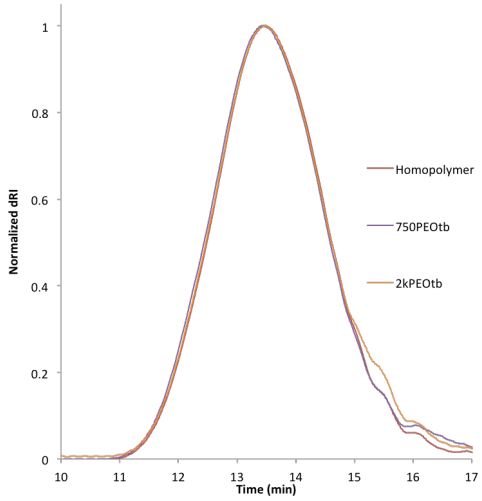

Figure S4.14. SEC for polymers 2.6, 2.9 and 2.10, run in DMF and calibrated against polystyrene standards.

Table S4.1. Results from SEC analysis of polymers 2.6, 2.9 and 2.10.

Polymer	Mn	Mw	PDI
Homopolymer	24000	40000	1.65
750PEOtb	23000	40000	1.76
2kPEOtb	25000	40000	1.62

4.4 Appendix 3: Supporting Information for Chapter 3

^{1}H NMR, ^{13}C NMR and FTIR

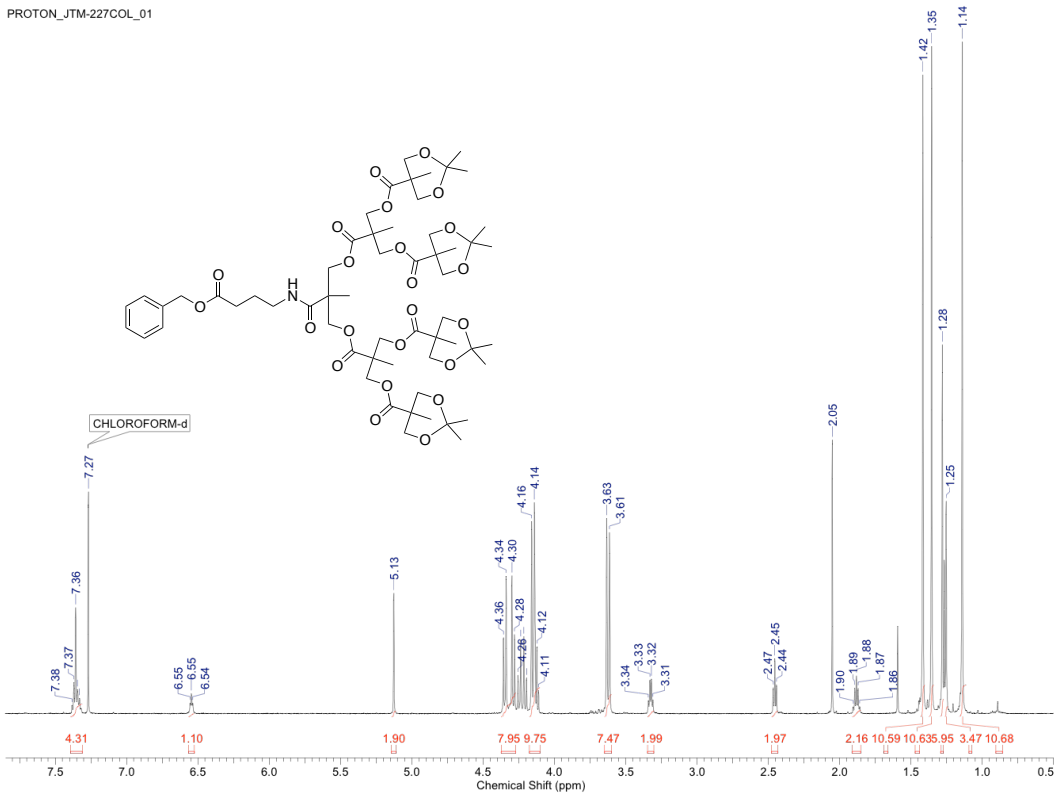

Figure S4.15. ^{1}H NMR (599MHz, $CDCl_3$) of 3.4.

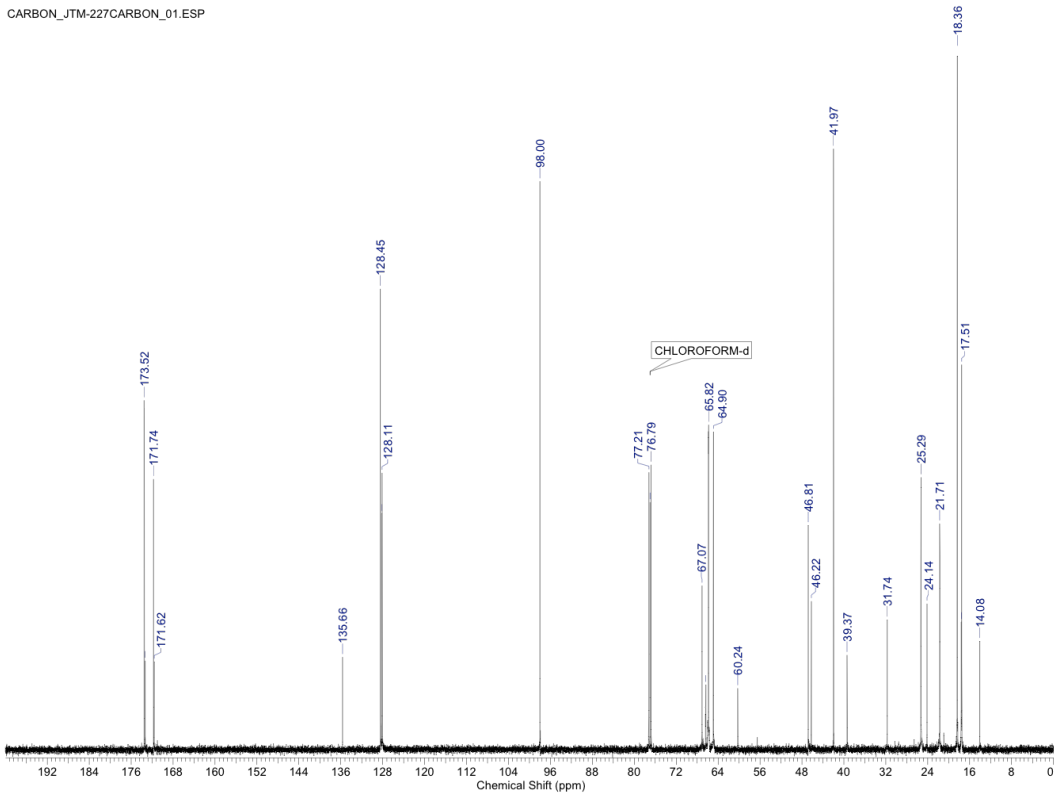

Figure S4.16. ^{13}C NMR (151MHz, $CDCl_3$) of 3.4.

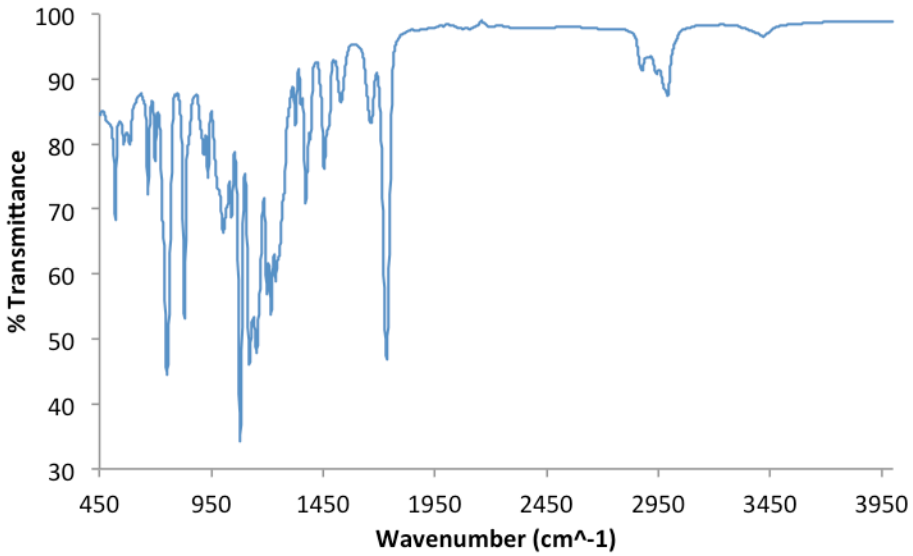

Figure S4.17. FTIR of 3.4.

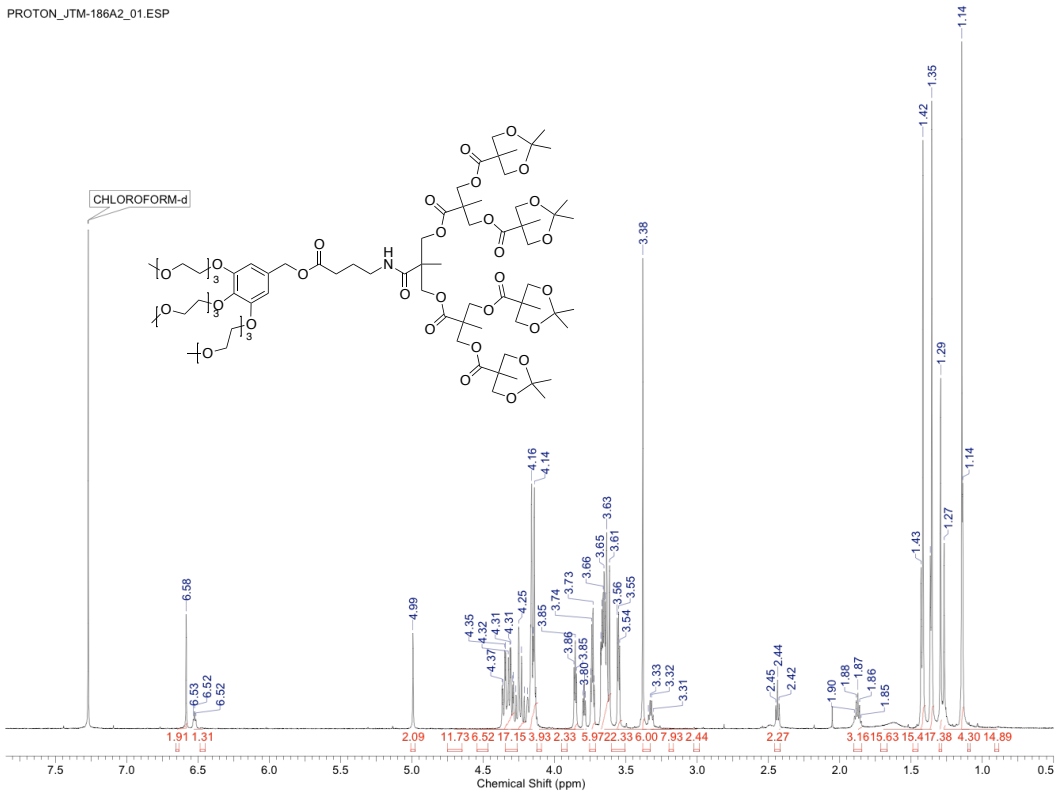

Figure S4.18. ^{1}H NMR (599MHz, $CDCl_3$) of 3.7.

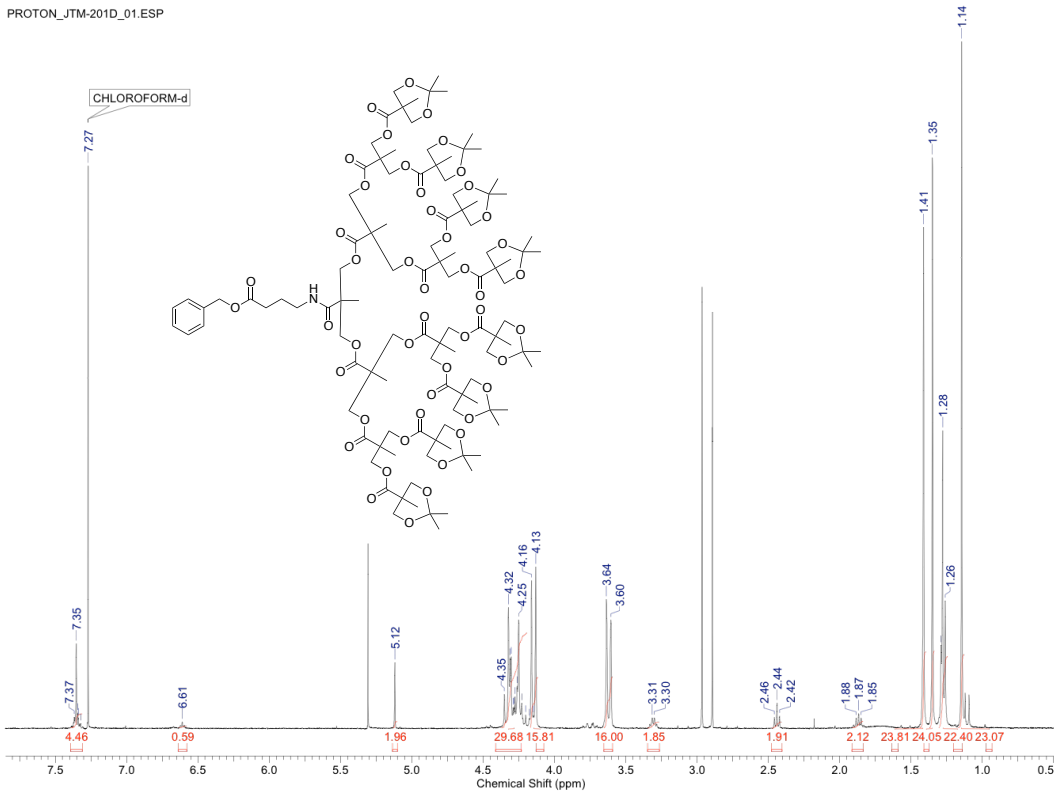

Figure S4.19. ^{1}H NMR (400MHz, $CDCl_3$) of 3.10.

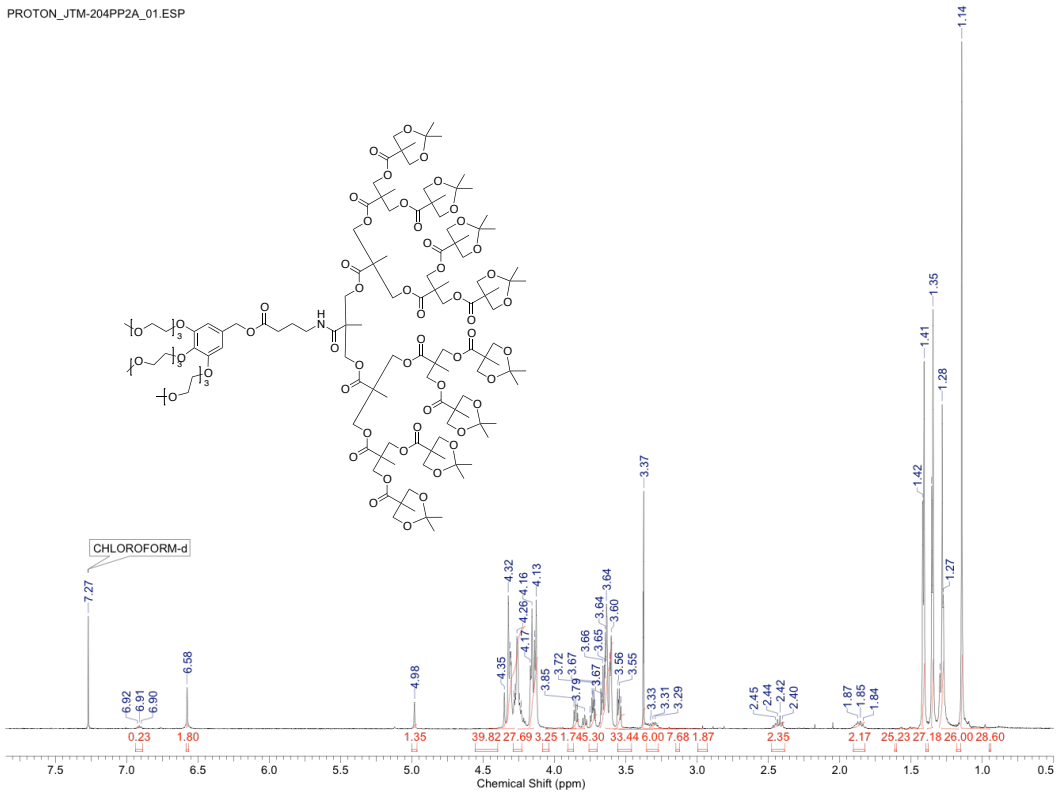

Figure S4.20. ^{1}H NMR (400MHz, $CDCl_3$) of 3.12.

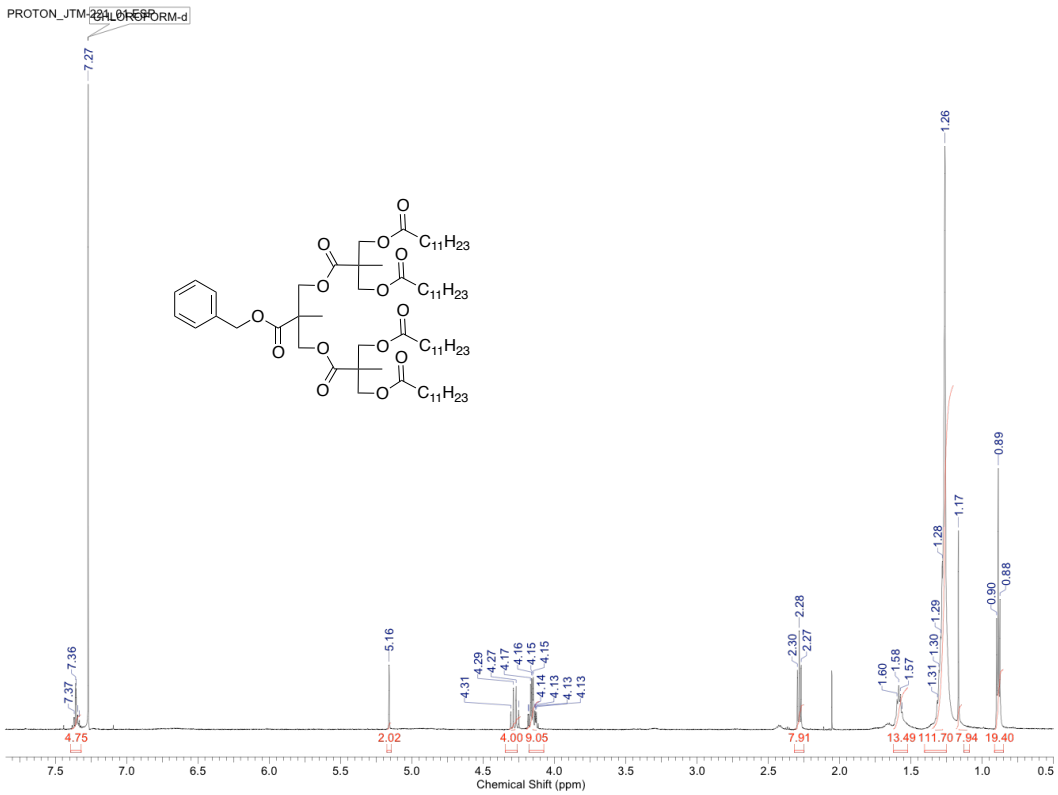

Figure S4.21. ^{1}H NMR (599MHz, $CDCl_3$) of 3.14.

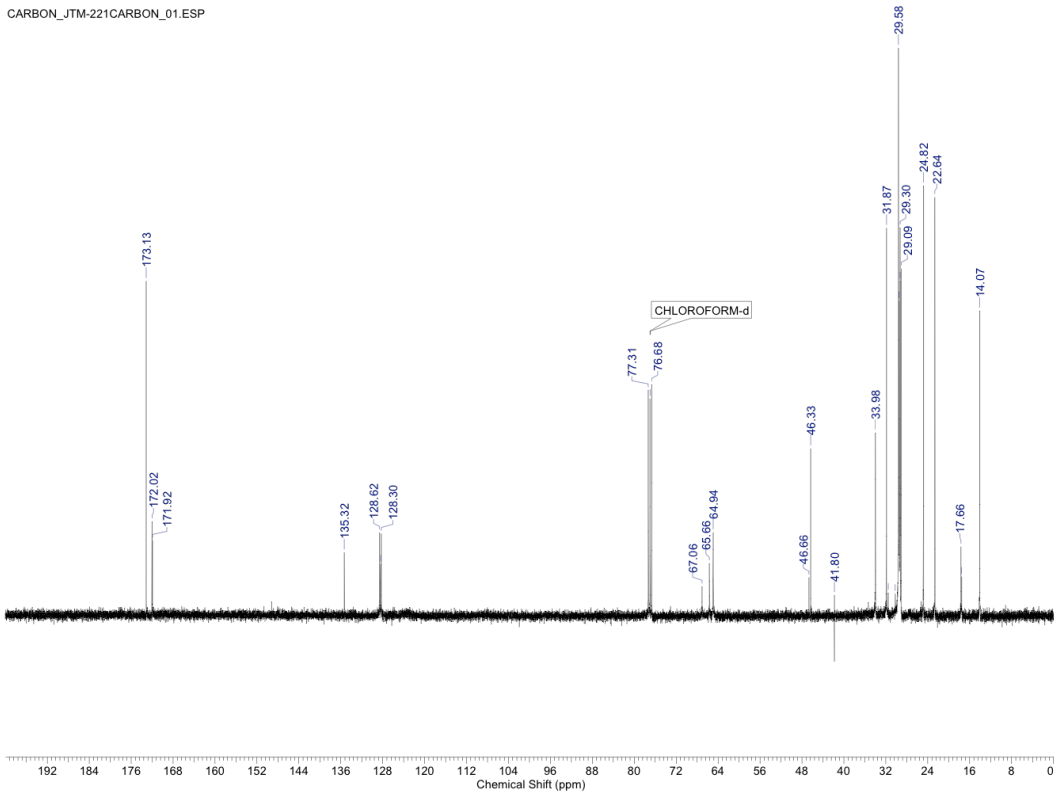

Figure S4.22. ^{13}C NMR (101MHz, $CDCl_3$) of 3.14.

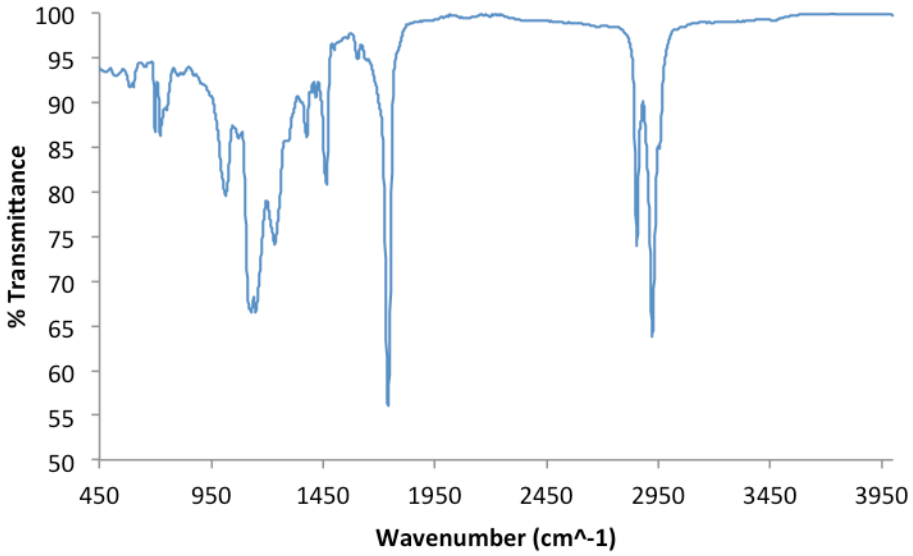

Figure S4.23. FTIR of 3.14.

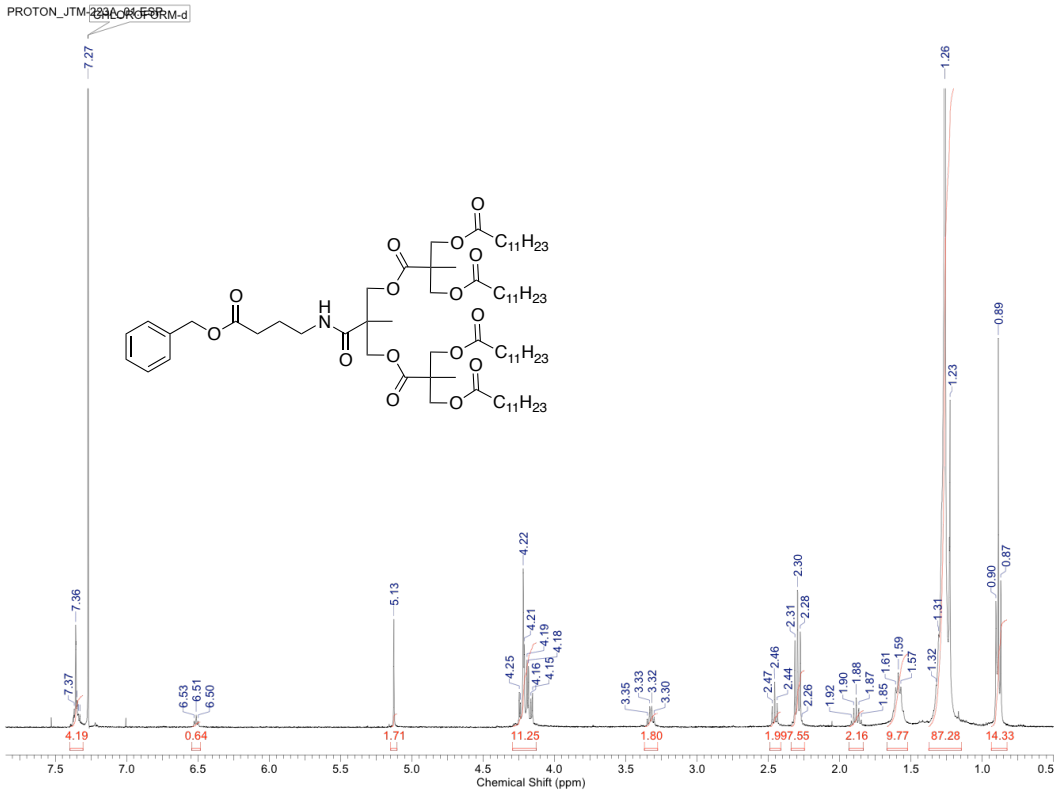

Figure S4.24. ^{1}H NMR (400MHz, $CDCl_3$) of 3.16.

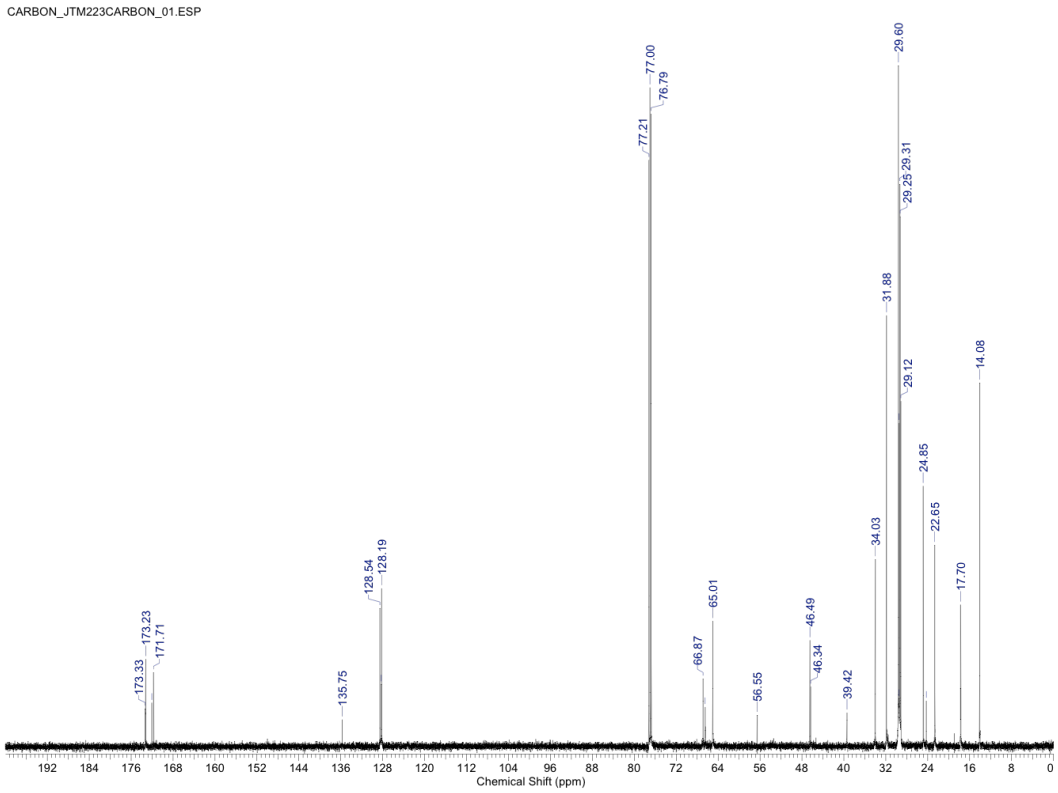

Figure S4.25. ^{13}C NMR (151MHz, $CDCl_3$) of 3.16.

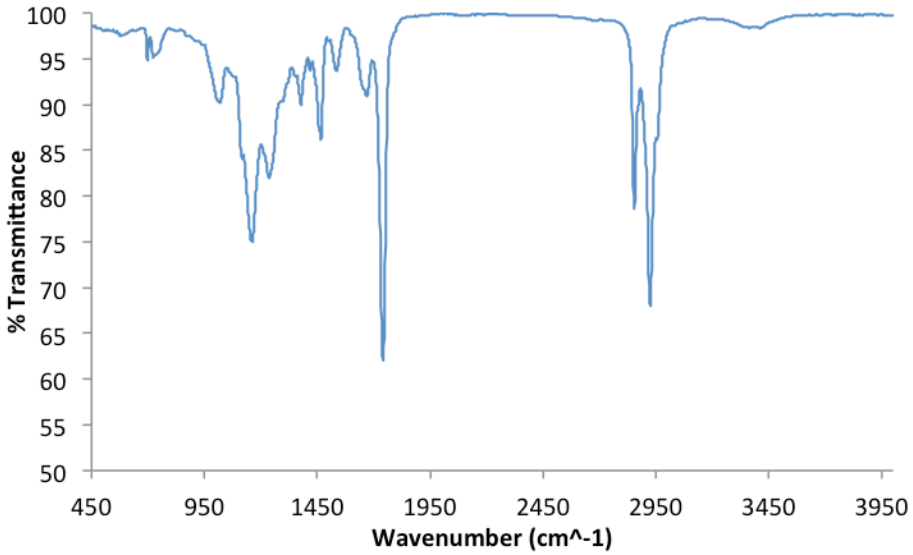

Figure S4.26. FTIR of 3.16.

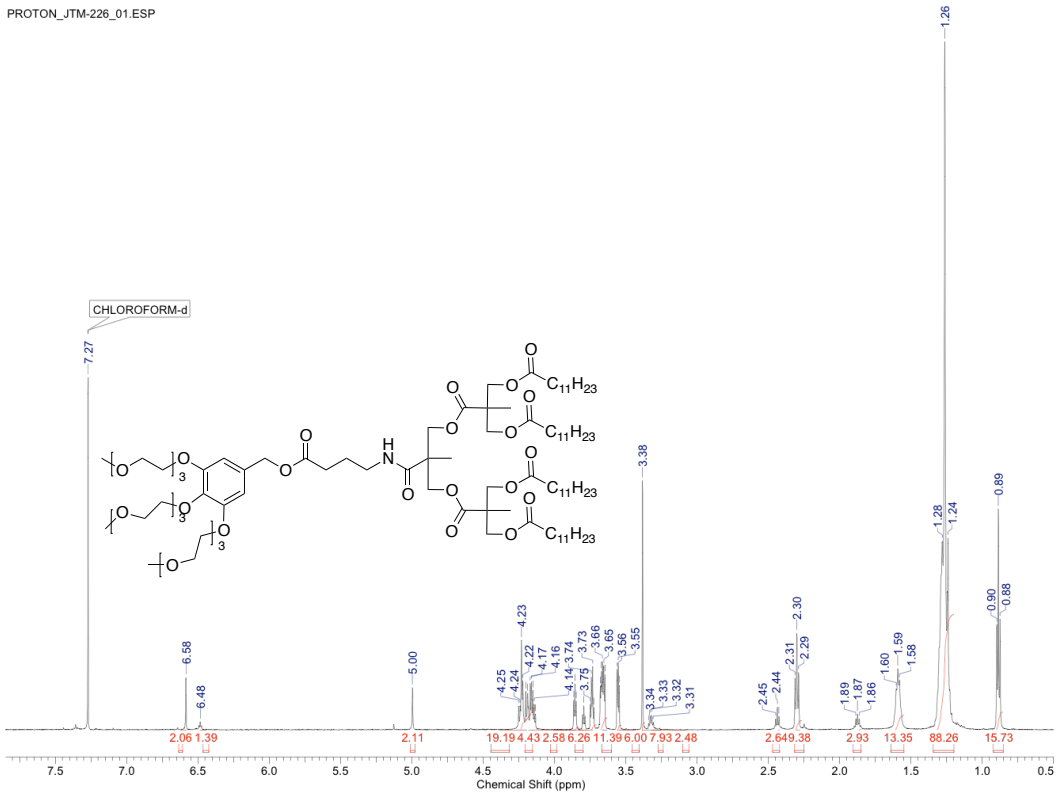

Figure S4.27. ^{1}H NMR (599MHz, $CDCl_3$) of 3.18.

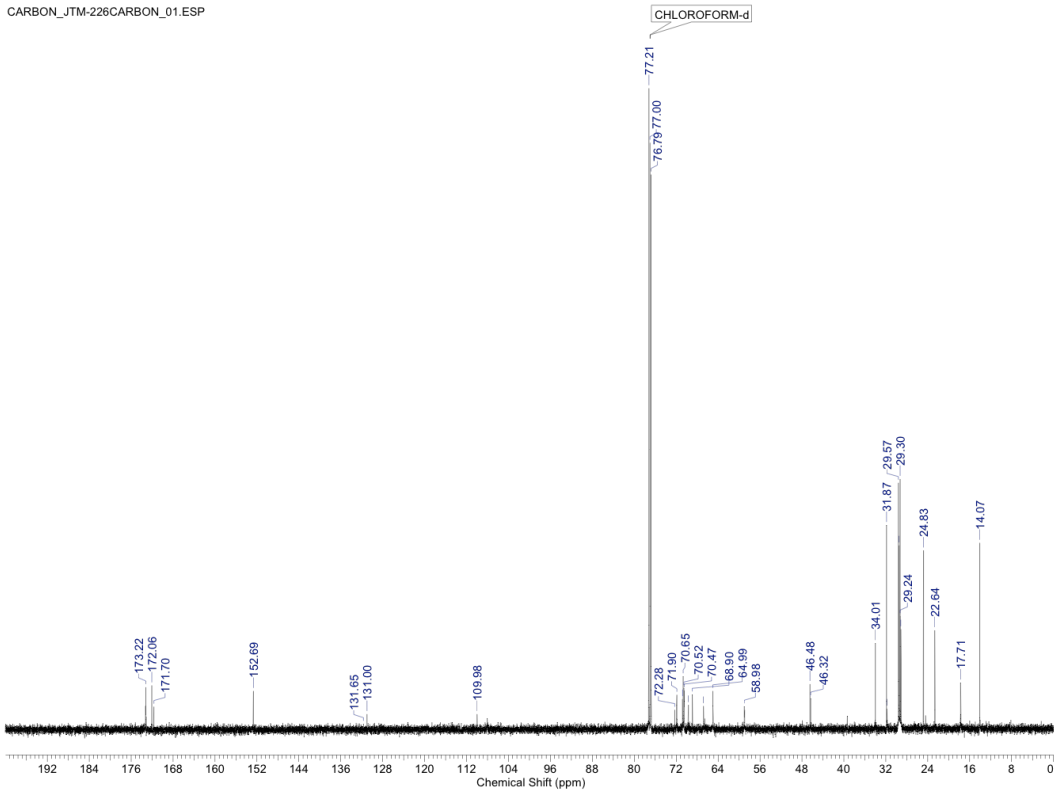

Figure S4.28. ^{13}C NMR (151MHz, $CDCl_3$) of 3.18.

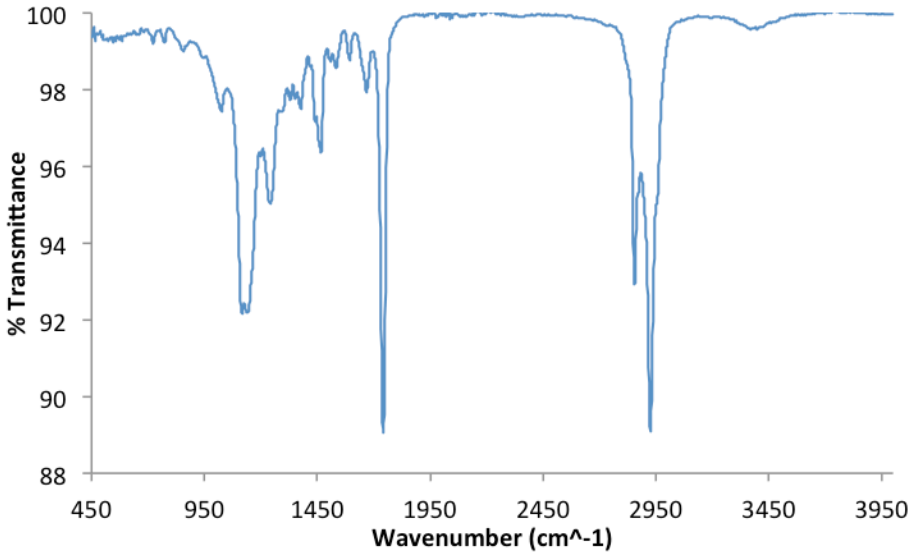

Figure S4.29. FTIR of 3.18.

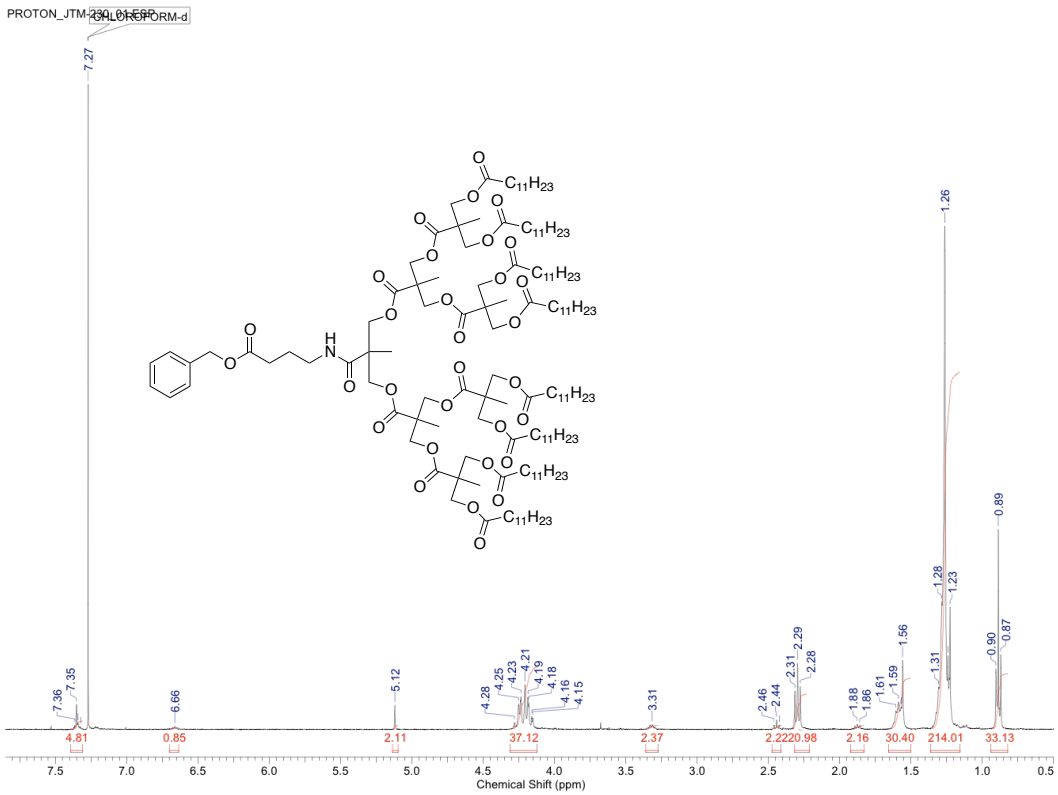

Figure S4.30. ^{1}H NMR (400MHz, $CDCl_3$) of 3.20.

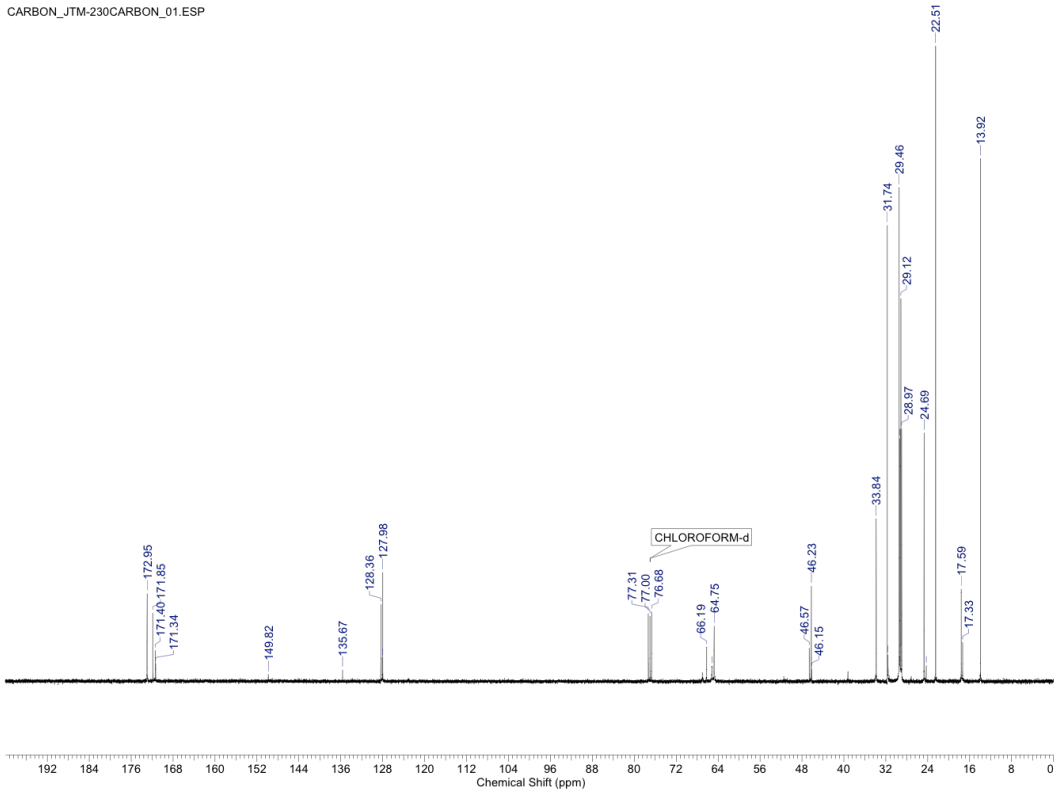

Figure S4.31. ^{13}C NMR (151MHz, $CDCl_3$) of 3.20.

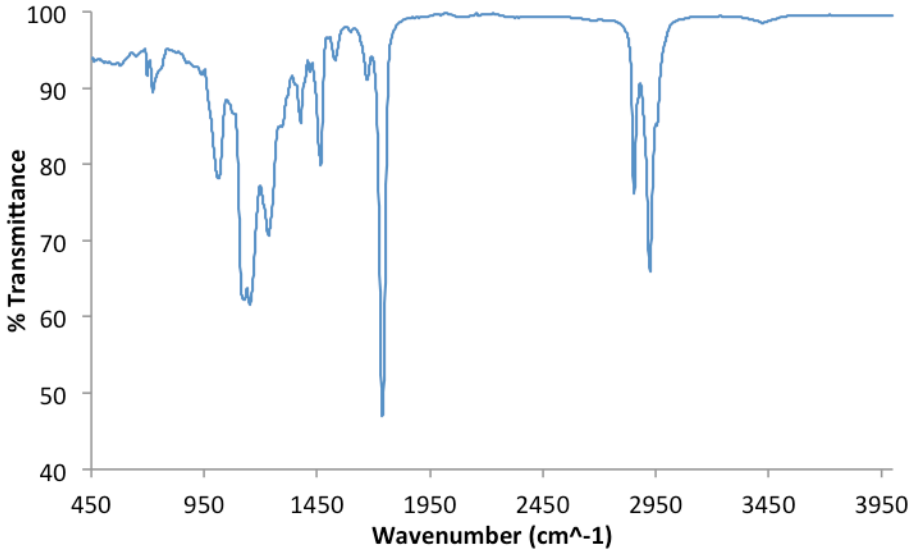

Figure S4.32. FTIR of 3.20.

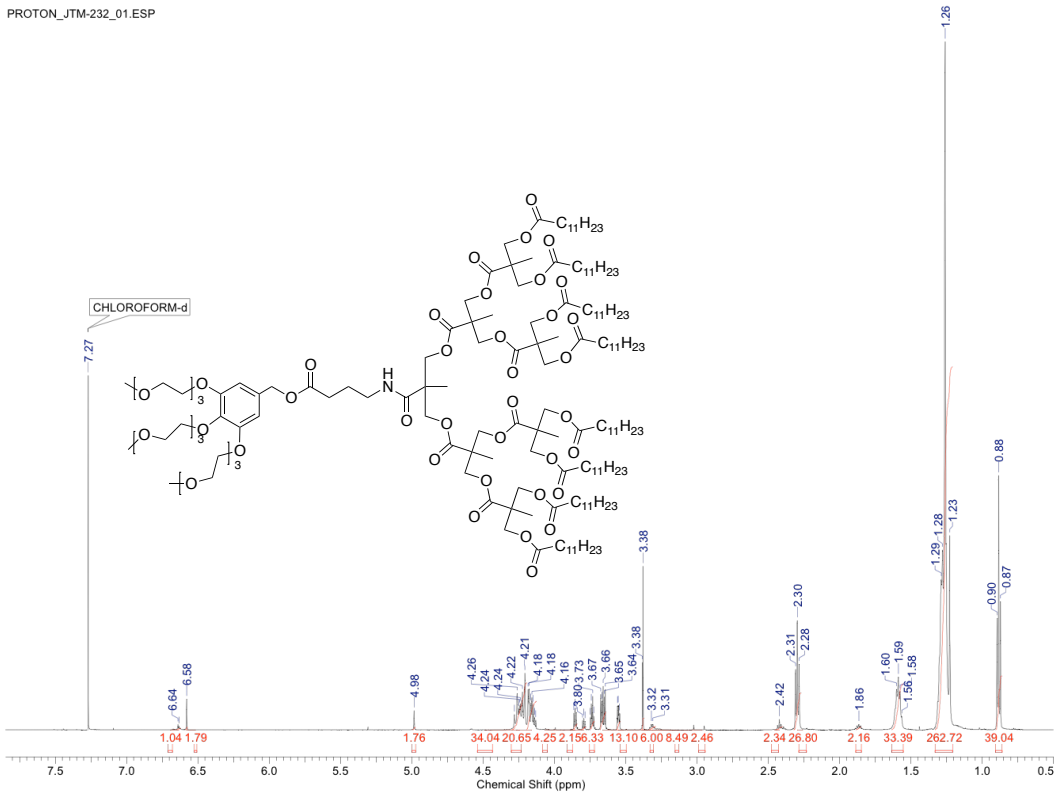

Figure S4.33. ^{1}H NMR (599MHz, $CDCl_3$) of 3.22.

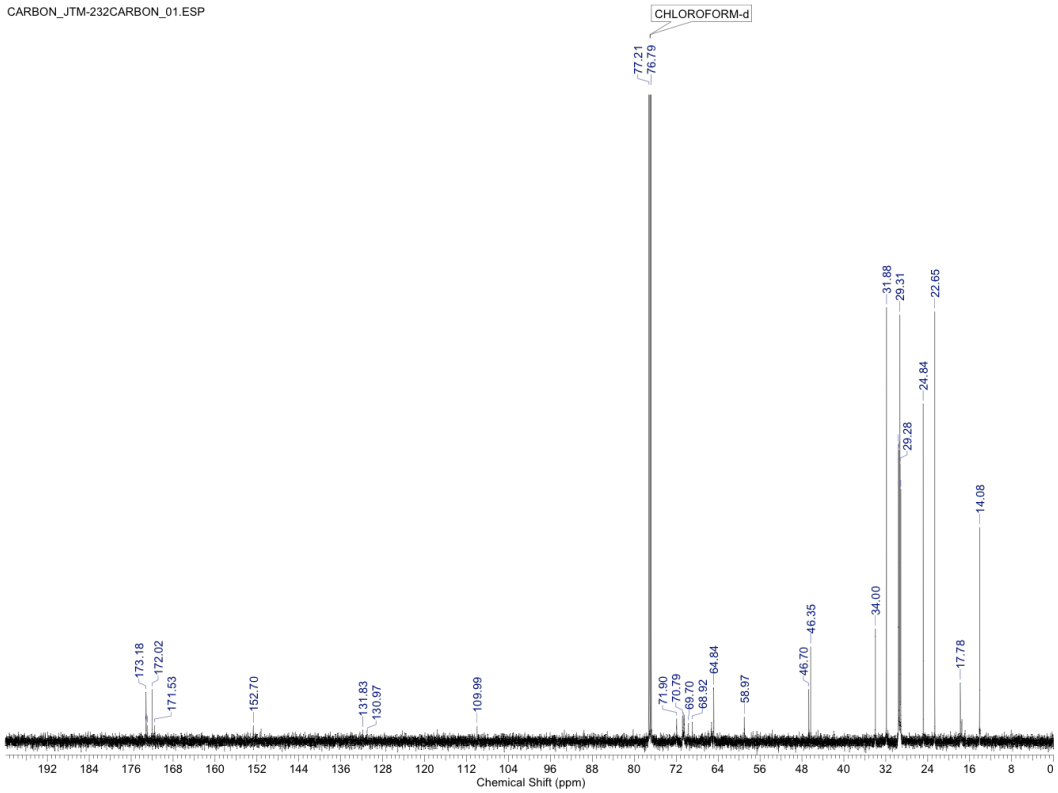

Figure S4.34. ^{13}C NMR (151MHz, $CDCl_3$) of 3.22.

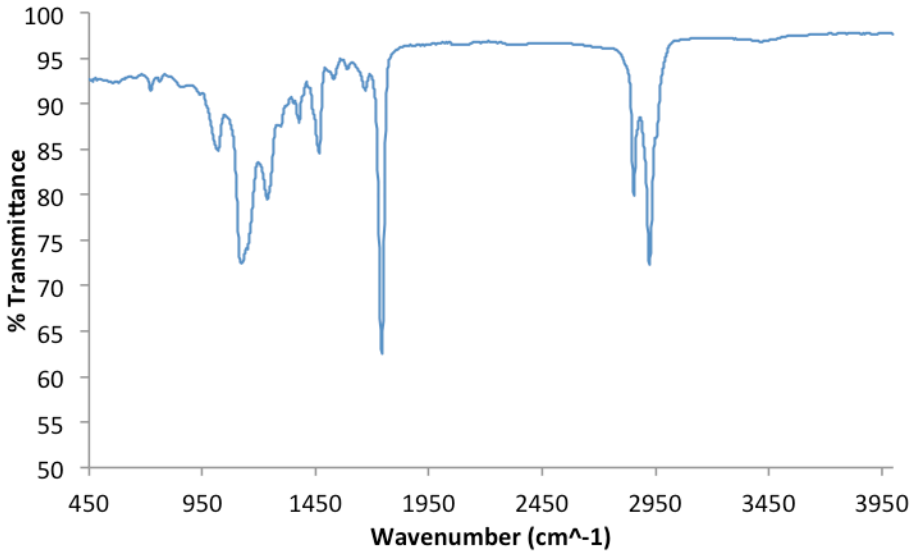

Figure S4.35. FTIR of 3.22.

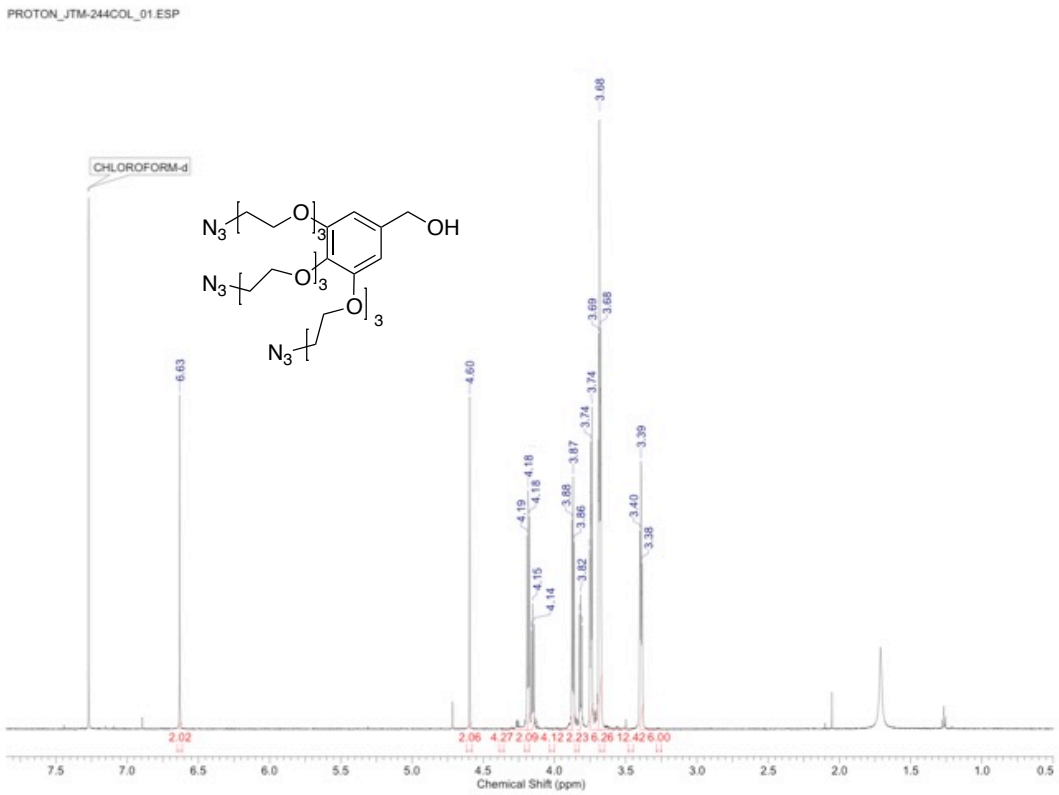

Figure S4.36. ^{1}H NMR (599MHz, $CDCl_3$) of 3.24.

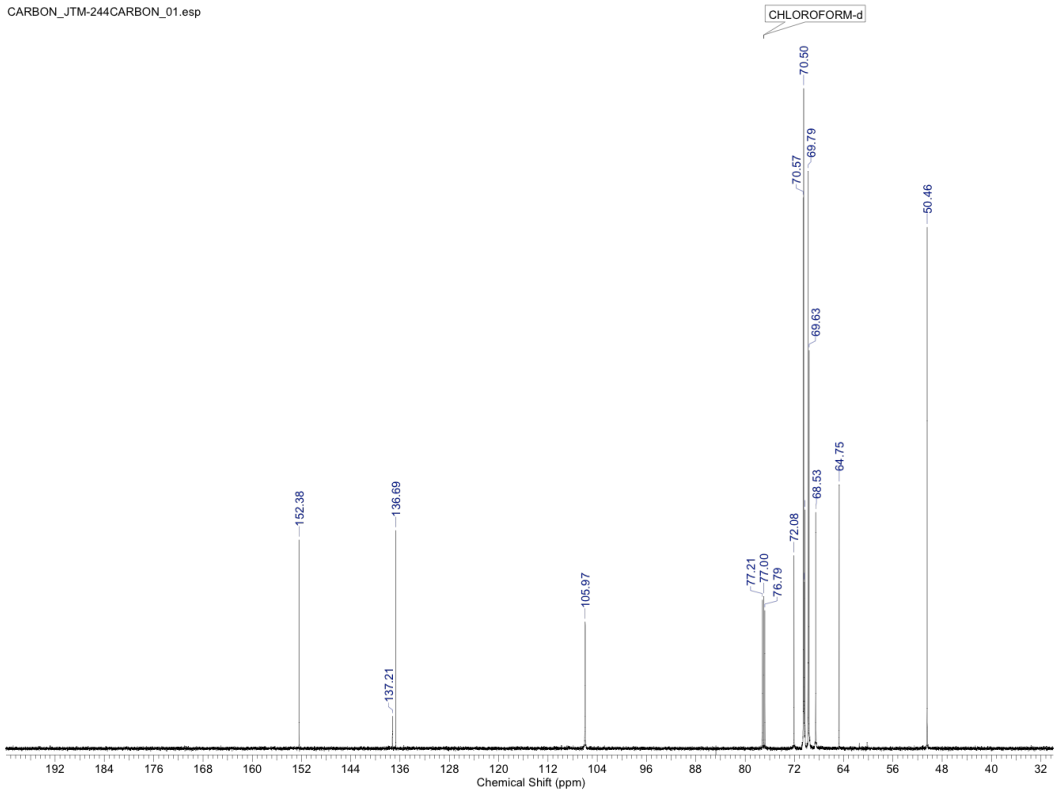

Figure S4.37. ^{13}C NMR (151MHz, $CDCl_3$) of 3.24.

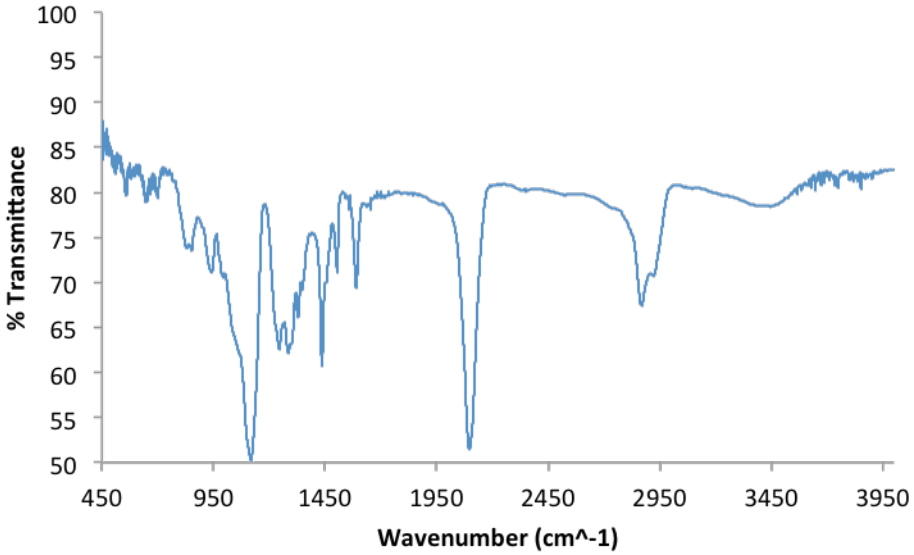

Figure S4.38. FTIR of 3.24.

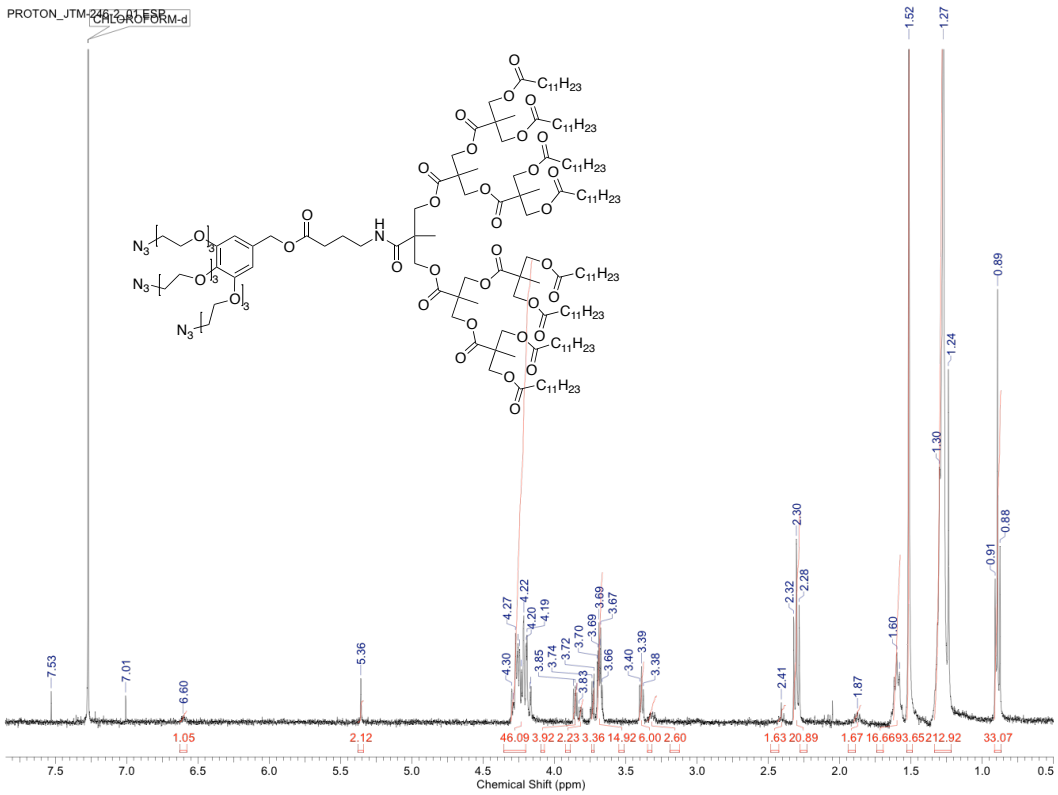

Figure S4.39. ^{1}H NMR (400MHz, $CDCl_3$) of 3.25.

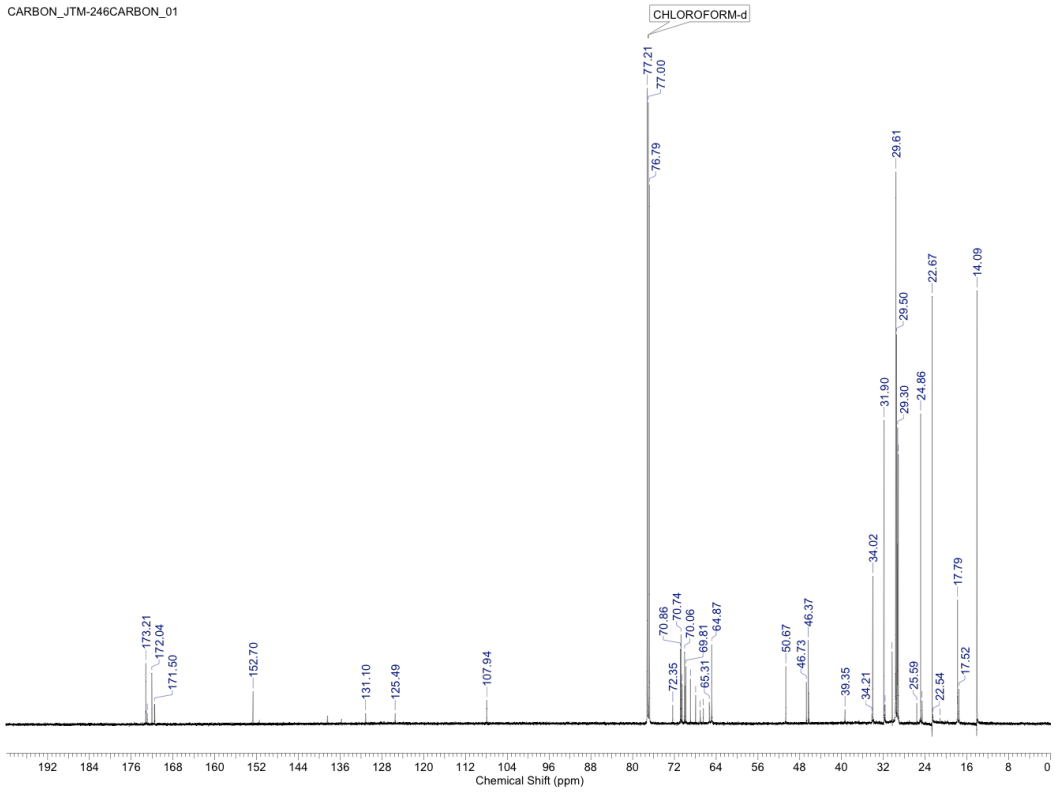

Figure S4.40. ^{13}C NMR (151MHz, $CDCl_3$) of 3.25.

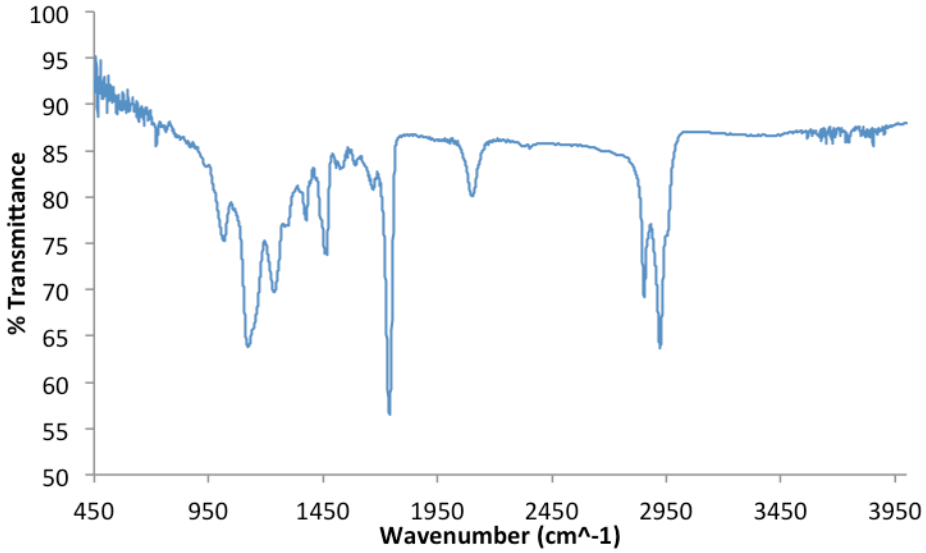

Figure S4.41. FTIR of 3.25.

Curriculum Vitae

EDUCATION

Western University, London, Canada

M.Sc., Organic and Polymer Chemistry — 2013-pres.
Research Supervisor: Dr. Elizabeth Gillies

B.Sc., Chemistry — 2008-2013
Honors Specialization in Biochemistry and Chemistry
4th year research project "Photodegradable Polymer Vesicles"
Research Supervisor: Dr. Elizabeth Gillies

RESEARCH EXPERIENCE

Graduate Research Assistant, Gillies Group — 2013-pres.
Western University, London, Canada

4th Year Undergraduate Project, Gillies Group — 2012-2013
Western University, London, Canada

16 Month Science Internship, Chemtura Canada, — 2011-2012
Chemtura Canada Agrosolutions, Guelph, Canada

PUBLICATION

McIntosh, J. T.; Nazemi, A; Bonduelle, C. V.; Lecommandoux, S.; Gillies, E. R. "Synthesis, self-assembly, and degradation of amphiphilic triblock copolymers with fully photodegradable hydrophobic blocks" *Can. J. Chem.* **2015**, (93), 126-133.

CONFERENCE PRESENTATIONS AND POSTERS

J. T. McIntosh, A. Nazemi, E. R. Gillies; "Dendrimersomes: Platforms for Photoresponsiveness and Surface Functionalization" *9th International Dendrimer Symposium,* Montreal, Quebec, July 12-17, 2015. [poster presentation]

J. T. McIntosh, A. Nazemi, E. R. Gillies; "Polymersomes and Dendrimersomes as Frameworks for Photoresponsiveness and Surface Functionalization" *CAMBR Distinguished Lecturer and Research Day,* London, Ontario, April 27, 2015. [oral presentation]